Episodic Air Pollution in Wisconsin (LADCO Winter Nitrate Study) and Georgia (SEARCH Network) During Jan-Mar 2009

Phase I Report

Jaemeen Baek[a]
Gregory Carmichael[a]
Sang Rin Lee[a]
Jacob Oleson[a]
Nicole Riemer[b]
Timothy Rohlf[a]
Sinan Sousan[a]
Scott Spak[a]
Charles Stanier[a]

[a]University of Iowa
[a]University of Illinois

October 2010

Prepared for the Lake Michigan Air Directors Consortium

Episodic Air Pollution in Wisconsin
(LADCO Winter Nitrate Study) and Georgia (SEARCH Network)
During Jan-Mar 2009

Acknowledgements

This document was made possible by the Electric Power Research Institute, Inc.,
and the Lake Michigan Air Directors Consortium

We would also like to acknowledge the measurement personnel involved in this project, and our colleagues who contributed data analysis products. Without their ingenuity and effort this study would not have been possible.

Eric Edgerton, ARA
Donna Kenski, LADCO
Mike Caughey, Illinois State Water Survey
Bill Adamski, WDNR
Joseph Hoch, WDNR
Joe Leair, WDNR
Jerry Medinger, WDNR
Dan Nickolie, WDNR
Mary Mertes, WDNR
Bruce Rodger, WDNR
Bart Sponseller, WDNR
John Hillery, WDNR
Janel Hanrahan, WDNR
Laura Carnahan, WDNR

Episodic Air Pollution in Wisconsin
(LADCO Winter Nitrate Study) and Georgia (SEARCH Network)
during January-March 2009

Jaemeen Baek, Gregory Carmichael, Sang Rin Lee, Jacob Oleson, Nicole Riemer, Timothy Rohlf, Sinan Sousan, Scott Spak, Charles Stanier

Phase I Report

Table of Contents

Appendices

12. A preliminary study of the long-term (2001-2009) characteristics of daily-averaged, filter-based concentrations of organic carbon (OC) and elemental carbon (EC) PM2.5 at monitoring sites in Milwaukee and Mayville, WI (Bill Adamski)
13. Literature review on nitrate formation
14. Fog time series
15. CART Analysis (Donna Kenski)

List of Figures

List of Tables

Episodic Air Pollution in Wisconsin (LADCO Winter Nitrate Study) and Georgia (SEARCH Network) during January-March 2009

Jaemeen Baek, Gregory Carmichael, Sang Rin Lee, Jacob Oleson, Nicole Riemer, Timothy Rohlf, Sinan Sousan, Scott Spak, Charles Stanier

Phase I Report

Executive Summary

Analysis of air quality and meteorology measurements obtained during the LADCO Winter Nitrate Study (WNS) was performed in order to better understand wintertime episodes of elevated fine particle ($PM_{2.5}$) concentrations in the Midwest. The analysis evaluated and compared the high time resolution surface observations taken during the three-month period (1 January - 31 March, 2009) at an urban Milwaukee site and a rural site in Mayville, Wisconsin. Contemporaneous observations at an urban-rural pairing of Southeastern Aerosol Research and Characterization (SEARCH) sites at Atlanta (Jefferson St.) and Yorkville, Georgia were similarly assessed to understand reasons for regional differences in episode chemistry, aerosol speciation, and intensity.

Refined conceptual model of wintertime nitrate PM episodes: The observations support a refinement of the current episode conceptual model. Wintertime fine particle episodes in the Upper Midwest occur when low pressure systems move into the region, and are marked by a shallow, stable planetary boundary layer, with increases in temperature and relative humidity, light southerly winds, and cloud cover. Strong late-season episodes occur in the presence of regional snow cover at temperatures near freezing, when snow melt and sublimation generate fog and strengthen the boundary layer inversion. These meteorological conditions alone raise concentrations of locally-emitted primary pollutants in urban areas to more than double seasonal background levels, and lead to further increases in the concentrations of secondary nitrate and ammonium aerosols due to preferential partitioning to the aerosol phase and ongoing conversion of NOx to nitrate during episodes. The rural response to episode meteorology is marked by less enhancement of primary pollutants due to lower local emissions, and by greater fractional contributions of ammonium nitrate. Nitrate, NOx for further nitrate production, and ammonia seem to be present in sufficient quantities so that these are not limiting; therefore, substantial $PM_{2.5}$ concentration increases are likely to ensue each time the required meteorological conditions occur. However, total ammonia and total nitrate (and, by extension, NOx) influence episode intensity. Controls of ammonia or nitrate are likely to decrease episode concentrations. Substantial contribution to nitrate production from nighttime chemistry of ozone and NO_2 to N_2O_5 and nitric acid is likely and can be investigated through

modeling of the field data. The refined conceptual model should probably include a decrease in ammonia availability as ammonium nitrate episodes progress to higher $PM_{2.5}$ concentrations. Confirmation of this shift would require corroboration by additional measurements, but the current evidence includes the two sites in the current study and multiple sites in a previous independent analysis of the Midwest Ammonia Monitoring network data. Finally, contribution of local urban emissions, particularly of organic aerosols from combustion, is important in urban locations and control of these emissions would decrease the urban excess that is observed.

The largest remaining uncertainties in the conceptual model are the variability from episode-to-episode in ammonia emissions, the balance of daytime and nighttime nitrate production, the relationship between NOx controls and nitrate reductions, and the extent to which snow and fog are causal (either through meteorological or chemical processes) rather than just correlated with episodes because of similar synoptic meteorological causes.

Additional policy-relevant findings include:

Episodes in Wisconsin showed strong enhancements in both primary and secondary aerosol compounds. The increase in $PM_{2.5}$ over typical conditions was due primarily to secondary nitrate and ammonium, which increased by a factor of 2-3 as a result of production and accumulation of nitrate together with preferential partitioning of nitrate and ammonia to the aerosol phase at low temperatures and high humidity. Increases in sulfate (factors of 2.2-2.9), organic carbon (factors of 1.4-1.7), and elemental carbon (factors of 1.9-2.0) were also noted. Analysis of nine years of organic carbon filters from the Wisconsin sites confirms the conceptual view that increases in wintertime organic carbon concentrations are from primary and not secondary sources.

There are significant differences in wintertime $PM_{2.5}$ episode frequency and chemical composition between urban and rural sites, and between Wisconsin and Georgia. Total $PM_{2.5}$ mass increased more during episodes at Mayville than at Milwaukee, but peak and average episode concentrations were higher at Milwaukee. All seven episodes at Mayville were coincident with episodes at Milwaukee, but Milwaukee also had six additional local late-winter episodes. Nitrate increased more at Milwaukee, near local sources, while ammonium increased more at Mayville. Preliminary analyses indicate that local sources of NOx (e.g., nearby highways) are important at Milwaukee, and regional sources of ammonia affect both Milwaukee and Mayville. Episode enhancements in $PM_{2.5}$ at the urban site in Georgia were as strong as in Milwaukee, but were less frequent during the study period. Episodes at both Georgia sites were due primarily to increases in organic matter, without such strong enhancements in other aerosol species.

Fine particle episodes during the WNS all began under similar synoptic conditions, with the arrival of a surface low pressure system. Episodes were marked by inversions with warm, moist air and low wind speeds. Snow cover and fog caused by sublimation of snow pack were both correlated with episode intensity; fog accompanied events at Mayville more often than at Milwaukee. Regional snow cover was present over southeastern Wisconsin and northern Illinois at the onset of late winter episodes and usually melted by the end of the episode, contributing moisture to the shallow boundary layer. Accurate predictions of boundary layer height, lapse rate, and surface wind speed are important for forecasting wintertime episode intensity.

Wintertime fine particle events in the upper Midwest vary year-by-year. The frequency, severity, and spatial extent of episodic $PM_{2.5}$ particle pollution in the upper Midwest varies from one year to the next depending on meteorology. Conditions (and episodes) during the Jan-Mar 2009 WNS were found to be above normal based on data for the period 2001-2009. Areas affected by wintertime $PM_{2.5}$ episodes include eastern Iowa, southeastern Minnesota, northern Illinois, and much of Wisconsin. (Note, the study did not examine wintertime events east of Lake Michigan.)

Several nitrate production pathways were important during episodes, and the thermodynamic sensitivity of episodes indicated that the importance of changes in ammonia and nitrate was affected by sulfate levels. During Wisconsin episodes, ammonium nitrate concentrations increased from a combination of stagnant inversion conditions, a shift in partitioning toward the condensed phase, and continued chemical production of nitric acid from NO_x. Preliminary analysis of potential nitrate production pathways and nitrate and ozone diurnal patterns were consistent with nitrate from both nighttime (O_3) and daytime (OH) pathways. Decreased solar insolation and decreased ozone during episodes, together with high RH and frequent fog, suggest that aqueous and heterogeneous pathways of aerosol production are as important (or more) than photochemical pathways during episodes. Thermodynamic sensitivity analysis found episodes sensitive to either ammonia or nitrate reductions. However, sensitivity was found to be different, especially at Mayville, during episode conditions than during average conditions, with a decrease in ammonia availability. This result was consistent with a reanalysis of previous thermodynamic sensitivity studies in the Upper Midwest. The relative effect of nitrate and ammonia on $PM_{2.5}$ was sensitive to sulfate levels. Decreases in sulfate (or nitrate) associated with ongoing implementation of the Clean Air Act decreased sensitivity of $PM_{2.5}$ levels to ammonia, and increased sensitivity to nitrate. In contrast, episodes in Georgia were associated with early morning $PM_{2.5}$ peaks, with organic carbon as the most prominent species leading to the buildup.

In Phase II, atmospheric chemical transport modeling with CMAQ and CAMx will be used to confirm these findings from a process-based perspective, and to:

- Identify important emission sources during wintertime episodes and determine whether they are local or a result of regional transport;
- Quantify the contributions of thermodynamic processes impacting $PM_{2.5}$ levels and their rural-urban gradients
- Determine the degree to which photochemical models can accurately predict $PM_{2.5}$ concentrations during observed wintertime episodes; and
- Understand how specific daytime and nighttime photochemical pathways contribute to nitrate formation

1.0 BACKGROUND

1.1 Introduction

The 2006 United States $PM_{2.5}$ standard under the Clean Air Act has two separate limits for $PM_{2.5}$. A short term limit is applied to peak 24-hour concentrations [35 micrograms per cubic meter of air ($\mu g\ m^{-3}$)].[i] There is also a limit on the annual average concentration (15 $\mu g\ m^{-3}$). The change in the 24-hour standard from 65 to 35 $\mu g\ m^{-3}$ has made attainment of ambient air quality standards much more difficult in locations that experience short-term episodes of moderately high PM levels (e.g., between 35 and 65 $\mu g\ m^{-3}$).

Figures 1-1 and 1-2 map a PM episode indicator. Two indicators of this type are used throughout this report and are explained in the endnote of this section.[ii] While Figure 1-1 shows the annual average behavior of the indicator, the seasonal behavior is shown in Figure 1-2. The four panels of Figure 1-2 sum to the values in Figure 1-1. For the states of Wisconsin, Minnesota, Iowa, and Northern Illinois, wintertime is the most active episode season.

A number of studies demonstrate that meteorology and high $PM_{2.5}$ episodes in the Midwestern U.S. are tightly linked. For example, the 2004 NARSTO PM Assessment (Chapter 10, Conceptual Models for PM for North American Regions) stated that the highest $PM_{2.5}$ values usually occur in the upper Midwest during summer and winter months, rather than the spring and fall. Furthermore, the episodes occur under stagnant high-pressure systems when there is shallow turbulent mixing (Chu 2004). At the time of the NARSTO assessment, nitrate and ammonia data were not available to show the extent of the short term winter episodes, so nitrate events were mentioned only in passing, and nitrate is listed as 11% of the annually averaged regional composition (McMurry, Shepherd et al. 2004, p. 363).

Recently published analysis by Pitchford et al. (2009) on high PM concentrations in the Midwest, used IMPROVE and STN data to estimate regional distributions of PM nitrate. They found a peak in Iowa (using 2005-2006 IMPROVE data) and a peak around the shore of southern Lake Michigan (using combined IMPROVE and CSN data for 2005-2006). Klatzman et al. (2009) also show that wintertime episodes tied to meteorological stagnation are important to NAAQS compliance in the Midwest, especially north of the southern boundary of the Great Lakes. The Jan 31-Feb 5, 2005 episode is analyzed by Katzman et al. and is shown to be dominated by nitrate.

High $PM_{2.5}$ episodes in urban cities generally occur during the winter. In the winter, high values occur during the warm front transition accompanying a surface low pressure system (Anderson, Martello et al. 2004). Chu (2004) suggested that in urban areas, meteorology and aerosol thermodynamics are as important, if not more important, as the photochemistry in determining high $PM_{2.5}$ concentrations.

Chu (2004) furthermore showed that nitrate events were concentrated in the Nov-Feb period. Chu (2004) identified nitrate events in five episodes during the Jan/Feb 2002 period. Detailed analysis is done by Chu on the Feb 6-8 2002 episode. Within the Midwest and Great Lakes, peak $PM_{2.5}$ occurred in Chicago with 34 $\mu g\ m^{-3}$, and concentrations in Iowa ranged from 18-26 $\mu g\ m^{-3}$. Approximately 40% of the filter mass in Iowa was nitrate, and peak nitrate was in Chicago. Chu (2004) further found that ammonia levels were almost sufficient for full neutralization of nitric acid in the Midwest, and acidic conditions occurred only southeast of the Ohio River.

Blanchard and Tanenbaum (2008) in collaboration with LADCO (Lake Michigan Air Directors Consortium) published a comprehensive study of PM sensitivity to total ammonia and total nitrate using extensive filter data taken as part of the 2003-2006 Midwest Ammonia Monitoring Project. Sites analyzed include Lake Sugema, IA, Bondville, IL, and Mayville, WI. A comparison between the 2008 PM sensitivity report and this work can be found in section 6, thermodynamic sensitivity. Other LADCO reports also address wintertime air quality in the upper Midwest. These include The Effects of Changes in Sulfate, Ammonia, and Nitric Acid on Fine PM Composition at Monitoring Sites in Illinois, Indiana, Michigan, Missouri, Ohio, and Wisconsin (Blanchard and Tanenbaum 2004), $PM_{2.5}$ in the Upper Midwest (LADCO 2003); $PM_{2.5}$ in the Urban Areas in the Upper Midwest (LADCO 2004), and the $PM_{2.5}$ Conceptual Model document (LADCO 2009). Stanier et al. (Stanier, Carmichael et al. 2009) also published a report on air quality in Iowa, which touches on many of the issues relevant for the LADCO winter nitrate study.

The LADCO Winter Nitrate Study is a measurement campaign designed to understand wintertime episodes of elevated fine particulate ($PM_{2.5}$) concentrations in the upper Midwest. These episodes are often regional and are characterized by low wind speeds, near-freezing temperatures, and elevated levels of ammonium nitrate.

From December 2008 to March 2009, an intensive monitoring campaign was conducted

by ARA Inc., the Wisconsin DNR, the Illinois State Water Survey, and LADCO. Continuous measurements of ammonia, ammonium, nitrate, nitric acid, ozone, NOx, NOy, and meteorology were conducted at an urban site (Milwaukee, Wisconsin), and an upwind rural site (Mayville, Wisconsin). Integrated samples of many species were also collected. Analysis of the study data was conducted by researchers from the University of Iowa and the University of Illinois. The analysis also included data from similar instruments at an urban-rural pair in the South Eastern Aerosol Research and Characterization (SEARCH) network around Atlanta, Georgia. Hourly inorganic species from both the SEARCH network and the Winter Nitrate Study are taken by the iCAMS (Inorganic Continuous Aerosol Measurement System), which is described in section 3 and in Appendix 2.

During the monitoring campaign, 13 episodes were recorded (defined by 7-hour average $PM_{2.5}$ exceeding 27 μg m^{-3}), with seven affecting both sites, and six affecting Milwaukee only. The most severe episode occurred January 21- 23, with average levels of 50 and 38 μg m^{-3} at the urban and rural sites, respectively.

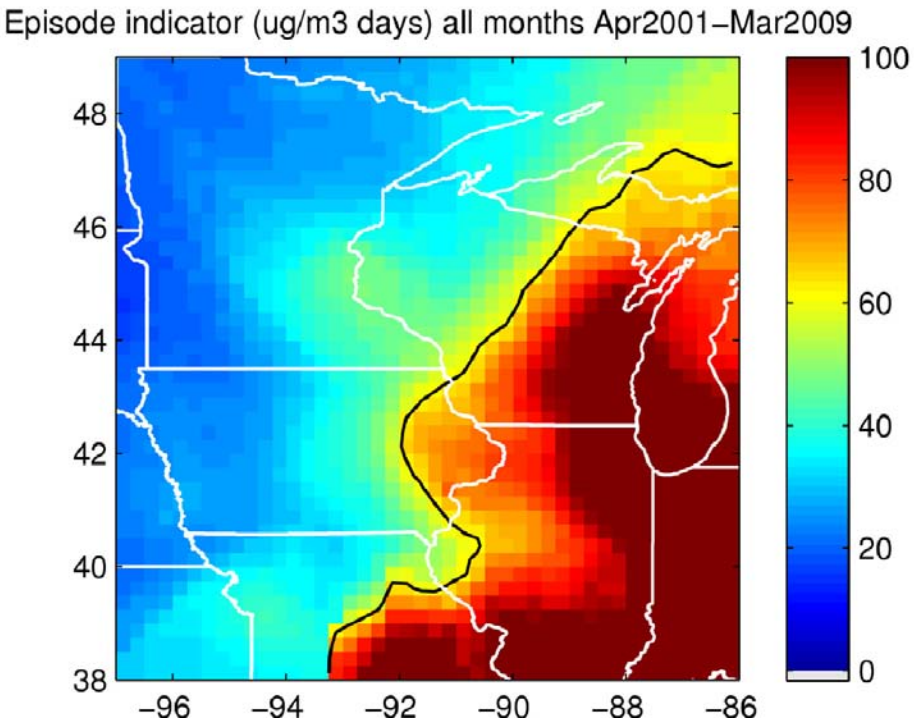

Figure 1-1. Eight year average of PM episode activity as quantified by a PM episode indicator (see note ii). Black line separates areas with an indicator > 62 from areas with an indicator < 62.

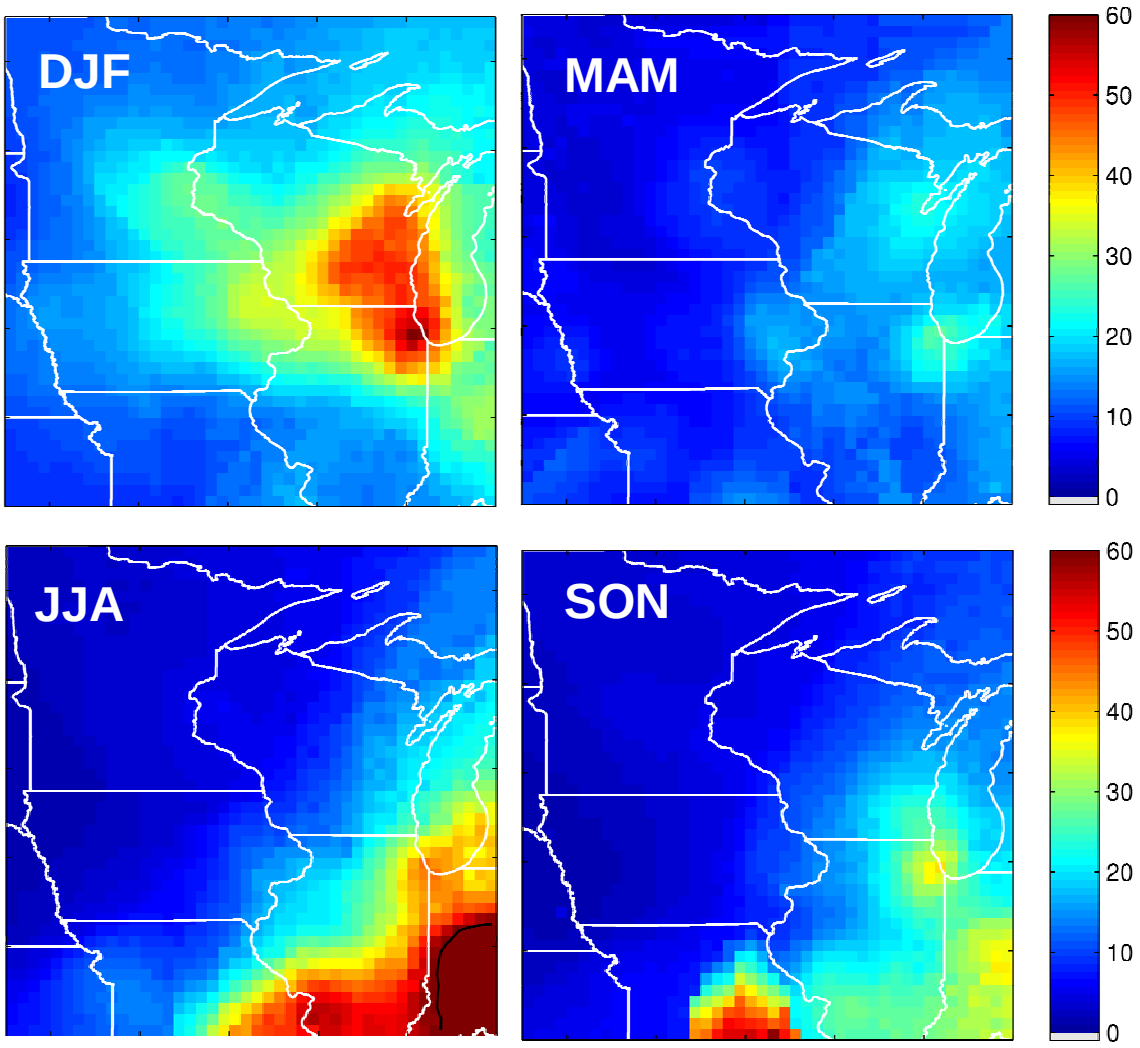

Figure 1-2. Eight year average of PM episode activity divided by season. Quantified by an episode indicator (see note ii).

1.2 Project Objectives

In response to the LADCO RFP for analysis of the Winter Nitrate Study, the following objectives were proposed. Those that are addressed in this phase I report are listed first. Those that will be addressed in a phase II report are listed second.

Phase I Objectives

Composition During Episodes:

- Divide measurement period into segments according to PM levels and meteorology;
- Assess the role of ammonia in forming particulate nitrate using a thermodynamic box model;
- Determine sensitivity of PM levels to reductions in nitric acid and ammonia using a thermodynamic box model(s);
- Assess hygroscopic state of aerosol using a thermodynamic box model;
- Assess data quality and uncertainty using continuous-filter comparison, charge balance, mass balance, and thermodynamic disequilibrium;
- Compare to previous thermodynamic box model analyses of the Midwest; and
- Compare severity and chemistry of episodes during the study to historical average episodes, and assess spatial extent of episodes sampled during the intensive.

Rural-Urban Gradients:

- Examine urban excess in particulate nitrate; and
- Analyze HYSPLIT back trajectories

Local Primary Sources:

- Perform wind sector analysis / conditional probability analysis / bivariate analysis.

Episode Meteorology:

- Identify meteorological unusual periods (fresh snow, snow melt, high actinic flux due to sun on snow, and fog);
- Conduct a CART multivariate analysis of meteorological variables

Nitrate Formation Chemistry:

- Examine diurnal pattern of nitrate and assess relative importance of daytime (OH) and nighttime (O_3 / N_2O_5) channels;
- Review state-of-science of PM nitrate formation; and
- Compare SEARCH (Atlanta) urban-rural pair data and Wisconsin data.

Phase II Objectives

3D Modeling

- Conduct 12-km CMAQ model runs for the measurement period on a Midwestern domain. This will support several of the analyses listed below
- PMCAMx modeling of the domain during the study period

Rural-Urban Gradients

- Model runs with various geographic areas perturbed for NO_x emissions to establish areas where emissions reduction lead to nitric acid reductions

Nitrate Formation Chemistry

- Determine sensitivity of PM nitrate levels to other factors (such as nitrate formation kinetics) using box modeling

Three Dimensional Model Implementation

- Conduct hybrid box model analysis replacing measured variables with modeled (one at a time) to determine areas where model inaccuracies contribute most to model-measurement error for ammonium nitrate
- Compare total measured ammonia concentrations versus total 3D modeled ammonia as a test of average ammonia emission levels and spatial-temporal patterns (II)
- Assess adequacy of PM nitrate chemistry used in photochemical models and recommend improvements
- Quantify model-measurement agreement during episodes (II), with comparison of CMAQ and PMCAMx

1.3 Glossary of Terms

Adjusted gas ratio: an alternate measure of ammonia availability defined in section 6.2. Abbreviation adjGR; Units: dimensionless.

ARA: LADCO subcontractor that developed and deployed the iCAMS in the winter nitrate study.

Gas ratio: a measure of ammonia availability discussed briefly in section 4.5, and defined and discussed in section 6.2. Abbreviation: GR; Units: dimensionless.

iCAMS: Abbreviation for Inorganic Continuous Measurement System, which provided the time resolved sulfate, nitrate, ammonium, ammonia, nitric acid, and NOy measurements.

FDMS TEOM: See TEOM.

NOy: NOx plus all reactive oxidation products of NOx. Find a table of information on all nitrogen species in Appendix 13. Units: typically in mixing ratio as ppb.

Relative sensitivity: the sensitivity of PM concentrations to a reduction in total nitrate divided by the sensitivity of PM concentrations to a reduction in total ammonia. Comes in two versions – fractional, and mass based, depending on whether the reduction is as an absolute mass or as a fraction of the total. See section 6.2 for detailed definition and discussion.

TEOM: Tapered Element Oscillating Microbalance, provides nearly continuous measurement of $PM_{2.5}$ mass. FDMS TEOM was used by Wisconsin DNR (Filter Dynamics Measurement System); FDMS TEOM has much better performance with semivolatile aerosols such as nitrate than the traditional TEOM.

Total ammonia: $NH_3(g) + NH_4$(particulate). In this work, $NH_4(p)$ is $PM_{2.5}$ ammonium. Typically

expressed as equivalent mass of $NH_4(p)$ and a conversion from ppb $NH_3(g)$ to mass concentration is done at atmospheric pressure and 273 K. See endnote i of section 3 for more information. Abbreviation: TNH3 or TA. Units: typically µg m^{-3} but can be expressed on molar basis or as ppb of equivalent $NH_3(g)$.

Total nitrate: $HNO_3(g) + NO_3$(particulate). In this work, $NO_3(p)$ is $PM_{2.5}$ nitrate. Typically expressed as equivalent mass of $NO_3(p)$ and a conversion from ppb $NH_3(g)$ to mass concentration is done at atmospheric pressure and 273 K. See endnote i of section 3 for more information. Abbreviation: TNO3 or TN. Units: typically µg m^{-3} but can be expressed on molar basis or as ppb of equivalent $HNO_3(g)$.

Total sulfate: $H_2SO_4(g) + HSO_4^-(p) + SO_4^{2-}(p)$. In this work, particulate species are limited to $PM_{2.5}$ size cut only. Typically expressed as equivalent mass of $SO_4^{2-}(p)$. As only measurements of $SO_4^{2-}(p)$ are availableand under relatively high gas ratios encountered $H_2SO_4(g)$ and $HSO_4^-(p)$ are negligible, total sulfate is well approximated as $SO_4^{2-}(p)$. Abbreviation: TSO4 or TS. Units: typically µg m^{-3} but can be expressed on molar basis.

WNS: Winter Nitrate Study, intensive field campaign from Dec 1, 2008 to Mar 31, 2009.

REFERENCES

Anderson, R. R., D. V. Martello, et al. (2004). "The regional nature of PM2.5 episodes in the upper Ohio River Valley." Journal of the Air & Waste Management Association **54**(8): 971-984.

Blanchard, C. L. and S. Tanenbaum (2004). The Effects of Changes in Sulfate, Ammonia, and Nitric Acid on Fine PM Composition at Monitoring Sites in Illinois, Indiana, Michigan, Missouri, Ohi, and Wisconsin, 2000-2002, Lake Michigan Air Directors Consortium.

Blanchard, C. L. and S. Tanenbaum (2008). Analysis of Inorganic Particulate Matter Formation in the Midwestern United States, Final Report. Prepared for Lake Michigan Air Directors Consortium. Albany, CA.

Chu, S. H. (2004). "PM2.5 episodes as observed in the speciation trends network." Atmospheric Environment **38**(31): 5237-5246.

Klatzman, T. L., A. P. Rutter, et al. (2009). "PM2.5 and PM10-2.5 Compositions during Wintertime Episodes of Elevated PM Concentration across the Midwestern USA." Aerosol and Air Quality Research **10**: 140-153.

LADCO (2003). PM2.5 in the Upper Midwest.

LADCO (2004). PM2.5 in Urban Areas in the Upper Midwest.

LADCO (2009). "Conceptual Model of PM2.5 Episodes in the Midwest."

McMurry, P., M. Shepherd, et al., Eds. (2004). NARSTO (2004) Particulate Matter Science for Policy Makers: A NARSTO Assessment. . Cambridge, England, Cambridge University Press.

Stanier, C., G. R. Carmichael, et al. (2009). Understanding Episodes of High Airborne Particulate Matter in Iowa, Center for Global and Regional Environmental Research. **http://www.engineering.uiowa.edu/~cs_proj/iowa_pm_project/iowa_pm.htm**.

NOTES

[i] Attainment or nonattainment of the Clean Air Act standards is determined by averaging the 98th percentile concentrations over a three year running average. For monitors with a full complement of 365 daily samples, the 98th percentile rule means that the 8th highest value in a given year determines attainment.

[ii] Two indicators are used in this work. One indicator uses max($PM2.5_i$-27.0) and the other uses max($PM2.5_i$-35.0). This metric can be used to quantify episode activity, by summing this metric over a period of time, and assigning units of µg m^{-3} days. Or it can be used to divide the measurement period into "episode" and "non episode" periods. For purposes of episode identification, some smoothing of the hourly values is required to avoid identifying short (several hour) periods of time as episodes. The smoothing procedure is described in Appendix 1.

The use of a threshold below 35, such as 27 is useful for highlighting areas or time periods where air quality is approaching the current short term standard. The threshold being below 35 is also appropriate since the standard may be lowered in the future. If the episode activity metric is based on 27 µg m^{-}3, an approximate value of this threshold necessary (but not sufficient) to cause compliance problems with the NAAQS is 0.02 x 365 x (35.5 – 27) or 62. The 0.02 is from the requirement that the 98th percentile day be above the $PM_{2.5}$ standard.

2.0 STUDY OVERVIEW

In the Great Lake Regions, fine PM ($PM_{2.5}$) has episodically high concentrations in winter. To investigate winter high PM episodes, high time resolution speciated $PM_{2.5}$ measurements were acquired, including gas phase ammonia and nitric acid, during a special study (the LADCO Winter Nitrate Study) using the iCAMS (Inorganic Continuous Aerosol Measurement System) instruments suite deployed by ARA. STN measurement sites at the Milwaukee-DNR SERHQ (AQS ID: 55-079-0026) and Mayville (AQS ID: 55-027-0007) (Figure 2.1) were supplemented with additional instruments for inorganic speciation from December 2008 – March 2009. Although some of the instruments deployed have data available starting in December 2008, data capture from the iCAMS instruments in December was inconsistent. Therefore, data analysis was conducted on the 3 month period (1/01/2009 to 3/31/2009). Analysis focused on Milwaukee as an urban site subject to higher levels of primary pollutants, and Mayville as a rural site to characterize the regional background.

The iCAMS system is part of routine measurements in the SEARCH network (Hansen et al., 2003) in the Southeastern U.S.. Therefore, to provide contrast to another rural-urban pair expected to have warmer temperatures and less nitrate pollution, selected measurements from the Atlanta (Jefferson St.) and Yorkville locations of the SEARCH network are included in the analysis.

The iCAMS (Edgerton et al., 2006) system utilized three instruments (described in more detail in Appendix 2). The first instrument measures NOy and NOy* (NOy* is NOy denuded to remove HNO_3). HNO_3 is then calculated as NOy-NOy*. The second instrument measures total nitrogen in one channel, and particular total nitrogen in the other channel (NH_3 has been denuded). NH_3(g) is calculated by difference. The third instrument measures inorganic ions (SO_4, NO_3, and NH_4) by conversion to SO_2 (for sulfate) and NOx (for NO_3 and NH_4).

2.1 Site descriptions

The Milwaukee site (DNR-SERHQ monitor) is located in a mixed-use urban area (commercial, retail, residential) just north of the city's downtown area and is exposed to considerable air pollution emanating from nearby highways (vehicular traffic) and industrial sources. The Mayville site, 65 km (40.5 mi) northwest of the Milwaukee site (Figure 2-1), is situated in an open, rural area that is largely surrounded by agricultural fields and has noticeably

less exposure to high primary pollutant levels than the Milwaukee site. The bearing from the Milwaukee site to the Mayville site is 310 degrees. Location of Jefferson Street in Atlanta, GA (Urban site) and Yorkville (Rural site) from SEARCH network can be found in Figure 2-2. (Hansen et al., 2003). Appendix 6 contains additional site photographs and maps for the Mayville and Milwaukee sites.

2.2 List of measurements

Four target chemical species (NO_3, SO_4, NH_4, and OC) in particulate matter were measured in both WNS sites. Gaseous chemical compounds (NH_3, HNO_3 and SO_2) were measured by 24 hr denuder for intercomparison with higher time resolution data. Unspeciated hourly $PM_{2.5}$ mass (TEOM, hourly) and speciated FRM were measured. Speciated filter measurements during this period were collected using the Speciation Aerosol Sampling System (SASS) instrument on a 1 in 3 day schedule. The SASS monitor collects integrated $PM_{2.5}$ mass samples for each 24 hour measurement period on a quartz filter. The $PM_{2.5}$ speciation filters are collected and sent to RTI Labs (US EPA contractor) for analysis by EPA-approved laboratory methods. RTI's laboratory analysis of each filter's mass yields 24 hr $PM_{2.5}$ concentrations for more than 50 separate compounds, including several ions (e.g., NO_3, SO_4, NH_4) and OC and EC. NO and NO_2 were measured at Milwaukee and SO_2 was measured at Mayville. Measured chemical species and method are summarized in Table 2-1. Table 2-2 summarized measured data used in this work from the SEARCH network (Hansen et al., 2003).

Table 2-1 Species measured at Milwaukee and Mayville site

Measurement	Time average	Units	Source	Method
$PM_{2.5}$	1hr	µg m^{-3}	WDNR	FDMS EPA Param 88500
SO_4	1hr	µg m^{-3}	ARA	See text
NO_3	1hr	µg m^{-3}	ARA	See text
NH_4	1hr	µg m^{-3}	ARA	See text
HNO_3	1hr	ppbv	ARA	See text
NH_3	1hr	ppbv	ARA	See text
NO_x[1]	1hr	ppbv	WDNR	EPA Param 42603
SO_2[2]	1hr	ppb	WDNR	EPA Param 42401
TEMP	1hr	Deg F	WDNR	
Wind Speed	1hr	mph	WDNR	
Wind direction	1hr	Comp Deg	WDNR	
NH_3	24hr	ppbv	ISWS	Denuder
HNO_3	24hr	ppbv	ISWS	Denuder
SO_2	24hr	ppbv	ISWS	Denuder
$PM_{2.5}$	24hr 1 in 3days	µg m^{-3}	WDNR	FRM EPA Param 88101
NH_4	24hr 1 in 3days	µg m^{-3}	WDNR	FRM EPA Param 88101
NO_3	24hr 1 in 3days	µg m^{-3}	WDNR	FRM EPA Param 88301
SO_4	24hr 1 in 3days	µg m^{-3}	WDNR	FRM EPA Param 88401
OC	24hr 1 in 3days	µg m^{-3}	WDNR	FRM EPA Param 88305
NOy	1hr	ppb	ARA	See text
O3	1hr	ppb	WDNR	
Relative Humidity[3]	1hr	%	NWS	
Surface pressure[3]	1hr	mbar	NWS	
Visibility[3]	1hr	km	NWS	
Precipitation[3]	1hr	mm	NWS	

[1.] hourly NOx is only available at Milwaukee
[2.] hourly SO_2 is only available at Mayville
[3.] Data were measured at the General Mitchell (MKE airport)

Table 2-2 Species data from SEARCH network[1.,2.]

Measurement	Time average	Units
$PM_{2.5}$	1hr	µg m^{-3}
SO_4	1hr	µg m^{-3}
NO_3	1hr	µg m^{-3}
NH_4	1hr	µg m^{-3}
HNO_3	1hr	ppb
NH_3	1hr	ppb
O_3	1hr	ppb
CO	1hr	ppb
SO_2	1hr	ppb
$NO/NO_2/NOx$	1hr	ppb
NO_y	1hr	ppb
BC	1hr	µg m^{-3}
TC	1hr	µg m^{-3}
OC	1hr	µg m^{-3}
Wind Speed	1hr	ms^{-1}
Wind direction	1hr	Compass Deg
TEMP	1hr	deg C
Relative Humidity	1hr	%
Station pressure	1hr	mbar
Precipitation	1hr	mm
Solar radiation	1hr	Wm^{-2}

[1.] Data were provided by ARA

[2.] This table shows only data used for this study.
Data are available at http://www.atmospheric-research.com/public/index.html .

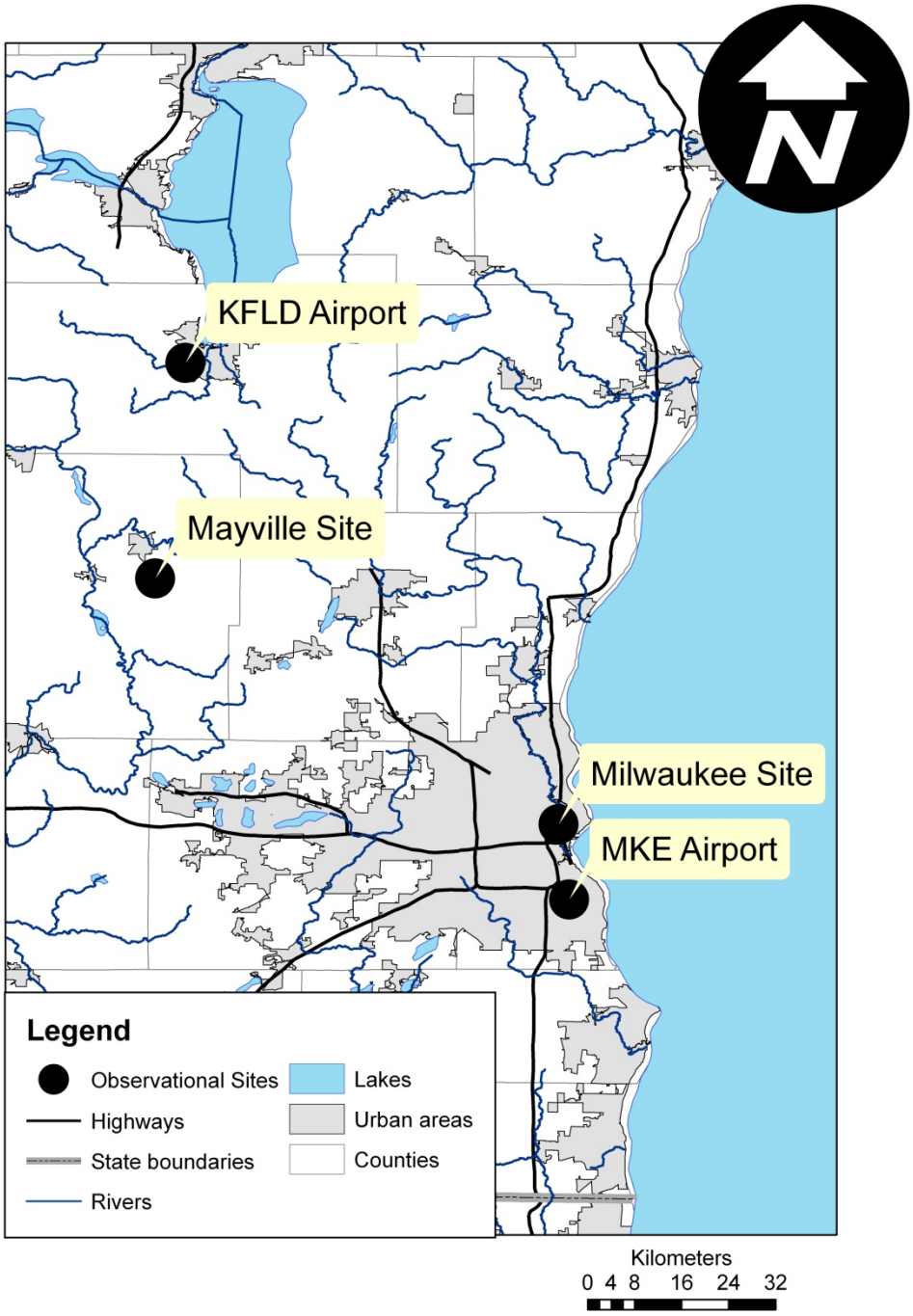

Figure 2-1 Area map showing Mayville site and Milwaukee site

Figure 2-2 Location of Yorkville and Jefferson Street at SEARCH Network

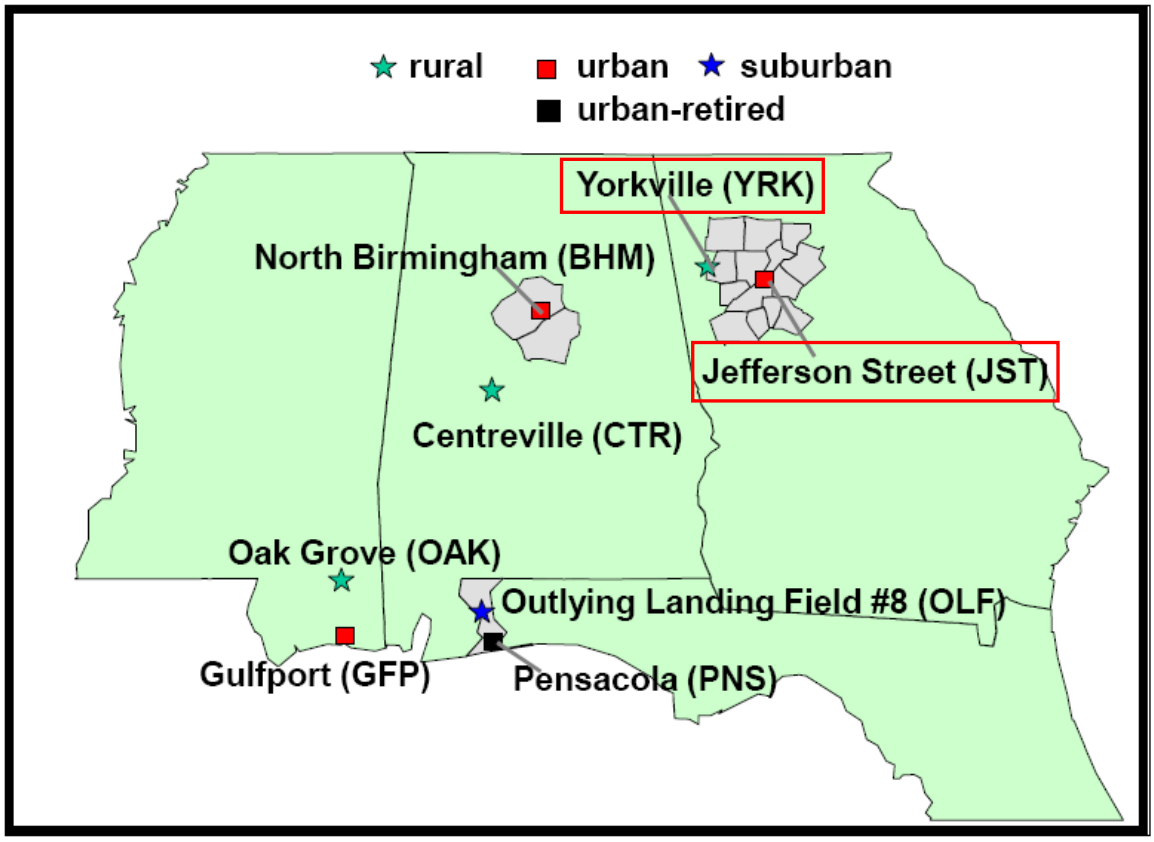

REFERENCES

Edgerton, E. S., B. E. Hartsell, et al. 2006. The Southeastern Aerosol Research and Characterization Study, part 3: Continuous measurements of fine particulate matter mass and composition. Journal Of The Air & Waste Management Association 56(9): 1325-1341.

Hansen, D. A., Edgerton, E.S., Hartsell, B. E., Jansen, J. J., Kandasmy, N., Hidy, G.M., and Blanchard, C.L. 2003, The southeastern aerosol research and characterization study: part 1-overview, *J. Air & Waste* **53**:1460-1471

3.0 WINTER NITRATE STUDY – SUMMARY OF MEASURED CONCENTRATIONS

3.1 Summary and Examples of Data Adjustments Made to the Wisconsin Semicontinuous Data

Data provided to the University of Iowa and Illinois team came from ARA (iCAMS), from ISWS, and from WDNR and had already gone through basic quality assurance checks and had missing values where data have been invalidated by the data originators. iCAMS data reflected on site calibrations; denuder data had been blank subtracted.

The data was then intercompared for this project. In order to maximize comparability with previous studies that assessed thermodynamic sensitivity using integrated filters, the hourly iCAMS data provided by ARA was adjusted to increase agreement with the integrated measurements (filters by WDNR / EPA STN and denuders by ISWS). This has also been employed in other locations (Wittig, Takahama et al. 2004). A full account of intercomparison and regression-based revision of Wisconsin data can be found in Appendix 2.

The degree of agreement between the integrated measurement and the iCAMS measurement (in terms of bias and correlation coefficient) were used to label the different iCAMS measurements with qualitative labels (very good, good, needs improvement, poor). These labels refer to the degree of agreement between the integrated and time-resolved measurements, and need to be interpreted carefully. In cases where the filter measurements are generally accepted as having low bias and high precision (such as 24 hour filter-based sulfate measurements), agreement between the iCAMS and integrated measurements is probably a good test of the iCAMS data quality. For other integrated measurements that are subject to potential measurement artifacts (e.g. aerosol nitrate) or that are performed less frequently (e.g. nitric acid and ammonia by denuder), a lack of agreement between the two techniques is more difficult to interpret.

Any 24 hour period with 19 or more hours of continuous inorganic data was averaged to form a 24-hour mean value, and these values were paired with their corresponding filter or denuder measurements for regression. The goals of the regression were twofold: (1) determine a slope and intercept for adjustment of the data (all corrections were assumed to be linear; there were insufficient comparison data points for nonlinear corrections); and (2) to determine a 95% confidence interval on the adjusted (or revised, the terms are used synonymously in the report)

iCAMS data.

The slopes, methods, intercepts and confidence intervals can be found in detail in Appendix 2. Figure 3-1 summarizes the overall comparison of the hourly and 24 hour data.

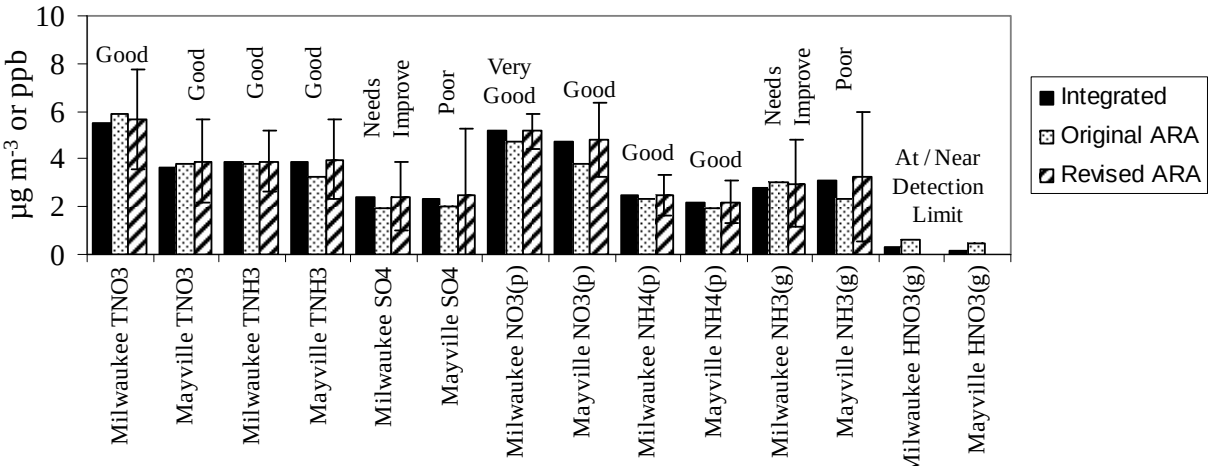

Figure 3-1. Comparison of 24 hour and hourly datasets. Y axis is the mean of the paired samples. Aerosols (labeled as (p) for particulate), total nitrate, and total ammonia as µg m^{-3}, and gases as ppb. Error bars show 95% confidence interval on an individual iCAMS hourly measurement at the mean concentration. Qualitative rating is a measure of agreement between the hourly and integrated techniques and is based on two factors: bias relative to 24 hour average measurement in the original iCAMS data, and size of confidence interval in the revised iCAMS data. See Table A2-4.

In summary, weighted least squares regression was performed with weights inversely proportional to the raw measured ARA values [e.g. $w_i=(ARA_i)^{-1}$]. For determining a confidence interval for every hourly ARA data point in the dataset, an error was assumed of the following form: the upper confidence value was $ARA_{corrected} + [f(ARA_{raw}) + \varepsilon]$ and the lower confidence value was $ARA_{corrected} - [f(ARA_{raw}) + \varepsilon]$. The values for f and ε were determined by linear regression of the prediction confidence intervals determined by the regression software (SAS).

An example of the best regression result was Milwaukee nitrate, and that is shown in Figure 3-2.

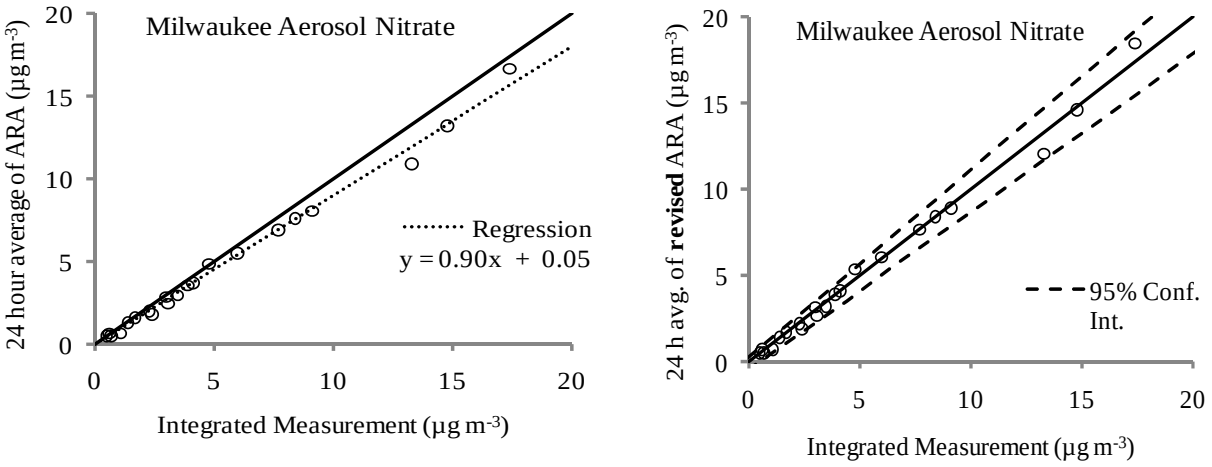

Figure 3-2. Comparison of iCAMS aerosol nitrate and filter readings at Milwaukee, with regression result and 95% confidence interval shown. Solid lines are 1:1 lines of agreement.

An example of a poor agreement between hourly and 24 hour samplers was for Mayville NH_3 (g), shown in Figure 3-3. As an independent check on the original and revised data, thermodynamic and charge balance was assessed before and after the revision. Figure 3-4 shows the result of the charge balance. The charge balance was very good prior to the revision, and improved in most cases upon adjustment.

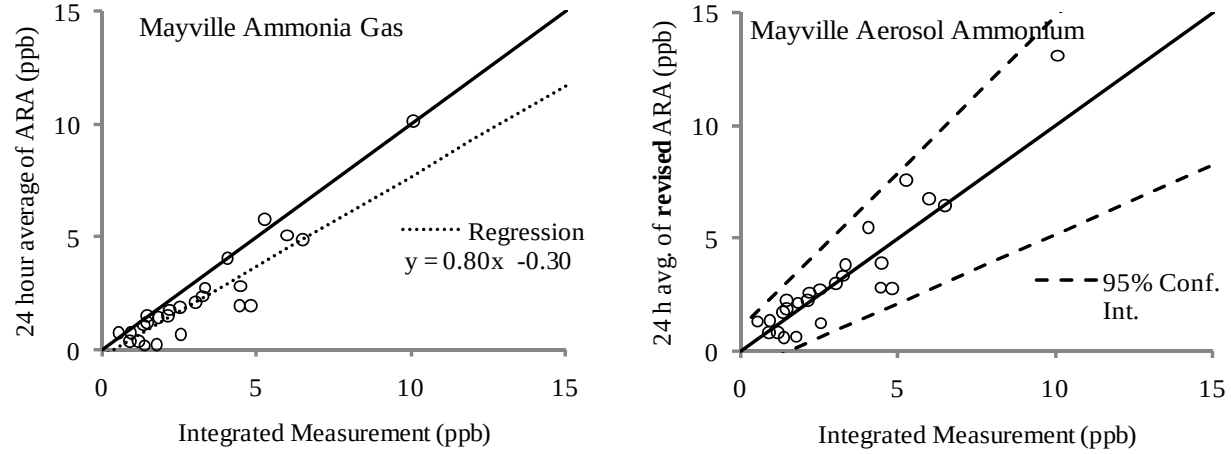

Figure 3-3. Comparison of ammonia gas between ARA and ISWS denuders at Mayville, with regression result and 95% confidence interval shown. Solid lines are 1:1 lines of agreement.

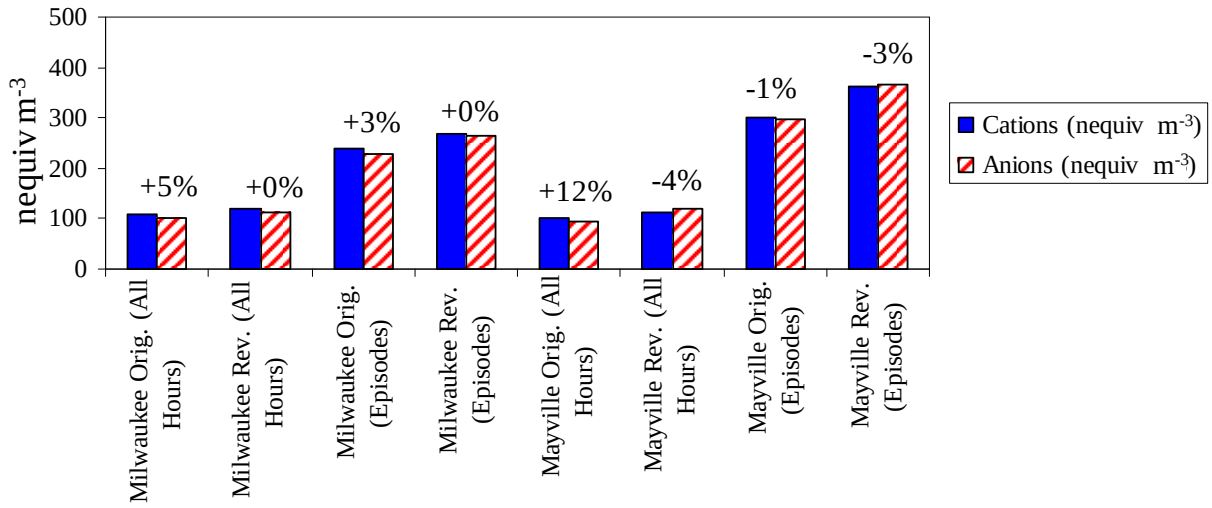

Figure 3-4. Charge balance in the original and revised ARA datasets. Bars indicate the mean values. Text values indicate the median charge balance of all hours with all valid ions. These may be different due to the different statistics of mean and median.

The experimental data was also evaluated using ISORROPIA. The measured total nitrate, total ammonia, and sulfate (both before data revision and after revision) were partitioned and compared to the measured phase partitioning (e.g. aerosol ammonium over total ammonia; aerosol nitrate / total nitrate). Total nitrate and total ammonium are defined in a note.[i] At both sites the NH_3 measured partitioning matched the modeled partitioning well in both the original and revised dataset; with confidence intervals taken into account, nearly all hours showed agreement between measured and modeled ammonia partitioning. For HNO_3, the nitrate fraction was not measured very accurately due to uncertainty in HNO_3. The majority of points have modeled nitrate / total nitrate ratios of > 0.8, but the measured dataset (original) has a large number of points with the measured partitioning in the 0.5-0.8 range. The data revision process alleviates this somewhat, but at the expense of large confidence intervals on HNO_3, on the nitrate aerosol fraction, and some negative HNO_3 values. See Figures A2-10 and A2-11. However, the large confidence intervals on the HNO_3 concentration was not directly critical to the thermodynamic sensitivity or nitrate chemical production investigations as these use total nitrate as their key input variable.

A further data quality check is examination of the sum of aerosol species mass by the iCAMS instruments versus the total mass recorded by the TEOM. Construction and

interpretation of the mass closure at the Wisconsin sites is complicated by the fact that there are no semicontinuous measurements of OC and EC. Mass closure is achieved to within 25% and hourly plots of mass closure are found in Appendix 2 for all sites using an OM/OC ratio of 1.4 (the ratio of organic mass, including all elements i.e. O and H, relative to the organic carbon mass). Taking into account uncertainties in the iCAMS revised data (e.g. the 95% confidence intervals shown in Figure 3-1) the mass balance is closed to within error at both sites. Even in locations where semicontinuous OC and EC are available (such as the SEARCH sites) the interpretation of the mass balance is somewhat difficult, as the OM/OC ratio of not well known. Although a value of 1.4 is used in this work,[ii] the main results of this study (focusing on inorganic constituents) are not sensitive to the OM/OC ratio. Future work in the Midwest should not adopt the 1.4 value used in this study, but rather rely on more recent research and independent data analysis on this topic. The results of this study are not sensitive to the value of the OM/OC ratio chosen. The value of 1.4 is the lowest in the range 1.6±0.2 proposed by Turpin and Lim (2001), but more recent studies have supported even higher values. Values of 1.8 have been used previously for the Midwestern domain (Brown, Hafner et al. 2006) for an annual average, and values of 1.77 (December) to 2.39 (July) have been determined for Atlanta (El-Zanan, Zielinska et al. 2009).

Considering the Wisconsin sites, mass closure is closer to 1:1 at Mayville using the OM/OC ratio of 1.4, while there is a slight mass deficit in the sum of species at Milwaukee. One interpretation of this is that the adjustments to aerosol species (all upward for sulfate, nitrate, and ammonium at both sites) were perhaps too large at the Mayville site. The largest uncertainties on these adjustments were for sulfate and nitrate at Mayville. Therefore, the mass balance closure is (within experimental error) consistent with equal OM/OC ratios at Milwaukee and Mayville.

3.2 Time Averaged Results

The overall results of the monitoring campaigns are summarized in Tables 3-2 through 3-5. These give the summary statistics of each measured variable at the two Wisconsin sites, and at the two SEARCH sites. Key variables to note from these tables are that the mean levels of pollutants or meteorological variables are ordered as follows:

- $PM_{2.5}$ Mil. (17.1) > Atlanta (12.1) > Mayville (11.7) > Yorkville (11.0)
- Total nitrate Mil. (5.6) > Mayville (4.8) > Atlanta (2.1) > Yorkville (1.8)

- Total ammonia Mayville (3.3) ~ Mil.(3.3) > Yorkville (3.1) > Atlanta (2.3)
- Gas ammonia Mayville (2.4) > Mil. (2.3) > Yorkville (2.1) > Atlanta (1.1)
- Nitrate / TNO_3 Mil. (78%) > Mayville (69%) > Atlanta (65%) > Yorkville (58%)
- NO_y Atlanta (36) > Milwaukee (27) > Mayville (6.3) > Yorkville (4.8)
- Temperature Atlanta (9) > Yorkville (8) > Mil. (-3) > Mayville (-5)
- Ozone Yorkville (32) > Mayville (31) > Mil. (22) ~ Atlanta (22)
- OC Atlanta (4.1) > Mil. (3.6) > Mayville (3.2) > Yorkville (2.2)
- EC Atlanta (0.75) > Mil. (0.52) > Mayville (0.3) ~ Yorkville (0.3)

In other words, total nitrate and nitrate partitioning to the aerosol were higher in Wisconsin than in Georgia. Total ammonia was also higher, but not by the same margin. NOy (and NOx, not shown) are urban pollutant, and are 4-5x higher at the urban sites. NOy, OC, and EC are all ordered in the same way, suggesting these are co-emitted pollutants of urban origin in both areas. Ozone is higher away from center city NOx emission hotspots; furthermore, mean ozone levels are not higher at the southern sites.

Table 3-2 has a footnote describing OC and EC values with and without the inclusion of the Milwaukee filter of January 22, 2009. The reading on this day in Milwaukee was an OC concentration of 45.1 µg m^{-3}, and FRM filter reading of 49.7 µg m^{-3}, with EC plus filter based inorganics totaling to 35.3 µg m^{-3}. In other words, the sum of species does not add up to the FRM. Therefore, this OC reading is suspect, either from a positive artifact, or from capturing a local source.[iii] Our recommendation is that analyses involving OC and EC should be done excluding the OC and EC values from January 22.

Table 3-2:Summary Statistics for Milwaukee Site During WNS (All Hours). Table Contains Revised Data Only

Variable	Units	Mean	Std. Dev	n	Min	10th	25th	Median	75th	90	Max
PM2.5	µg m^{-3}	17.1	11.4	2142	-2.9	5.5	8.7	14.4	22.7	32.7	72.7
NOx	ppb	22.7	23.3	2033	5.0	5.0	10.0	17.0	29.0	43.0	304.0
Temp	C	-2.7	7.5	2160	-23.6	-12.1	-8.3	-2.5	2.5	6.3	24.2
Wind Speed	m/s	3.0	1.3	2160	0.3	1.3	2.0	3.0	3.8	4.7	8.0
Wind Direction	Degrees	NA	NA	2160	0			see wind rose			360
NOy	ppb	26.5	24.3	1849	2.1	7.8	12.8	19.9	32.9	48.1	342.4
O3	ppb	22.2	10.7	2135	2.0	7	14	23	31	35	53
NO	ppb	6.6	15.8	2105	-1.0	0.0	1.0	2.0	7.0	13.0	254.0
NO2	ppb	16.3	10.1	2105	2.0	5.0	9.0	14.0	23.0	31.0	57.0
SO4	µg m^{-3}	2.03	1.57	1668	-0.50	0.49	0.97	1.72	2.80	3.81	14.53
NO3	µg m^{-3}	4.35	4.37	1742	-0.20	0.49	1.17	3.03	6.18	10.09	35.48
NH4	µg m^{-3}	2.13	1.73	1793	0.01	0.39	0.85	1.75	2.96	4.14	11.35
NH3	ppb	2.27	1.84	1683	0.29	0.61	0.97	1.71	3.00	4.74	18.48
TNO3	µg m^{-3}	5.57	5.20	1604	-0.80	0.78	1.72	3.96	7.90	13.07	42.17
TNH3	µg m^{-3}	3.28	2.61	1575	-0.51	0.49	1.31	2.82	4.70	6.64	18.62
HNO3	ppb	0.49	1.02	1604	-0.60	-0.14	0.02	0.24	0.60	1.28	14.13
Dry Bulb Temp	C	-2.90	7.48	2159	-24.25	-12.01	-8.30	-2.83	2.20	6.00	23.30
Wet Bulb Temp	C	-4.75	6.79	2159	-24.65	-13.21	-9.80	-4.54	0.42	3.55	14.20
RH (Mitchell Airport)	0-100	64.4	13.6	2159	22.0	47.0	55.1	64.6	73.7	83.0	98.5
Pressure	mbar	991.9	9.6	2159	964.3	979.2	985.3	992.1	999.8	1004.7	1013.8
Rainfall	mm/hr	0.08	0.43	2160	0.0	0.00	0.00	0.00	0.00	0.00	6.86
PM2.5, 24 hr	µg m^{-3}	18.3	11.0	29	4.2	4.9	10.3	17.2	21.1	39.0	49.7
NO3, 24 hr	µg m^{-3}	4.9	4.4	28	0.5	0.7	2.2	3.4	6.4	13.3	17.4
SO4, 24 hr	µg m^{-3}	2.2	1.2	28	0.8	1.0	1.4	2.0	2.8	4.0	5.9
NH4, 24 hr	µg m^{-3}	2.3	1.8	28	0.4	0.4	1.0	2.0	3.0	5.0	8.0
EC[a]	µg m^{-3}	0.52	0.69	28	0.12	0.1	0.3	0.4	0.5	0.8	4.0
OC[a]	µg m^{-3}	5.1	7.9	28	1.2	1.9	2.3	3.1	5.1	6.8	45.1
EC/OC[a]	Unitless	0.11	0.04	28	0.04	0.05	0.08	0.11	0.14	0.16	0.20
EC[b]	µg m^{-3}	0.39	0.20	27	0.12	0.1	0.3	0.4	0.5	0.7	0.83
OC[b]	µg m^{-3}	3.6	1.8	27	1.2	1.9	2.2	3.1	5.1	6.3	7.8
EC/OC[b]	Unitless	0.11	0.04	27	0.04	0.05	0.07	0.12	0.14	0.16	0.20
NH3	ppb	1.9	1.0	27	0.7	0.9	1.2	1.6	2.4	3.1	5.3
HNO3	ppb	0.3	0.2	27	0.09	0.1	0.15	0.21	0.35	0.5	0.83
SO2	ppb	0.7	1.1	28	0.09	0.12	0.17	0.33	0.92	1.66	5.02

[a] includes Jan 22 OC and EC values – see text and endnotes for explanation of this

[b] does not include Jan 22 OC and EC values. While the OC and EC statistics change significantly, the EC/OC ratio on Jan 22 (0.09) is similar to the mean (0.11) and median (0.11) ratios, so the overall mean, median, and distribution stay almost unchanged.

Table 3-3. Summary Statistics for Mayville Site During WNS (All Hours). Table Contains Revised Data Only

Variable	Units	Mean	Std. Dev	n	Min	10th	25th	Median	75th	90	Max
PM2.5	µg m^{-3}	11.7	8.8	2148	-2.7	2.9	5.2	9.6	16.4	23.6	63.1
PM2.5b	µg m^{-3}	11.5	9.4	1979	-6.3	2	4.9	9.31	16.1	24.7	62.8
SO2	ppb	1.5	1.2	2019	0.1	0.4	0.8	1.3	2.0	3.0	13.8
Temp	Deg C	-5.3	8.4	2160	-28.3	-15.5	-11.7	-5.4	1	5.6	21.4
Wind Speed	m/s	3.9	6.1	2160	-49.6	2.0	3.1	4.3	5.9	7.3	11.3
Wind Direction	Degrees	NA	NA	2160	0			see wind rose			360
RH	0-100	72.2	14.4	2160	30.0	53.0	62.0	72.0	83.0	93.0	96.0
Dew Point	Deg C	-9.7	8.5	2160	-32.2	-21.0	-16.2	-9.3	-3.2	1.2	9.2
NOy	ppb	6.3	4.6	2075	1.1	2.4	3.3	5.3	7.9	11.5	57.2
O3	ppb	30.8	7.6	2038	0	21.0	26.0	31.0	36.0	39.0	58.0
SO4	µg m^{-3}	2.20	1.7	1809	-0.5	0.4	1.0	1.9	3.1	4.3	10.1
NO3	µg m^{-3}	3.3	3.6	1816	-0.2	0.2	0.6	2.0	4.6	7.9	27.3
NH4	µg m^{-3}	2.1	1.8	1800	0.0	0.4	0.7	1.5	2.9	4.3	12.6
NH3	ppb	2.4	2.2	1990	0.3	0.6	0.8	1.7	3.0	5.2	16.2
TNO3	µg m^{-3}	4.8	3.6	1679	-0.2	1.1	2.1	3.6	7.2	9.9	22.1
TNH3	µg m^{-3}	3.3	2.2	1673	0.5	1.1	1.6	2.6	4.5	6.4	12.1
HNO3	ppb	0.2	0.5	1679	-0.9	-0.2	-0.1	0.1	0.4	0.8	4.9
Dry Bulb Temp	Deg C	-5.0	8.3	2157	-28.6	-15.4	-11.3	-5.2	1.31	5.17	20.9
Wet Bulb Temp	Deg C	-6.5	7.6	2157	-28.8	-16.1	-12.3	-6.5	-0.5	3.1	14.1
RH	0-100	69.2	12.3	2157	27.3	52.4	60.6	69.0	78.2	85.9	95.9
Pressure	mbar	987.6	9.6	2157	960.2	974.5	981.0	987.9	995.0	1000.7	1010.0
PM2.5, 24 hr	µg m^{-3}	15.8	8.9	30	4.2	6.9	9.9	14.4	17.5	32.2	38
NO3, 24 hr	µg m^{-3}	4.9	4.1	27	0.6	1.3	1.8	3.5	6.5	11.9	14.4
SO4, 24 hr	µg m^{-3}	2.25	0.9	27	0.9	1.2	1.6	2.0	2.8	3.3	4.8
NH4, 24 hr	µg m^{-3}	2.2	1.6	27	0.1	0.6	1.2	1.7	3.1	4.6	6.3
EC, 24 hr	µg m^{-3}	0.3	0.2	28	0.1	0.1	0.1	0.3	0.4	0.5	0.6
OC, 24 hr	µg m^{-3}	3.2	2.1	28	1.1	1.2	1.9	2.9	4	5.4	11.8
NH3, 24 hr	ppbv	2.2	1.7	27	0	0.7	1.0	1.7	3.3	4.5	7.6
EC/OC	Unitless	0.09	0.03	27	0.01	0.04	0.07	0.09	0.12	0.13	0.14
HNO3, 24 hr	ppbv	0.2	0.1	27	0	0.06	0.08	0.2	0.2	0.4	0.5
SO2, 24 hr	ppbv	0.4	0.4	27	0	0.1	0.2	0.3	0.5	0.9	2.2

Table 3-4. Summary Statistics for Jefferson St. Site (Atlanta, GA) (All Hours).

Variable	Units	Mean	Std. Dev	n	Min	10th	25th	Median	75th	90	Max
SO4	µg m^{-3}	2.67	1.80	2023	-0.09	0.79	1.44	2.30	3.44	5.01	15.2
NO3	µg m^{-3}	1.37	1.41	2075	-0.14	0.14	0.38	0.99	1.93	2.95	10.9
NH4	µg m^{-3}	1.37	0.93	2090	-0.01	0.38	0.75	1.17	1.76	2.58	6.28
HNO3	ppb	0.29	0.27	1859	-0.11	0.06	0.12	0.22	0.37	0.64	1.95
NH3	ppb	1.17	0.79	1939	0.02	0.39	0.62	0.97	1.52	2.11	6.18
TNO3	µg m^{-3}	2.12	1.50	1797	-0.11	0.58	1.12	1.89	2.77	3.77	11.5
TNH3	µg m^{-3}	2.31	1.16	1881	0.12	0.94	1.50	2.19	2.89	3.85	8.0
O3	ppb	21.7	13.7	2143	-0.35	1.97	10.5	22.4	31.2	38.9	65.5
CO	ppb	312	234	2062	104	172	201	241	322	493	2266
SO2	ppb	3.03	5.25	2130	0	0.28	0.61	1.35	2.94	7.51	86.3
NO	ppb	17.2	43.6	2140	0.01	0.37	1.02	3.22	10.12	39.2	393.9
NO2	ppb	16.9	11.4	2128	1.17	5.05	8.34	13.83	23.1	33.4	65.4
NOx	ppb	32.8	46.9	2126	1.41	6.14	10.23	17.5	32.2	68.6	431.0
NOy	ppb	35.8	53.3	2140	2.21	7.26	11.44	18.3	33.7	74.1	421.9
Wind Speed	m/s	1.93	1.03	2151	0.07	0.64	1.15	1.83	2.58	3.38	5.73
Wind Direction	Degrees	NA	NA	2151				see wind rose			
Temperature	Deg C	9.25	7.2	2158	-11.7	-0.9	4.4	9.93	14.46	18.3	27.6
RH %	Unitless	65.0	24.3	2157	17.1	31.9	44.9	63.7	87.9	98.6	101.8
Station Pressure	mbar	985.0	6.55	2157	964.5	975.7	982.1	986.0	989.3	993.2	1002.2
Solar Radiation	W m-2	139	228	2157	0.22	0.23	0.25	0.70	188.1	564.8	944.6
Rainfall	mm	63.8	77.1	2155	0	0	1.52	24.13	119.1	173.7	261.4
PM2.5	µg m^{-3}	12.1	7.0	2081	1.3	4.7	6.79	10.48	15.8	21.7	51.0
BC	µg m^{-3}	0.75	0.72	1838	0.03	0.21	0.35	0.54	0.88	1.41	6.3
TC	µg m^{-3}	4.72	3.86	1874	0.23	1.40	1.95	3.46	5.98	9.95	26.1
OC	µg m^{-3}	4.10	3.38	1613	0.12	1.21	1.71	2.93	5.16	8.89	22.7
BC / OC	Unitless	0.18	0.12	1613	0.04	0.10	0.13	0.18	0.25	0.34	1.90

Table 3-5. Summary Statistics for Yorkville, GA (All Hours)

Variable	Units	Mean	Std. Dev	n	Min	10th	25th	Median	75th	90	Max
SO4	µg m^{-3}	2.33	1.54	2729	-0.21	0.66	1.19	2.07	3.13	4.30	10.46
NO3	µg m^{-3}	1.04	1.15	2773	-0.06	0.12	0.26	0.69	1.44	2.32	10.32
NH4	µg m^{-3}	1.15	0.74	2778	0	0.34	0.63	1.05	1.49	2.05	5.98
HNO3	ppb	0.28	0.26	2846	-0.05	0.04	0.11	0.20	0.37	0.62	2.05
NH3	ppb	2.06	3.41	2810	0.09	0.3	0.66	1.21	2.32	4.11	68.69
TNO3	µg m^{-3}	1.8	1.4	2011	-0.02	0.4	0.8	1.5	2.4	3.6	11.2
TNH3	µg m^{-3}	3.1	3.3	1993	0.2	1.1	1.6	2.4	3.7	5.6	56.3
O3	ppb	31.62	11.57	2869	-0.04	16.41	24.15	31.97	39.05	45.70	68.40
CO	ppb	176.34	44.48	2642	82.52	129.67	148.77	168.91	195.22	230.63	452.33
SO2	ppb	1.54	2.71	2864	-0.01	0.10	0.34	0.88	1.86	3.36	59.07
NO	ppb	0.40	1.32	2877	-0.05	-0.01	0	0.02	0.25	1.01	25.26
NO2	ppb	3.08	3.17	2875	0.13	0.67	1.11	2.02	3.79	6.983	31.12
NOx	ppb	3.5	4.0	2874	0.2	0.7	1.2	2.2	4.3	7.4	43.1
NOy	ppb	4.8	4.3	2874	0.21	1.5	2.2	3.5	5.9	9.3	45.1
Wind Speed	m/s	3.4	1.6	2888	0.2	1.4	2.2	3.3	4.5	5.6	10.5
Wind Direction	Degrees	NA	NA	2891			see wind rose				
Temperature	Degree C	8.1	7.1	2893	-13.3	-1.8	3.2	8.6	13.8	16.8	25.3
RH %	Unitless	70.0	23.2	2895	19.8	37.8	50.2	70.4	92.5	100.3	103.0
Station Pressure	mbar	972.4	6.3	2879	951.6	963.6	969.4	973.4	976.5	989.4	988.9
Solar Rad	W m^{-2}	128.3	215.4	2896	0	1.0	1.1	1.5	162.5	512.0	926.5
Rainfall	mm	27.11	32.60	2889	0	0	2.03	10.67	41.15	82.80	120.40
PM 2.5	µg m^{-3}	11.0	5.9	2651	1.2	4.8	7.2	9.9	13.6	18.5	59.4
BC	µg m^{-3}	0.3	0.3	2626	0.01	0.1	0.1	0.2	0.4	0.6	2.2
TC	µg m^{-3}	2.4	2.1	2848	0.1	0.8	1.2	1.9	3.0	4.9	22.0
OC	µg m^{-3}	2.2	1.9	2574	0.01	0.7	1.1	1.7	2.6	4.2	19.8
BC / OC	Unitless	0.16	0.37	1872	0.03	0.07	0.09	0.13	0.17	0.24	15.8

3.3 Episode Identification

Episodes were defined as periods where the smoothed $PM_{2.5}$ hourly concentration (7 hour running average) exceeded 27 μg m^{-3} for 4 or more consecutive hours. The detailed procedure for episode identification and the detailed episode list can be found in Appendix 1. A low threshold was selected for episodes (27 threshold instead of 35 or 35.5 μg m^{-3} and 4 hour duration rather than 24 hour duration) to increase the number of episodes isolated for study. A $PM_{2.5}$ concentration of 27 μg m^{-3} is a relevant indicator of "high" concentrations in light of the current $PM_{2.5}$ standard (i.e., 75% of 35 μg m^{-3}) and possible future $PM_{2.5}$ standards (i.e., 90% of 30 μg m^{-3}, which is the lowest daily level identified by USEPA (2010).

The Milwaukee site had the highest number of episodes (13), while the Mayville site had 7 episodes. All episodes that occurred at Mayville also had a concurrent Milwaukee episode. Therefore episodes could be classified as "shared" between the two sites or "Milwaukee only." The exact start and end times of shared episodes were not identical.

The urban Atlanta site (Jefferson St.) experienced 6 episodes using the same episode definition, and the rural Atlanta site (Yorkville) experienced 2 episodes. Similar to the Wisconsin sites, episodes were either shared or urban only. There were no rural only episodes.

The episodes are shown in a $PM_{2.5}$ time series for the Wisconsin sites, and in a $PM_{2.5}$ time series for the Georgia sites.

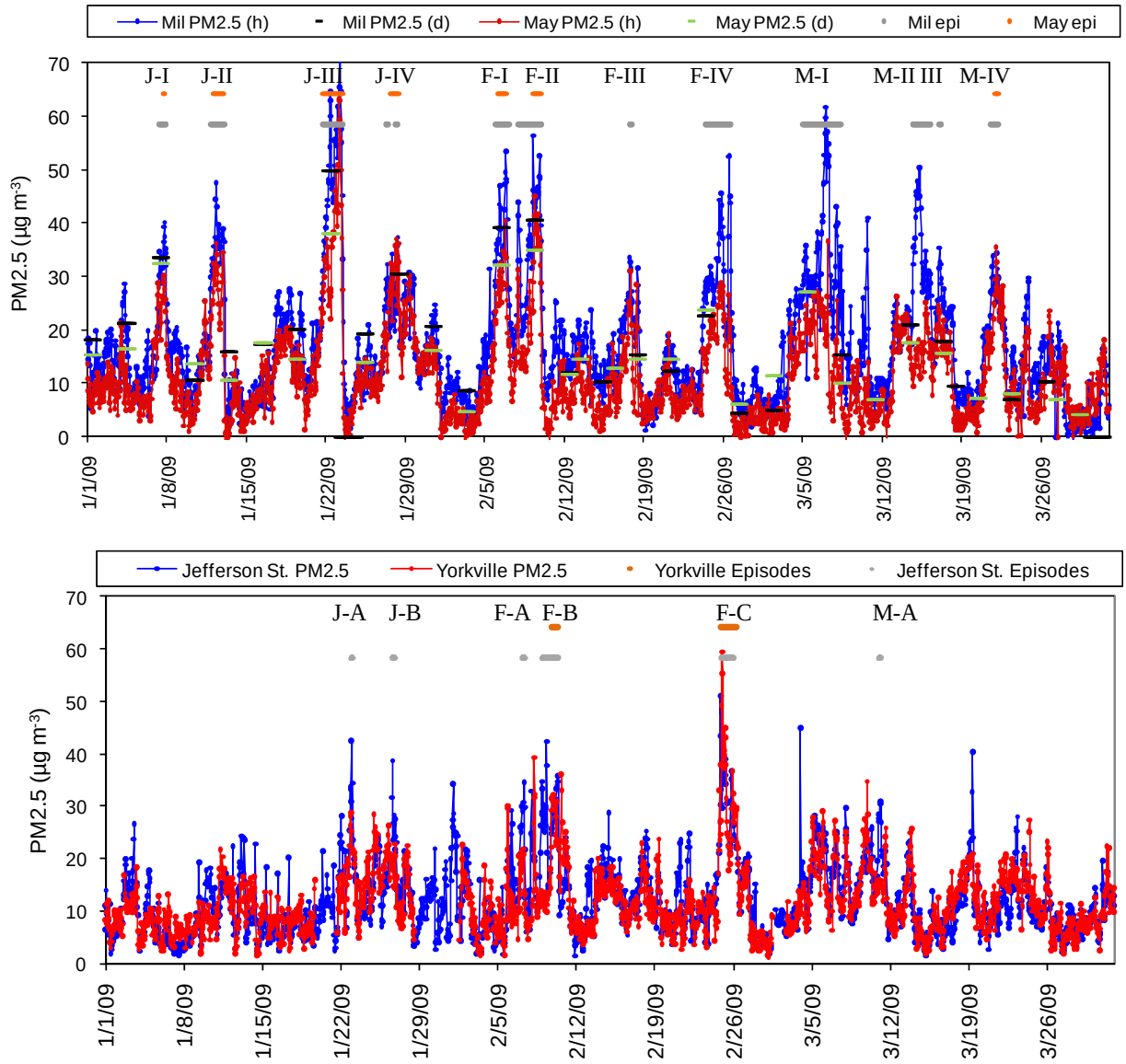

Figure 3-5. Hourly and daily $PM_{2.5}$ at the Wisconsin and SEARCH sites.

Top panel Wisconsin: Blue (hourly) and black (24 hr) $PM_{2.5}$ concentrations are shown for Milwaukee. Red (hourly) and green (daily) $PM_{2.5}$ concentrations are for Mayville. Grey and orange bands indicate hours that have been designated as episode hours. Grey is for Milwaukee while orange is for Mayville. The episode number is indicated above the episode bands, with J-I being Jan-I, F-I for Feb-I, and M-I for Mar-I.

Bottom panel SEARCH: Blue (hourly) $PM_{2.5}$ concentrations are shown for Jefferson St. (Atlanta). Red (hourly) $PM_{2.5}$ concentrations are for the rural site in Yorkville. Grey (urban) and orange (rural) bands indicate episode hours.

Table 3-5. Summary table for Wisconsin episodes – see Appendix 1 for more detail

Episode Name	Start Date	End Date	Milwaukee Peak 7hr $PM_{2.5}$	Milwaukee Avg. $PM_{2.5}$ during period	Mayville Peak 7hr $PM_{2.5}$	Mayville Avg. $PM_{2.5}$ during period
JAN-I	7-Jan	7-Jan	36.4	33.6	30.1	29.0
JAN-II	11-Jan	13-Jan	40.1	36.1	36.2	28.7
JAN-III	21-Jan	23-Jan	64.5	50.3	55.0	37.9
JAN-IV	27-Jan	27-Jan	28.1	28.9		
JAN-V	27-Jan	28-Jan	31.4	31.4	32.3	30.5
FEB-I	5-Feb	7-Feb	47.0	37.6	34.3	30.7
FEB-II	7-Feb	10-Feb	47.5	35.4	40.3	36.9
FEB-III	17-Feb	17-Feb	29.8	30.3		
FEB-IV	24-Feb	26-Feb	41.9	31.3		
MAR-I	5-Mar	8-Mar	54.6	33.8		
MAR-II	14-Mar	16-Mar	47.2	35.5		
MAR-III	17-Mar	17-Mar	30.8	31.6		
MAR-IV	21-Mar	22-Mar	30.0	29.4	29.8	29.8

Table 3-6. Summary table for Georgia episodes – see Appendix 1 for more detail

Episode Name	Start Date	End Date	Jefferson St. / Atlanta Peak 7hr $PM_{2.5}$	Jefferson St. / Atlanta Avg. $PM_{2.5}$ during period	Yorkville Peak 7hr $PM_{2.5}$	Yorkville Avg. $PM_{2.5}$ during period
JAN-A	22-Jan	23-Jan	32.5	33.7		
JAN-B	26-Jan	26-Jan	28.8	28.6		
FEB-A	7-Feb	7-Feb	30.0	30.6		
FEB-B	8-Feb	10-Feb	31.9	27.3	31.2	29.0
FEB-C	24-Feb	26-Feb	38.1	32.2	46.2	31.9
MAR-A	10-Mar	11-Mar	28.8	29.1		

3.4 Diurnal Patterns

A complete set of diurnal averaged patterns for both the Atlanta and Wisconsin sites can be found in Appendix 3. Some representative patterns are repeated here and discussed in subsequent sections. Diurnal patterns were produced by averaging all episode hours occurring within a common time bin (e.g. 1-2 AM), and therefore there may be a different number of hours in each time bin since episodes did not all start and end at a fixed time of day.

Mean and episode conditions for $PM_{2.5}$ are shown in Figure 3-6. The Georgia sites display a slightly more distinctive diurnal pattern with a peak at 09:00 and a minimum at 13:00. Elevated PM during episodes is most pronounced during nighttime hours. In Wisconsin sites, the diurnal patterns for $PM_{2.5}$ are very flat during episodes and non-episodes, with a slight (a few microgram per m^3) increase at Milwaukee during episodes at 8 AM and a small increase at the beginning of the night. This contrast suggests that variations in $PM_{2.5}$ in Wisconsin are not caused so much by diurnal changes in boundary layer height and wind speed, but rather by regional meteorology. Another possibility is that boundary layer and wind speeds remain low during daytime hours of episodes.

The diurnal patterns for total nitrate are shown in Figure 3-7. Perhaps the most striking feature of these is that they are relatively flat. The morning peak in Milwaukee may be a sampling error where some fraction of the high NOx levels are reported as nitrate. Another important feature in 3-7 is the higher level of nitrate in Wisconsin, and the greater involvement of nitrate in episodes at the Wisconsin sites. Weekday/weekend patterns are analyzed and discussed in section 7.

Ozone diurnal patterns (Figure 3-8) show how similar the ozone patterns are at the two urban sites (in both magnitude and diurnal pattern) with the morning decrease in O_3 due to the reaction of O_3 and NO during periods of elevated motor vehicle NOx and poor mixing. This early morning dip in O_3 is not present at the rural sites. Rural levels exceed urban levels. For example, the ozone mean in Mayville is 41% higher than the ozone mean in Milwaukee.

Key points from diurnal patterns in the appendix are listed below:

- Sulfate at WNS sites shows a peak during daytime, presumably from OH-driven sulfate production.
- Ammonia has a relatively flat diurnal pattern, but has slightly higher average levels during the late afternoon.

- Milwaukee episodes tend to be 5 degrees warmer than climatological mean conditions. Mayville episodes are also warmer than the climatological mean, but warmer in the afternoon (relative to climatological mean) than the morning.

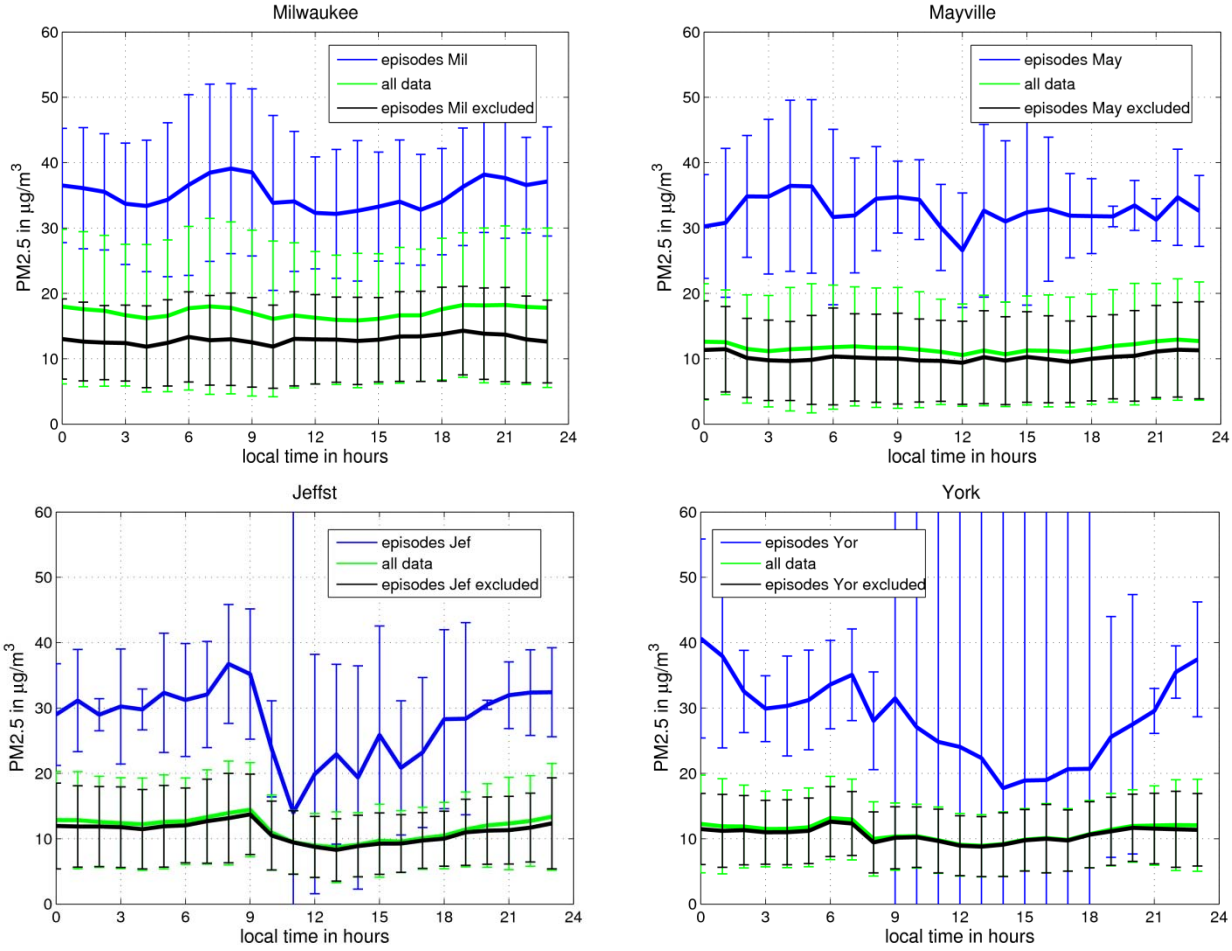

Figure 3-6. Diurnal pattern for $PM_{2.5}$ in urban sites (left), rural sites (left), Wisconsin sites (top) and Georgia sites (bottom).

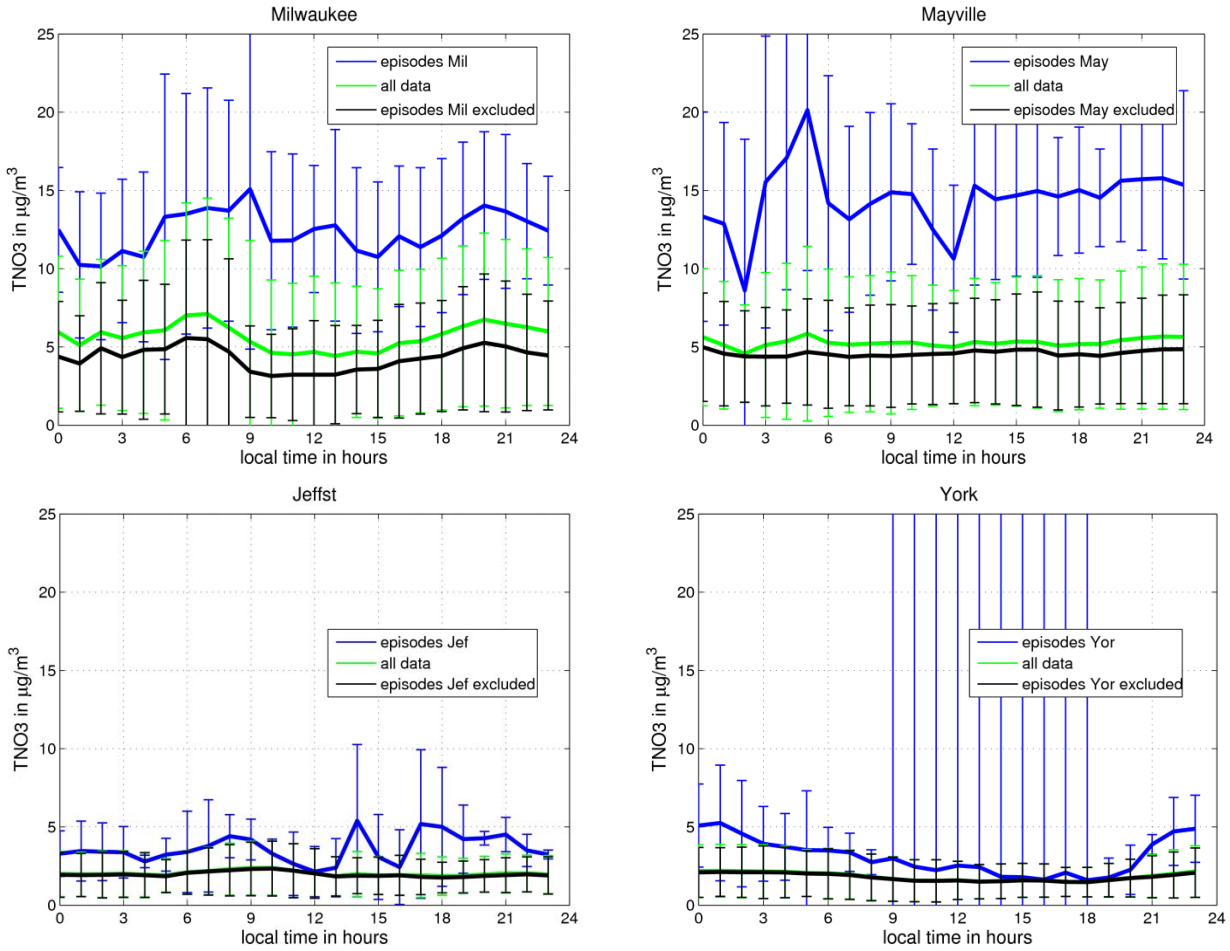

Figure 3-7. Diurnal pattern for total nitrate in urban sites (left), rural sites (left), Wisconsin sites (top) and Georgia sites (bottom).

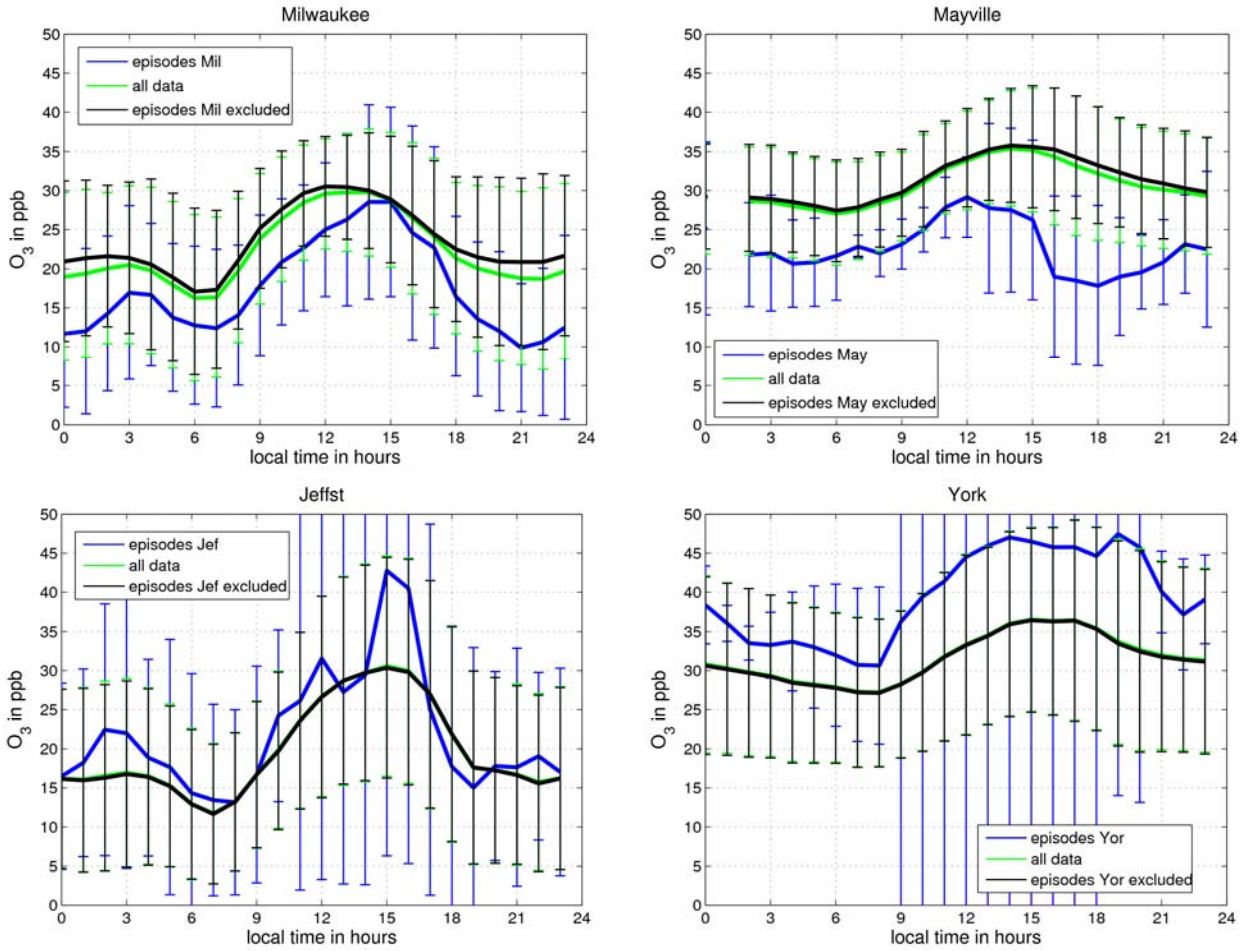

Figure 3-8. Diurnal pattern for ozone in urban sites (left), rural sites (left), Wisconsin sites (top) and Georgia sites (bottom).

3.5 *Aerosol Composition*

Appendix 4 contains detailed figures and tables of aerosol and gas composition during the overall study period, during episodes, during non-episodes, and during individual episodes. Appendix 4 also includes values for the OC/EC ratio, information on mass balance closure, and values for the degree of sulfate neutralization, gas ratio, and adjusted gas ratio. In this section, the results are reported graphically, and average episode (rather than episode specific) chemical composition is shown. Graphs of concentrations that are episode specific are also in Appendix 4. These analyses are the same for the Wisconsin and Georgia sites.

Due to the different hours with missing data (either from flagged hourly data or from 1 in 3 day sampling), there are different numbers of hours available for different studies of relative composition. Accordingly, three composition analysis were completed:

- Analysis 1 – Inorganic aerosol composition, using all simultaneous hours where SO_4, NO_3, NH_4, and $PM_{2.5}$ were available.
- Analysis 2 – inorganic aerosol composition plus OC and EC (carbonaceous compounds).
- Analysis 3 – inorganic aerosol plus inorganic gas (NH_3 and HNO_3) composition analysis.

Since inorganic aerosol species are included in all three analyses, questions requiring inorganic concentrations or fractions them can usually be addressed with all three analysis types. However, for assessing fractional composition most accurately, sampling periods without missing data in any species need to be isolated. Where multiple composition analyses are available (e.g. SO_4, NH_4, NO_3) the differences between the analyses are not significant for most questions. The exception is where ratios of these species to OC and EC, where the low number of samples can cause non-representative data due to the low number of OC and EC samples during the study. The number of data values in any particular average can be found in Appendix 4. These range from approximately 1100-1600 for all hours and non-episode cases, to 37-200 for all episode variables (lowest in Yorkville, highest in Milwaukee), to as low as 7 for individual episode variables.

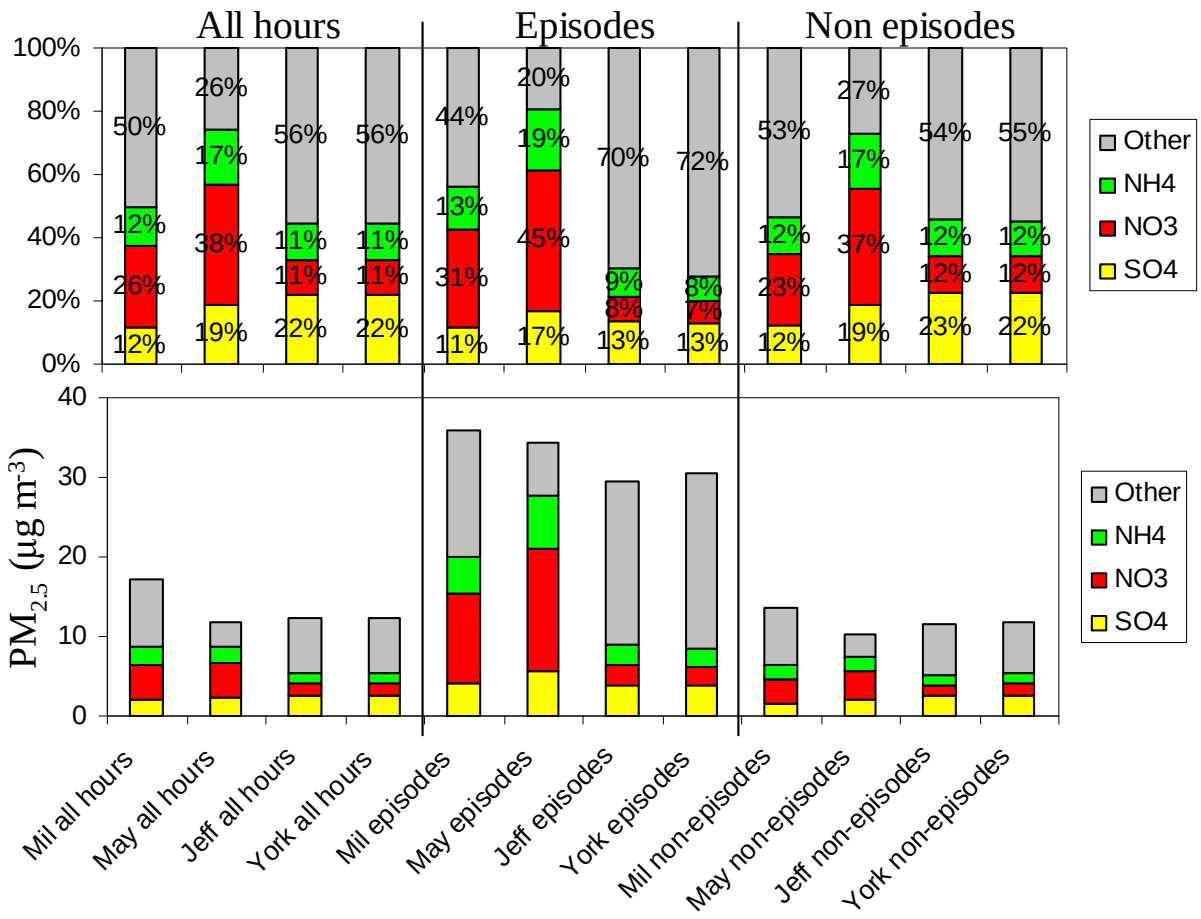

Figure 3-9. Basic chemical composition analysis, using mean values for all hours with available SO_4, NH_4, NO_3, and $PM_{2.5}$ values. Top panel has fractional composition and bottom panel are absolute values.

Figure 3-9 shows that the other (mainly OC) contribution is very important at both urban sites, and at Yorkville. Nitrate is much more important at the WNS study than at the SEARCH sites.

The second type of chemical composition analysis pulls in available OC and EC data, showing that (at most sites) the other can be accounted for by the measured organic matter (OC x 1.4 OM/OC ratio) and EC.[ii] The mass balance at Mayville is not satisfied as well as at the other sites, possibly due to a small number of OC samples with potential positive artifacts.

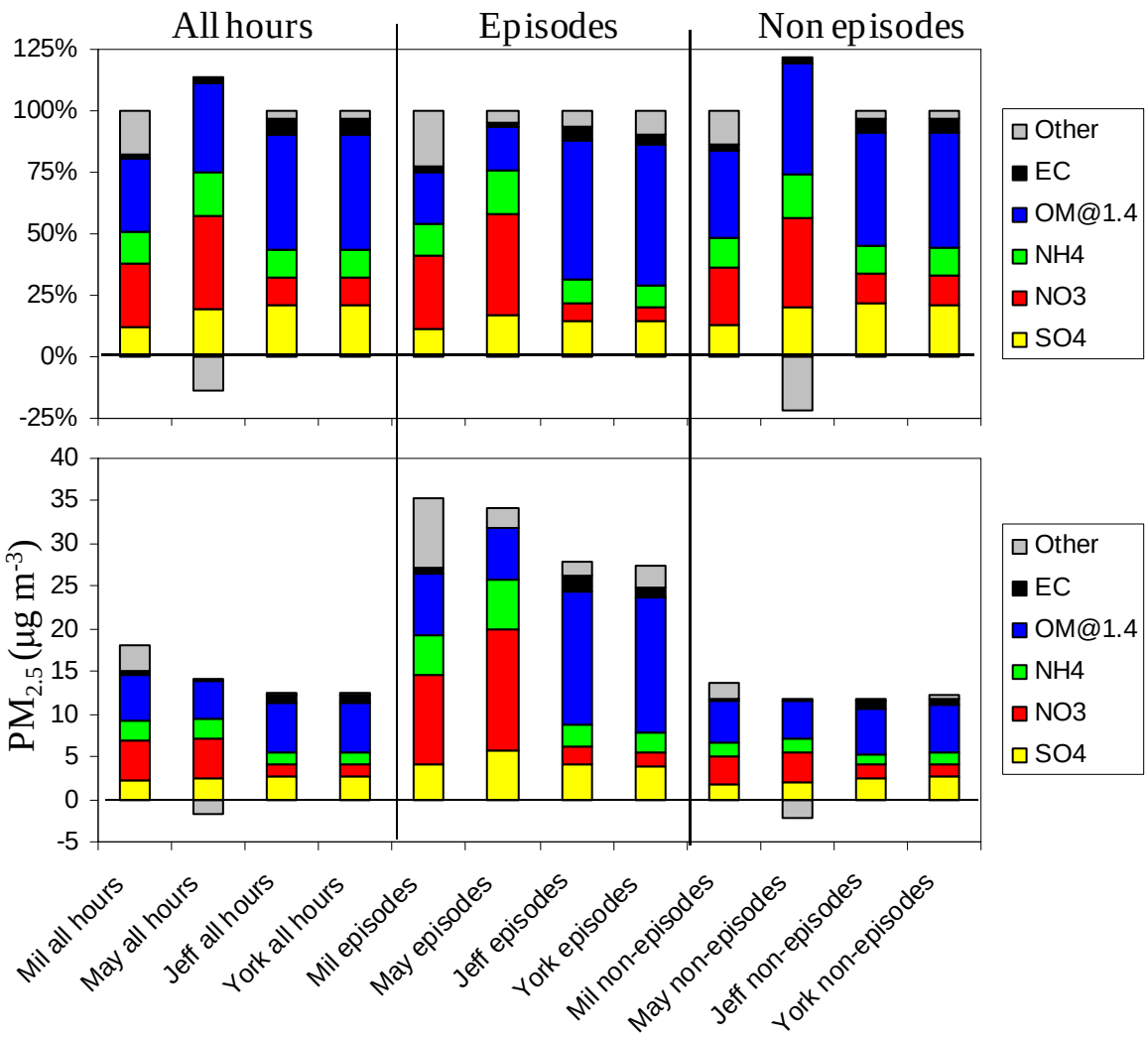

Figure 3-10. Chemical composition analysis, using mean values for all hours with available SO_4, NH_4, NO_3, OC, EC and $PM_{2.5}$ values. Top panel has fractional composition and bottom panel are absolute values. (Jan 22 OC and EC filters at Milwaukee are excluded).

OC/EC ratios are shown in Figure 3-11. The data show that OC/EC ratios decrease during episodes, indicative of higher contribution of primary OC emissions relative to secondary (assuming the primary emission OC/EC ratio remains constant). While secondary organic aerosol was not expected in winter, the high contribution of OC to episodes in Milwaukee, coupled with high OC values during January episodes and during fog events, made confirmation of this assumption necessary. Further investigation of this assumption using a multiyear OC/EC record can be found below.

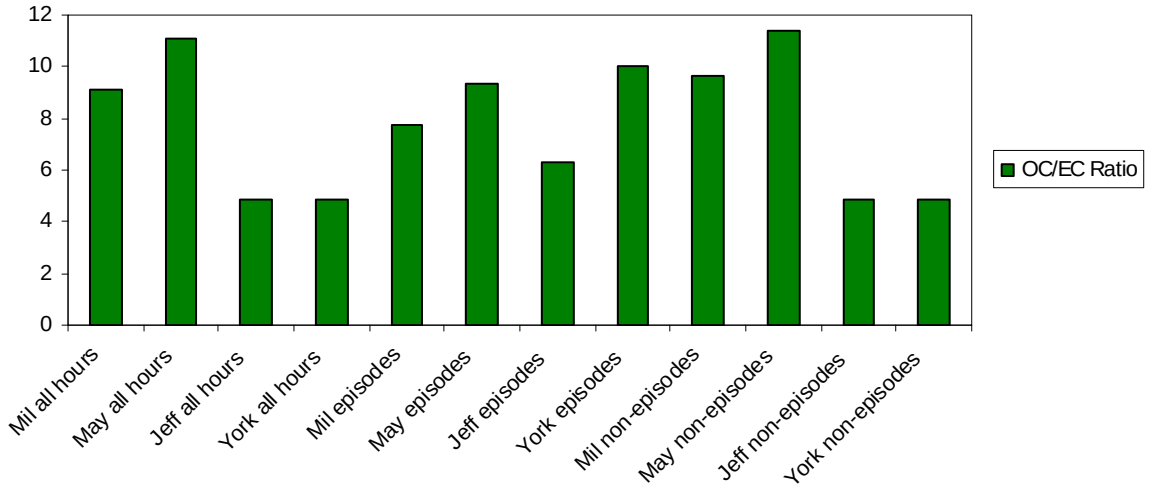

Figure 3-11. OC/EC ratio. Note: instrumentation is consistent between Milwaukee and Mayville, and between Jefferson St. and Yorkville, but not necessarily between the Wisconsin and SEARCH sites.

The third type of chemical composition analysis includes NH_3 and HNO_3 gases. For Figure 3-12, gases are shown as negative concentrations. Perhaps the most striking features about these figures is that the gas concentrations are low compared to the aerosols, even in the Georgia sites. Furthermore, gas concentrations are (on average) much more constant than their aerosol counterparts. In other words, during episodes, the total concentration of nitrate and ammonia goes up, and the increase is mainly in the particulate phase.

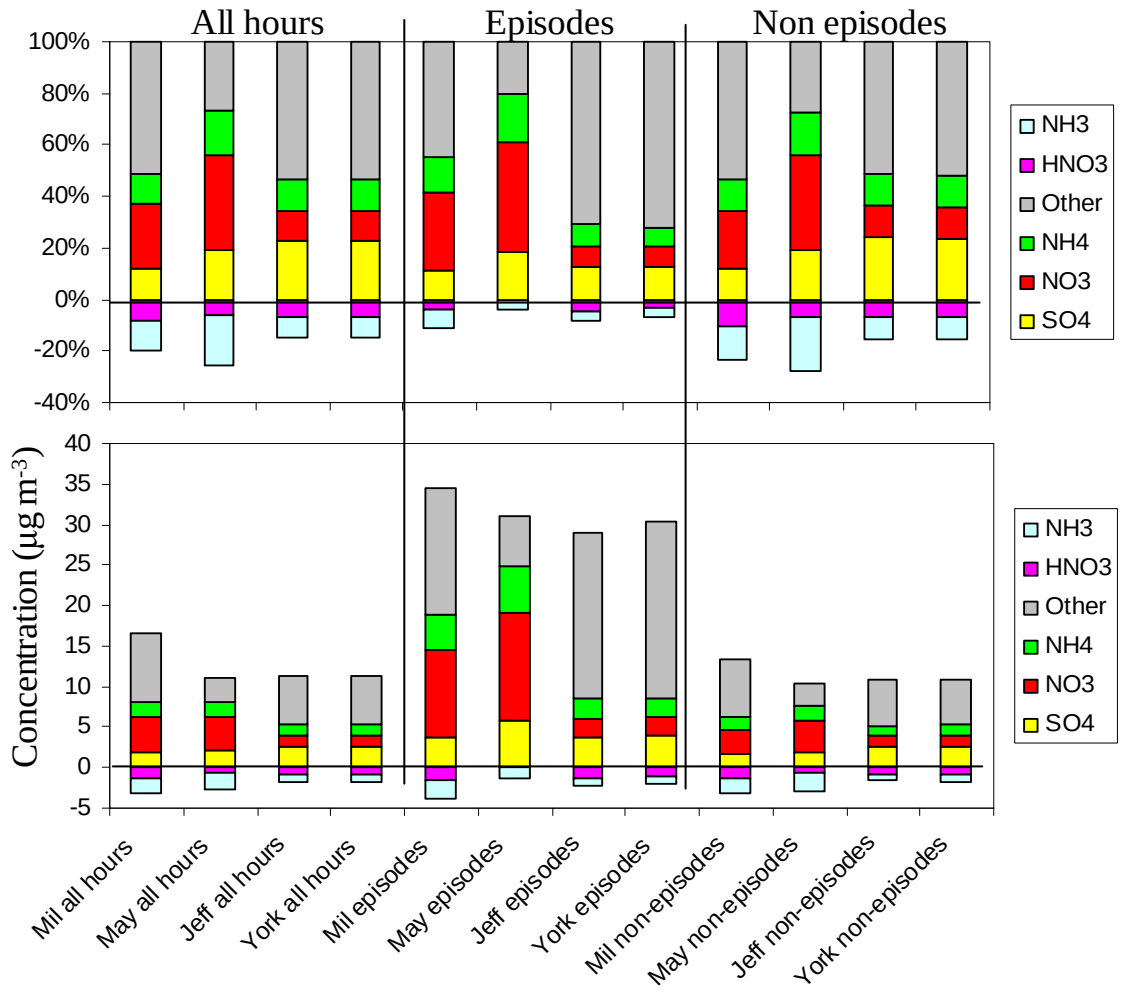

Figure 3-12. Chemical composition analysis including inorganic gases, using mean values for all hours with available SO_4, NH_4, NO_3, HNO_3, NH_3 and $PM_{2.5}$ values. Top panel has fractional composition and bottom panel are absolute values with gas species shown as negative.

Gas ratio, an indicator of available ammonia discussed in more depth in section 6, is graphed in Figure 3-13. Gas ratio is the calculated by $(TNH_3\text{-}2TS)/TNO_3$ where TS is total sulfate and all terms are on a molar basis (Ansari and Pandis 1998). Except for Mayville during episodes (at a gas ratio of 0.98) all the gas ratios are above 1, the typical threshold for ammonia sensitive conditions. The gas ratio is highest at the Georgia sites. At Wisconsin sites, it is higher at Mayville during non-episode periods, but higher in Milwaukee during episode periods. The gas ratio drops slightly during episodes (on average) at both Wisconsin sites.

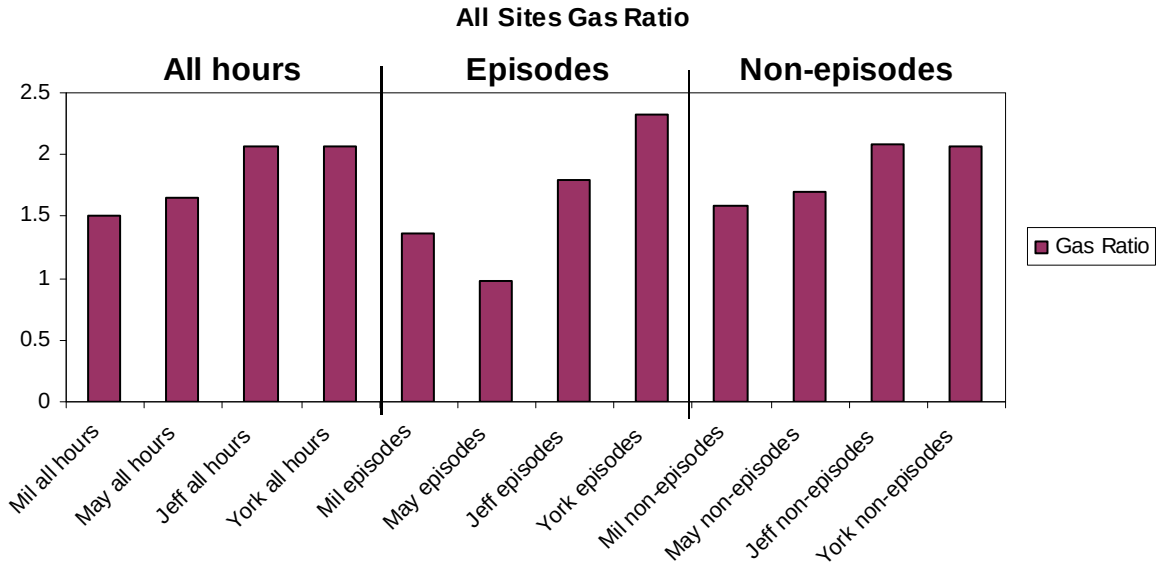

Figure 3-13. Gas ratio for the four sites during episode and non episode periods.

By examining the enrichment or enhancement ratios of compounds (the ratio of the concentration during episodes to that during non-episode periods), some insight can be gained toward what sources become more prevalent (on a relative basis) during episodes. The results of this calculation are shown in Table 3-7. Other important enhancement ratios are those for NO_x and NO_y. The NO_x enhancement ratio is ~1.9-2.0 for Milwaukee and ~1.7 for Mayville. The NO_y enhancement ratios are 2.1 and 2.5 for Milwaukee and Mayville, respectively.

Table 3-7. Enhancement ratios for key chemical compounds

	SO_4	NO_3	NH_4	OC	EC	HNO_3	NH_3	TNO_3	TNH_3	$PM_{2.5}$
Milwaukee[a]	2.53	3.64	3.02	1.53	1.96	1.05	1.33	2.70	2.25	2.65
Milwaukee[b]	2.19	2.68	2.57	1.73	1.91	0.41	1.09	1.57	1.67	2.32
Milwaukee[c]	2.59	3.94	3.03	1.37	1.99	1.72	1.10	3.36	2.17	2.71
Mayville	2.91	4.05	3.73	1.38	1.91	< 1	0.57	2.73	1.84	3.33
Jefferson St.	1.52	1.81	1.96	2.92	2.30	1.74	1.08	1.77	1.56	2.58
Yorkville	1.48	1.65	1.76	2.78	1.47	1.33	1.05	1.57	1.48	1.31

All Milwaukee entrees (a-c) have the Jan 22 OC and EC values excluded.
[a]Milwaukee enhancement – "all episode hours" relative to non episode average conditions.
[b]Milwaukee enhancement for Milwaukee only episodes calculated as the average of enhancement factors for episodes occurring at Milwaukee but not at Mayville and having 7 or more hours of OC data.
[c]Milwaukee enhancement for episodes occurring at both Mayville and Milwaukee and having 7 or more hours of data.

The enhancement ratios can indicate the source or aerosol types that are most "characteristic" of an episode. The data from Table 3-7 is graphed in Figure 3-14, and enhancement ratios from the table have been divided by the enhancement of $PM_{2.5}$. Therefore, species >1 are enhanced more than $PM_{2.5}$.

- Milwaukee episodes are marked by enhancements in sulfate, nitrate (mainly through repartitioning), and ammonium (mainly through repartitioning). OC also builds up more than total nitrate or total ammonia, but its relative contribution to the aerosol falls (consistent with Figure 3-9).
- Both site episodes, whether at Milwaukee or at Mayville, have a similar profile of enhancements. Total nitrate builds up faster than total ammonia. Sulfate is enhanced, and the shift in partitioning from gas to aerosol for ammonia is evident.
- The enhancement of total ammonia at Wisconsin sites is similar to that of local primary sources NOx, OC, and EC, while the enhancement of NOy and total nitrate is larger.
- At the Georgia sites, episodes are dominated by OC (and by EC also at Jefferson St.).

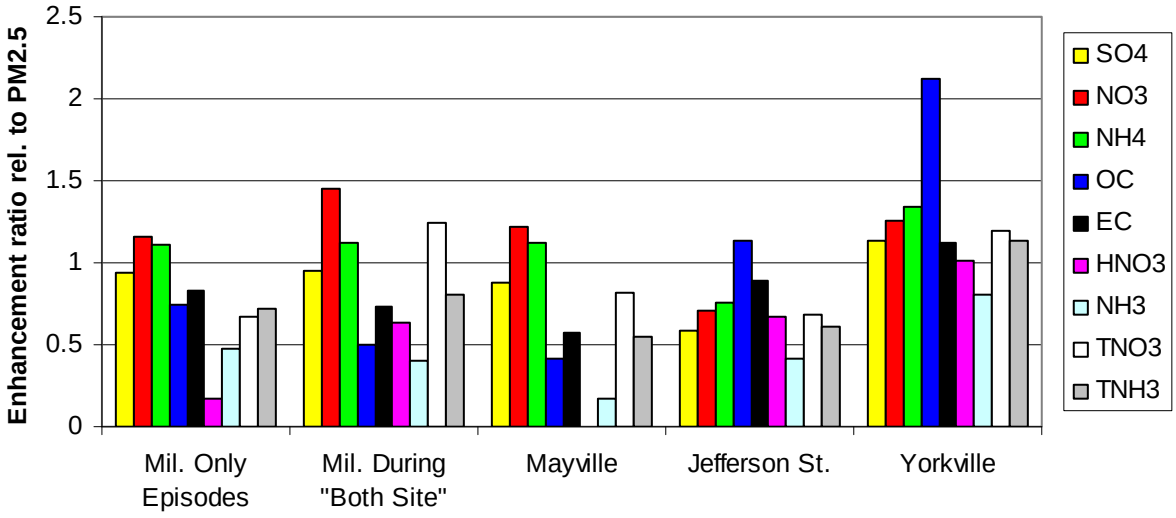

Figure 3-14. Enhancement Ratios relative to Enhancement Ratio of $PM_{2.5}$.
Ratios are from Table 3-7 and are based on episode vs. non-episode conditions. "Mil Only" section is from line b of Table 3-7, and "Mil During Both Site" entry is from line c of Table 3-7.

The shifting of the PM chemistry as $PM_{2.5}$ increases can be seen in the following figures, which graph various PM composition indicators for different episodes, for all episodes, for all hours, and for non-episodes.

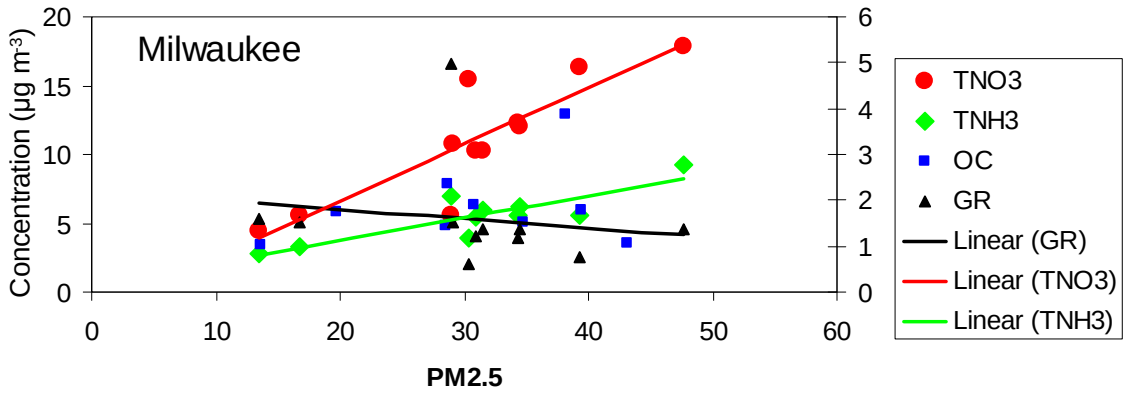

Figure 3-15. Total nitrate, total ammonia, OC, and gas ratio as a function of $PM_{2.5}$ for various periods in the Milwaukee dataset. Jan 22 datapoint for OC is excluded. Lines are linear fits. Gas ratio decreases slightly with increasing $PM_{2.5}$.

Figure 3-15 shows the widening ratio (enhancement) of total nitrate relative to total ammonia at the Milwaukee site and the slight decrease in gas ratio. The high gas ratio period is the Mar I episode. Total ammonia increase is similar to the increase for OC, suggesting possibly that these are both building up during stagnation, while total nitrate is enhanced due to chemical production during the episode.

Figure 3-16 repeats the treatment of Figure 3-15 for Mayville. Here the same pattern is evident, but the drop in gas ratio is clearer since there is less scatter in the data. Total ammonia builds up similarly to OC, while total nitrate buildup is enhanced.

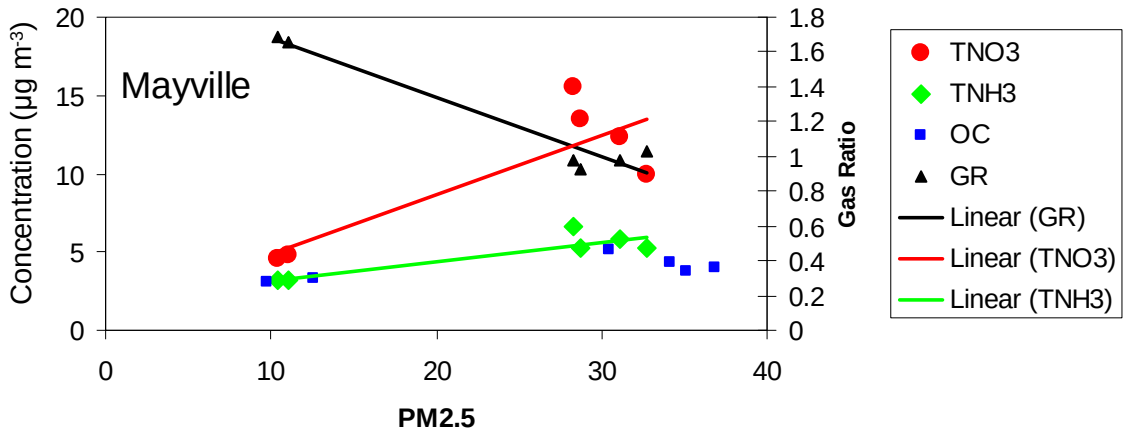

Figure 3-16. Total nitrate, total ammonia, OC, and gas ratio as a function of $PM_{2.5}$ for various periods in the Mayville dataset. Gas ratio decreases slightly with increasing $PM_{2.5}$, reflecting greater enhancement of total nitrate than of total ammonia.

Bill Adamski of WDNR analyzed OC/FRM, EC/FRM, and OC/EC ratios for the Milwaukee and Mayville sites for all samples from Jan 001 to Oct 2009, and this can be found in Appendix 15. This was done to look for patterns in these ratios as a function of season, ozone levels, RH, temperature, and $PM_{2.5}$ concentration. The purpose was to overcome the limited dataset for OC and EC during the study period. These data were insufficient to rule out significant secondary organic aerosol production during wintertime episodes. The key result from this appendix is that OC/EC ratios depend on season (highest ratio in summer, lowest in winter, at both sites). This is shown in Figures A15-6 and A15-18 of the appendix. At Milwaukee, OC/EC ratios decrease with increasing $PM_{2.5}$ in both warm and cold seasons, suggesting impact of primary emissions during both summer and winter $PM_{2.5}$ episodes. But the decrease is slightly more pronounced in winter, consistent with our assumption that secondary production is a summertime phenomenon (Figure A15-4). In Mayville, OC/EC ratios increase slightly with $PM_{2.5}$ in summer, and decrease with $PM_{2.5}$ in winter. Thus, the long term record confirms the initial assumption of negligible involvement of secondary organic aerosol during winter episodes (on average).

Ansari, A. S. and S. N. Pandis (1998). "Response of inorganic PM to precursor concentrations." Environmental Science & Technology **32**(18): 2706-2714.

Brown, S. G., H. R. Hafner, et al. (2006). Integration of Results for the Upper Midwest Urban Organics Study, Lake Michigan Air Directors Consortium.

El-Zanan, H. S., B. Zielinska, et al. (2009). "Analytical Determination of the Aerosol Organic

Mass-to-Organic Carbon Ratio." Journal Of The Air & Waste Management Association **59**(1): 58-69.
Turpin, B. J. and H. J. Lim (2001). "Species contributions to PM2.5 mass concentrations: Revisiting common assumptions for estimating organic mass." Aerosol Science And Technology **35**(1): 602-610.
USEPA (2010). Policy Assessment for the Review of the Particulate Matter NAAQS, Second External Review Draft (June 2010).
Wittig, A. E., S. Takahama, et al. (2004). "Semi-continuous PM2.5 inorganic composition measurements during the Pittsburgh air quality study." Atmospheric Environment **38**(20): 3201-3213.

[i] Total nitrate is defined as the measured aerosol nitrate plus the measured nitric acid (converted to its equivalent mass concentration of aerosol nitrate). Total ammonia is defined as the measured aerosol ammonium plus the measured ammonia (converted to its equivalent mass concentration of ammonium). Conversions from ppb gas (which the original results were reported as) to mass concentrations were done using an assumed temperature of 273 K. The potential error from using a standard temperature rather than a measurement specific temperature is small compared to the measurement error itself; furthermore, average temperatures at the Wisconsin sites were within 6 degrees of 273 K.

[ii] The selection of the OM/OC ratio of 1.4 is based on the value needed to best achieve mass balance at the Wisconsin sites. Comparing PM_{other} = TEOM – sum species other than OC vs. OM, gives the following. Using OM/OC 1.4: Mayville OM is too high by 13% of total $PM_{2.5}$ and Milwaukee OM is too low by 17% of total $PM_{2.5}$. OM/OC 1.6: Mayville OM is too high by 19% of total $PM_{2.5}$ and Milwaukee OM is too low by 14% of total $PM_{2.5}$. OM/OC 1.8: Mayville OM is too high by 24% of total $PM_{2.5}$ and Milwaukee OM is too low by 9% of total $PM_{2.5}$. A value of 1.6 provides the best fit for mass balance closure in the Georgia sites. Another value recently used in Midwestern analysis is 1.8 in the LADCO report "Integration Of Results For The Upper Midwest Urban Organics Study Final Report STI-903520-2942-FR." Furthermore, the acknowledged negative bias in nitrate in Brown et al. (2006) can be compensated by a high OM/OC ratio. Values of 1.77 (December) to 2.39 (July) have been determined for Atlanta (El-Zanan, Zielinska et al. 2009). For reference, 1.4 is the lowest value of OM/OC recommended in Turpin and Lim (2001). The actual OM/OC ratio may be different in Milwaukee and in Mayville, and the mass balance closure is likely influenced by sampling artifacts in OC and OM and nitrate.

[iii] Concentrations for the Milwaukee station on Jan 22, were (24 hr averages): FRM 49.7, OC 45.1, EC 3.96, NO_3 17.4, NH_4 7.99, SO_4 5.92. The next highest value in that calendar year for OC is 11.5, and the next highest for EC is 1.21 µg m^{-3}. This was the strongest episode whether the measure is peak $PM_{2.5}$, or $PM_{2.5}$ concentrations integrated over the length of the episode. TEOM levels rose steadily at sites all over Wisconsin, so the FRM value for Milwaukee seems robust. Unfortunately, for Jan 22 - the other 2 Wisconsin speciation $PM_{2.5}$ monitoring sites (Waukesha, Perkinstown) - did not get a sample to lab to analyze for species. The Jan 22 sample from Waukesha would have been especially comparable because its FRM $PM_{2.5}$ concentration for that day was 44.5 µg m^{-3}. Milw-SER (30 air miles to the east of Waukesha) had a FRM $PM_{2.5}$ reading of 49.7 µg m^{-3}. The very high $PM_{2.5}$ concentrations of Jan 22 were not the result of any "exceptional" event (e.g., fire). Instead, the extraordinarily high $PM_{2.5}$ values of Jan 22 were the result of synoptic-scale meteorological conditions that were very favorable to high $PM_{2.5}$ throughout the state - weather features that started on Jan 21 (i.e., episode ramp-up day) and increased through Jan 22, peaking in early Jan 23 before a strong cold front quickly ended the episode that day.

4. METEOROLOGICAL AND HISTORICAL CONTEXT FOR THE 2009 LADCO WNS

4.1 Meteorology

The 2009 WNS took place during a winter that featured considerable departures from 1971-2000 climatology of Southeastern Wisconsin. The preceding December was marked by record snowfall across the region, with 9.5" of snow in Milwaukee and 40.4" in Madison. January 2009 was 2.72 ºC colder than normal and much drier, with only 48% of the climatological average of 47 mm of precipitation in eight days of measurable precipitation. In particular, the 21-day period from 18 January to 8 February had only a trace (0.25 mm) of precipitation and two days of measurable snowfall at Milwaukee, and featured four pollution episodes. February and March were slightly warmer than normal (+0.94 ºC and +0.67 ºC, respectively) with unusually high precipitation (39% and 42% above normal). More than half of the 0.96 m of snowfall recorded at Milwaukee General Mitchell Airport during the three-month study period occurred in March (0.50 m). Milwaukee had snow cover in SNODAS assimilated snow data (NOHRSC, 2009) for all 31 days in January, 18 days in February, and 10 days in March, consistent with reports at the airport (31, 14, and 7 days, respectively).

Fine particle episodes during the WNS all began under similar synoptic conditions, characterized by an approaching high level ridge/surface low pressure system moving into the region, bringing warm, moist, stagnant air. These findings from the 2009 WNS conform to the existing LADCO conceptual model of $PM_{2.5}$ episodes throughout the year (LADCO, 2009) and the empirical Classification and Regression Tree (CART) for Midwestern daily average $PM_{2.5}$ concentrations. CART analysis performed for the 2009 WNS by LADCO's Donna Kenski for Milwaukee and Mayville using upper air soundings from Green Bay identified temperature aloft (850 mb) and the boundary layer lapse rate quantified in aloft-surface temperature difference as the two most important meteorological variables associated with $PM_{2.5}$ events. These variables are indicators of inversion conditions, and their change is strongly correlated with synpotic systems. In CART, observations at Mayville and Milwaukee were not good predictors of $PM_{2.5}$ surface concentrations at the other site. Ozone, CO, NO_x, and NO_y were better predictors for $PM_{2.5}$ than surface meteorological values, and also better than more direct $PM_{2.5}$ precursors NH_3 and HNO_3.

Local conditions during episodes were consistent with this synoptic context. Figures 4-1

and 4-2 show daily average time series of observed temperature and relative humidity at the Mayville and Milwaukee sites, augmented with daily surface pressure observations at Fond du Lac County and Milwaukee General Mitchell airports. Falling surface pressure and increases in temperatures and relative humidity coincident with the arrival of a low pressure system were the primary local signals for the initiation of a wintertime episode. Mayville experienced the same local meteorological changes as Milwaukee during the Milwaukee-only episodes, even when local fine particle concentrations were not high enough to qualify as an episode.

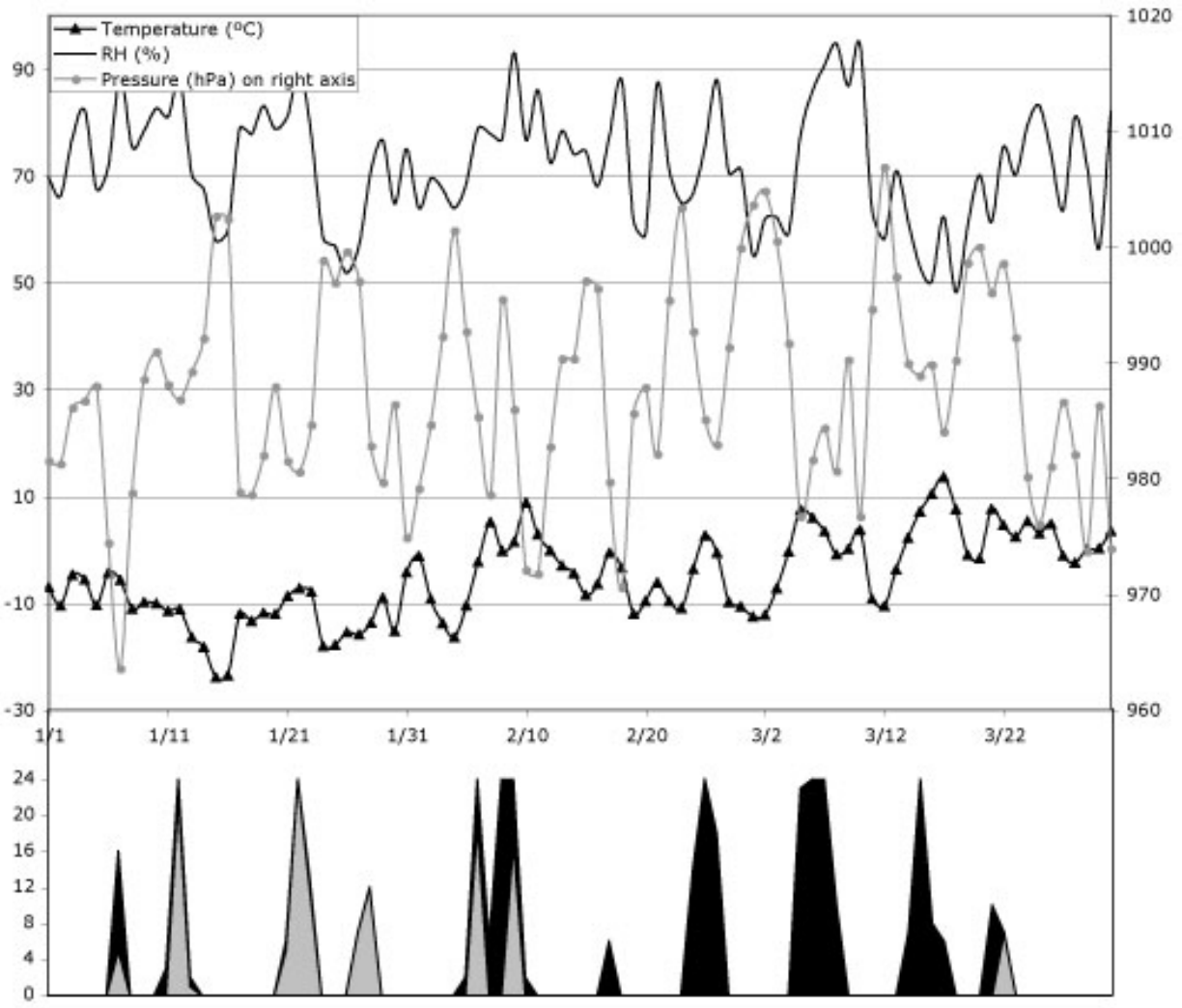

Figure 4-1. Mayville daily average temperature, relative humidity, and surface pressure, along with daily number of episode hours at Milwaukee (black) and Mayville (gray).

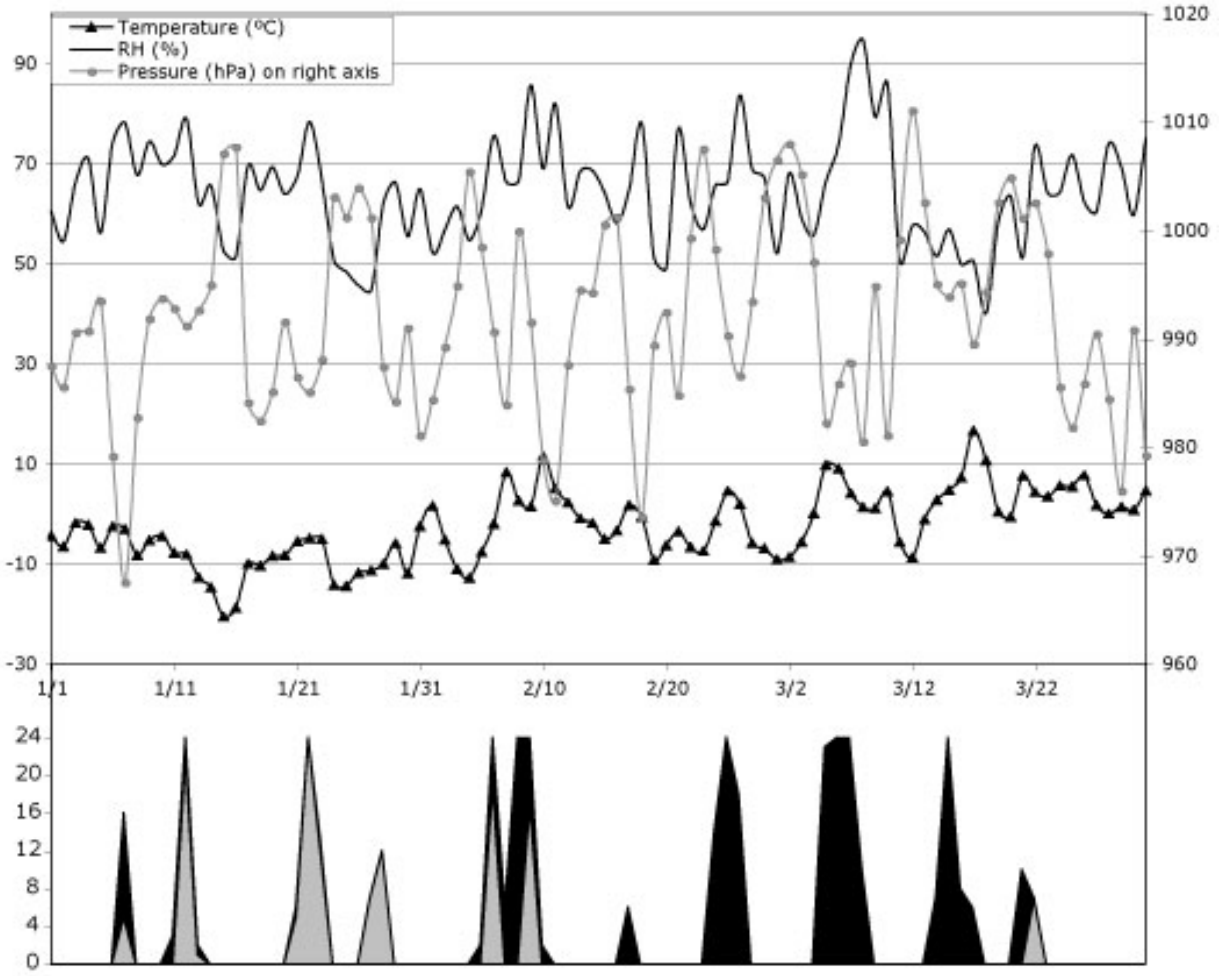

Figure 4-2. Milwaukee daily average temperature, relative humidity, and surface pressure, along with daily number of episode hours at Milwaukee (black) and Mayville (gray).

Meteorological conditions during events were distinct from the rest of the study period (Table 4-1). Local episodes at both sites were defined throughout primarily by high relative humidity, low pressure, lower visibility, and lighter, more southerly winds. Using a quantitative definition of fog as a difference between temperature and dew point of 2.5 ºC or less, Mayville episodes were strongly correlated with fog, with 74% of episode hours marked by fog at the Mayville site, as compared to 23% of non-episode hours. Fog occurred frequently at Mayville, on 58 of the 90 days of the study, including 10 of 11 episode days. Fog occurred at Milwaukee General Mitchell Airport on 29 days of the study, during nearly every episode, and often during the night immediately after the end of an episode. The last two episodes in March had no fog, due to high temperature and low relative humidity. The strongest episodes at Milwaukee were

marked by fog throughout the day (Appendix 14). These values are likely underestimates, as the Milwaukee monitoring site is closer to the lake than the airport, and may have been foggier. While it is clear that strong fog events are correlated with fine particle episodes, much of this correlation is due to the fact that fog and particle events are caused by the same low, stable boundary layer conditions, and the foggy days were directly attributable to snowpack melting and sublimation. While aqueous chemistry in fog is known to enhance the generation of secondary fine particles and to maintain stable inversions, there is not a statistically significant quantitative residual relationship between fog and fine particle concentration observations that conclusively identifies fog as an important additional contributor to episode intensity during the 2009 WNS.

There was never any liquid precipitation at either site on the first day of an episode or on the preceding day, although snow commonly accompanied episodes. Nine of the thirteen episodes concluded with rain (two), snow (four), or a combination (three) in SNODAS, often accompanying frontal systems. However, the strongest event (1/21-1/23) concluded without precipitation. Thus, while rainout cleared the air after most episodes, it was not as necessary for the termination of an event as the passage of a frontal system advecting the polluted air away. Snow cover was an important source of ambient moisture, enhancing particle growth and increasing aerosol water mass during many of the events. Snow melt and sublimation may also have released deposited aerosol precursors during episodes, including nitric acid and ammonia.

Only the last three episodes in March occurred without snow on the ground. January featured widespread regional snow cover across southeastern Wisconsin and northern Illinois throughout the month, while snow cover was lower in February and not consistently present in March (Figure 4-3). However, all four episodes in February and the first in March began on days with at least 0.5” of snow cover at both sites, and all of them ended with the snow completely melted at Milwaukee. On the days when February and March events began, snow covered the southern half of the region, and SNODAS snow depth was 2 to 4 times the average for the two months. These were among the most severe and long-lived episodes sampled during the WNS, including four of the five most severe events. All February and March days without snow cover occurred after fine particle episodes with consecutive days of temperatures above freezing. Sublimation of snow cover occurred during all episodes with snow cover. These strong February and March episodes were also marked by strong sublimation from the snowpack, with each

including one of the 10 days with the highest level of sublimation in SNODAS during the study. Thus, melting and sublimation of regional snowpack during particle events featuring a warm, stagnant, shallow boundary layer provided a source of moisture that contributed to event severity.

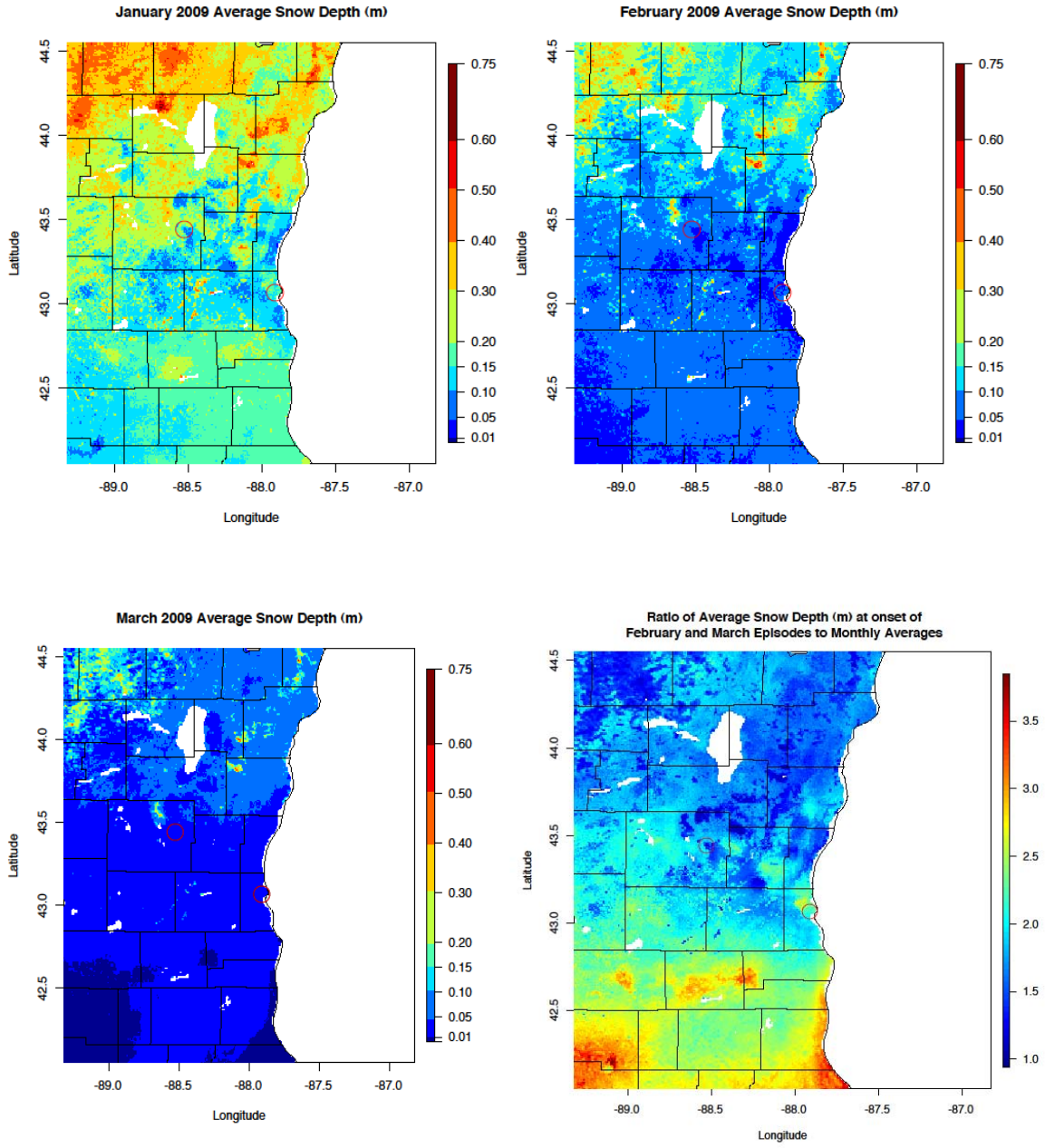

Figure 4-3. Average SNODAS assimilated 1 km snow depth (m) for each of the three months of the study, and the ratio of average snow depth on the first days of February and March episodes to the 2-month average. Mayville and Milwaukee sites circled.

Winds at Milwaukee, more than precipitation or snow cover, help explain why the two days that otherwise met the general criteria for fine particle episodes (1/17 and 2/21) did not generate strong events. The existing conceptual model for wintertime episodes, augmented by CART analyses throughout the region and WNS observations, is that low pressure, increasing temperature, high humidity, and slack winds coincided with a shallow and/or inverted boundary layer to reduce ventilation and increase conversion of precursors to the aerosol phase. Winds at Milwaukee during the WNS averaged 2.97 m/s, dropping to 2.30 m/s during local episodes (Table 4-1). On 1/17, despite a strong drop in pressure, rising temperatures, and high RH, hourly average wind speeds up to 4.56 m/s prevented $PM_{2.5}$ concentrations from building beyond 27 $\mu g/m^3$. On 2/21, high winds (averaging 4.12 m/s throughout the day and reaching 5.95 m/s), prevented $PM_{2.5}$ from reaching 20 $\mu g/m^3$. The absence of snowpack and 5.5" of snowfall may have further contributed. In both of these cases, winds were from the south, as during episodes, but were abnormally strong. Likewise, winds explain why Chicago did not experience a strong local fine particle event during the peak of the strongest episode at Mayville and Milwaukee on 1/22, when 24 hour average $PM_{2.5}$ concentrations were 34.6 $\mu g/m^3$ and 50.4 $\mu g/m^3$, respectively. Chicago had similar temperature, pressure, and relative humidity throughout the episode, but with wind speeds twice as high as Milwaukee that day, and so did not record an episode.

The impacts of actinic flux on rates of photochemical reactions has been hypothesized as a potential factor in wintertime particle events, but the lack of local observations of insolation made this factor difficult to address conclusively. The study sites are more than 100 km from the nearest site with direct insolation data, the University of Wisconsin Extension Automated Weather Observation Network station at Arlington, Wisconsin. Half-hourly insolation at this site was dramatically lower during Milwaukee episodes, by 30-50% in the mornings and by 10% at the noon daily maximum (Appendix 4-1), but similar during the afternoon. Visibility statistics at Milwaukee (Appendix 4-2) generally agree. As the decreases in insolation during episodes are greater than the extinction caused by aerosols at these concentrations, results suggest lower photolysis rates during fine particle episodes due to adsorption and scattering by clouds. Co-located photometer, nephelometer, and ceilometer observations may be useful additions to future studies.

Table 4-1. Hourly meteorological conditions averaged by fine particle episode status, January 1/1—3/31 2009. The fog binary is for a definition of fog as a difference between temperature and dew point of 2.5 ºC or less.

Site	Location	Variable	Units	Mayville Episode Hours	Milwaukee Episode Hours	No Episode	All Hours
Mayville	Site	Temperature	ºC	-6.36	-0.21	-5.21	-5.28
		Wind speed	m/s	3.75	3.84	3.98	3.96
		Wind direction	º	199.95	194.21	215.49	214.55
		Fog	1/0	0.74	0.51	0.23	0.28
		RH	%	83.82	79.27	71.42	72.18
	KFLD	Visibility	Km	9.49	11.91	14.76	14.44
		Fog	1/0	0.45	0.37	0.12	0.16
	Airport	RH	%	79.40	76.55	68.51	69.17
		Dry bulb	ºC	-6.61	-0.68	-4.93	-5.03
		Wet bulb	ºC	-7.46	-2.10	-6.44	-6.50
		Dew point	ºC	-9.69	-4.55	-10.10	-10.08
		Pressure	hPa	983.73	984.62	987.83	987.58
Milwaukee	Site	Temperature	ºC	-4.23	1.37	-3.61	-2.72
		Wind speed	m/s	2.33	2.30	3.11	2.97
		Wind direction	º	225.76	201.52	229.79	224.72
	MKE	Visibility	km	7.29	8.69	14.01	13.05
	Airport	Fog	1/0	0.18	0.21	0.08	0.10
		RH	%	74.93	72.84	62.60	64.44
		Dry bulb	ºC	-4.62	0.71	-3.69	-2.90
		Wet bulb	ºC	-5.74	-1.00	-5.56	-4.75
		Dew point	ºC	-8.54	-3.87	-10.14	-9.02
		Pressure	hPa	988.24	989.18	992.50	991.91

4.2 Airmass Back Trajectories

Air mass back trajectories from the Mayville and the Milwaukee sites were analyzed using the NOAA HYSPLIT model from January 1st to April 3rd, 2009 by D. Kenski at LADCO. 3-hourly meteorology input for trajectory calculations was taken from 40 km resolution NOAA Eta Data Assimilation System (EDAS). Starting times of back trajectories were 6 am, noon, 6 pm and midnight. Figures 4-4 to 4-9 show composite plots of back trajectories at 0, 500, and 1000 m in each month. Red dot trajectories indicate periods with $PM_{2.5}$ episodes at both sites, green dots for Milwaukee-only episodes, and blue dots for clean periods. Back trajectories that started closest to the first hour of a $PM_{2.5}$ episode were chosen for the analysis, in order to highlight conditions that initiated episodes. Appendix 9 contains a larger set of back trajectory plots, and also contains larger versions of Figures 4-4 to 4-9.

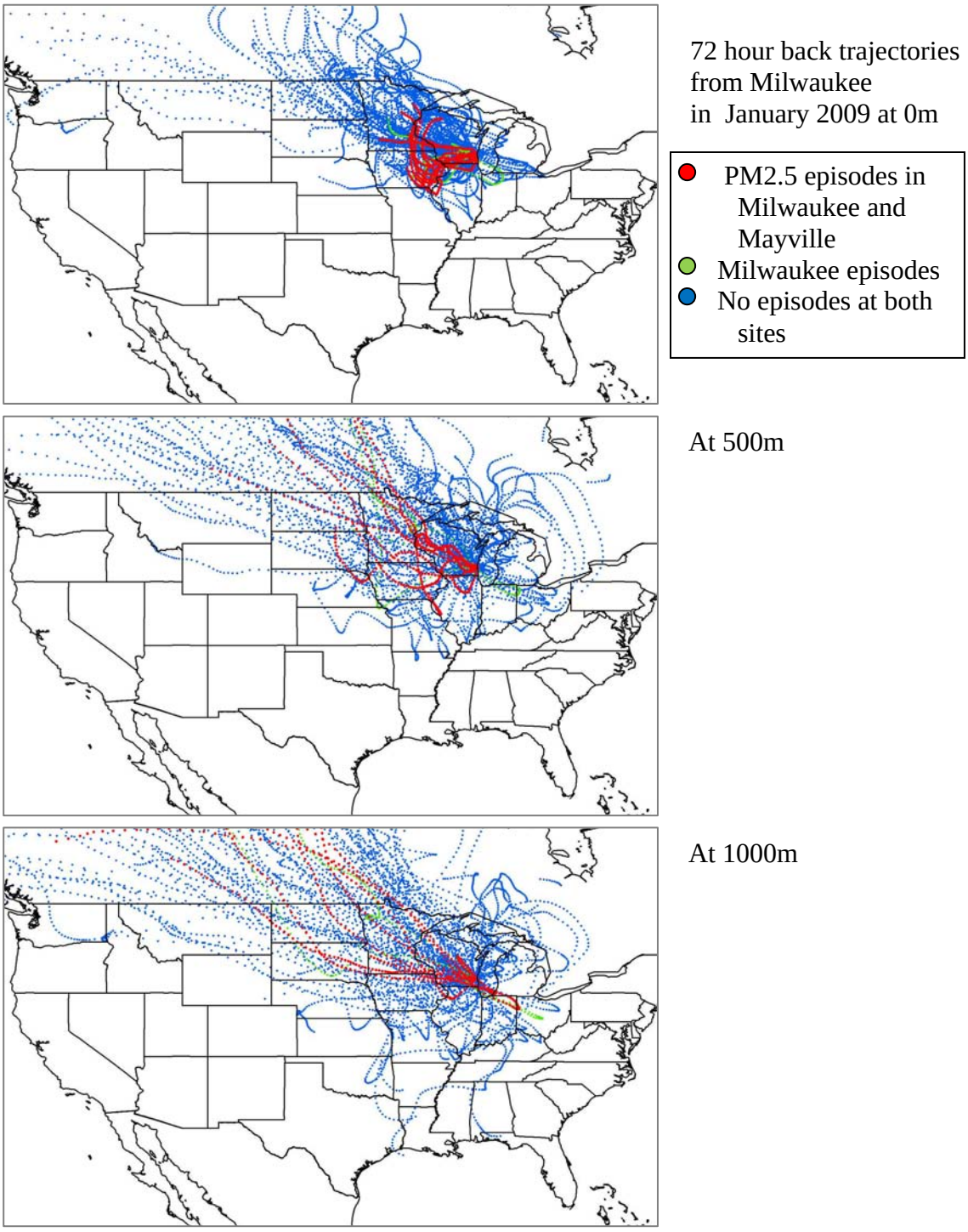

Figure 4-4. 72 hour back trajectories from the Milwaukee site in January 2009 at 0m, 500m, and 1000m. Back trajectories are analyzed at 6am, noon, 6pm and midnight every day.

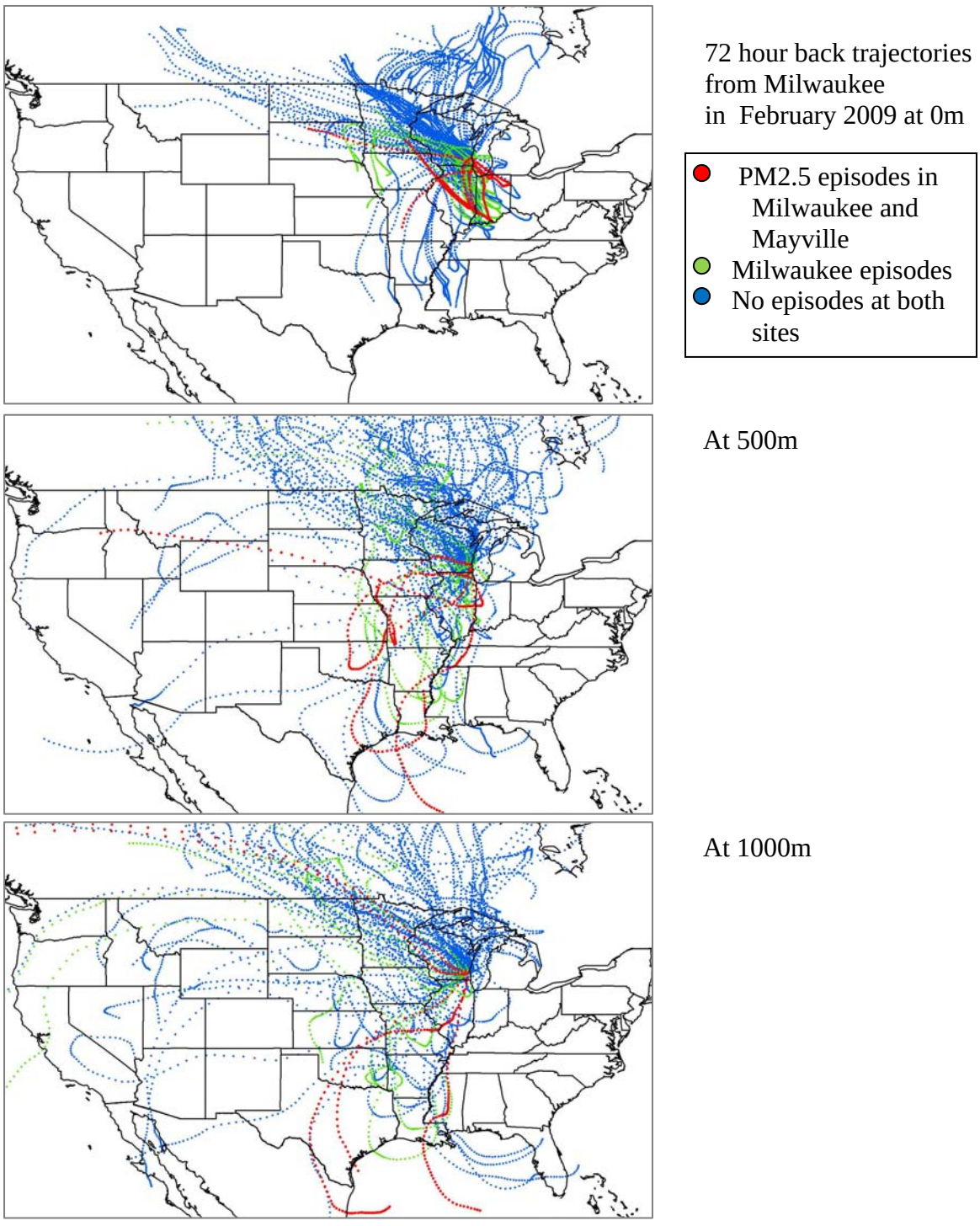

Figure 4-5. 72 hour back trajectories from the Milwaukee site in February 2009 at 0m, 500m, and 1000m. Back trajectories are analyzed at 6am, noon, 6pm and midnight every day.

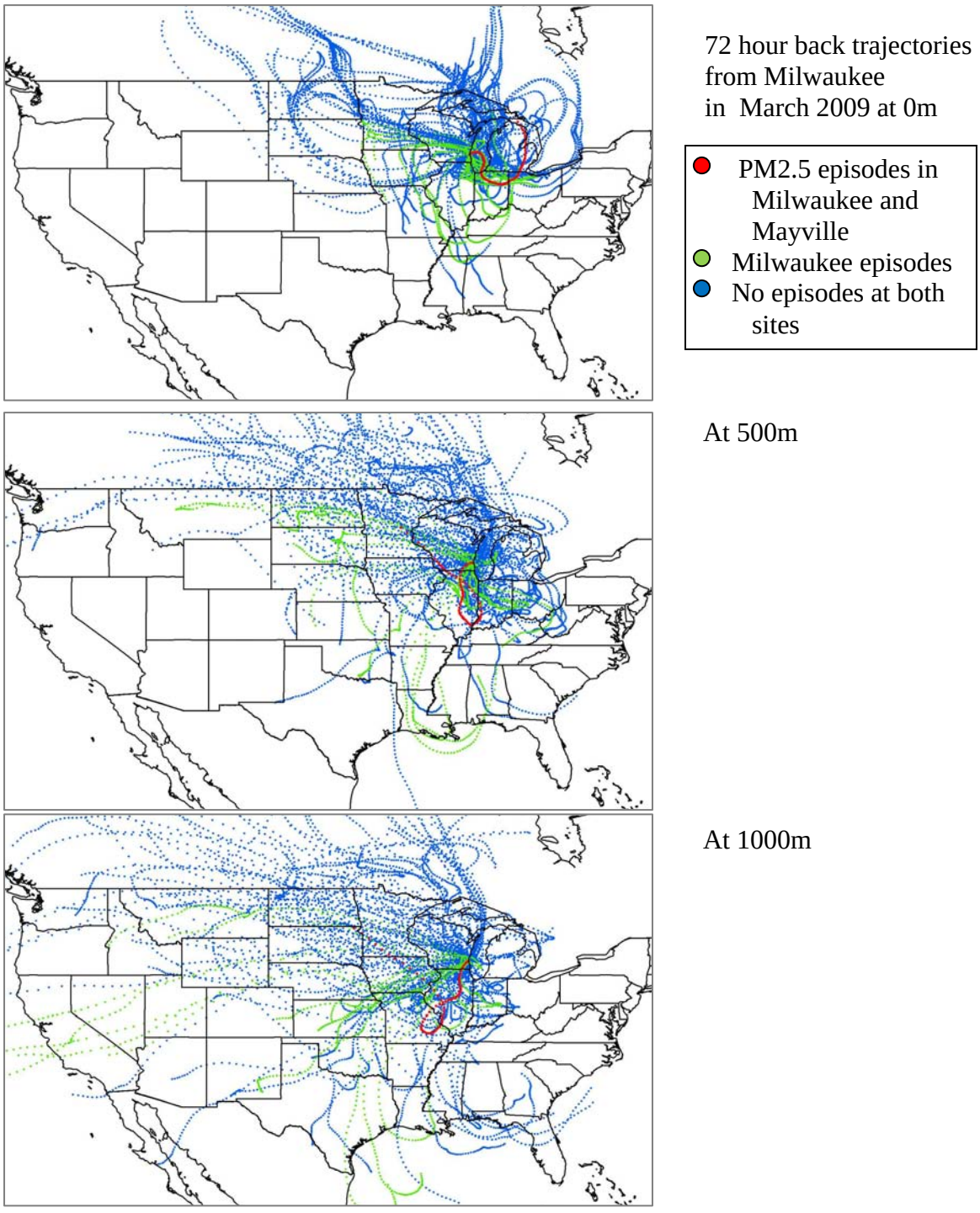

Figure 4-6. 72 hour back trajectories from the Milwaukee site in March 2009 at 0m, 500m, and 1000m. Back trajectories are analyzed at 6am, noon, 6pm and midnight every day.

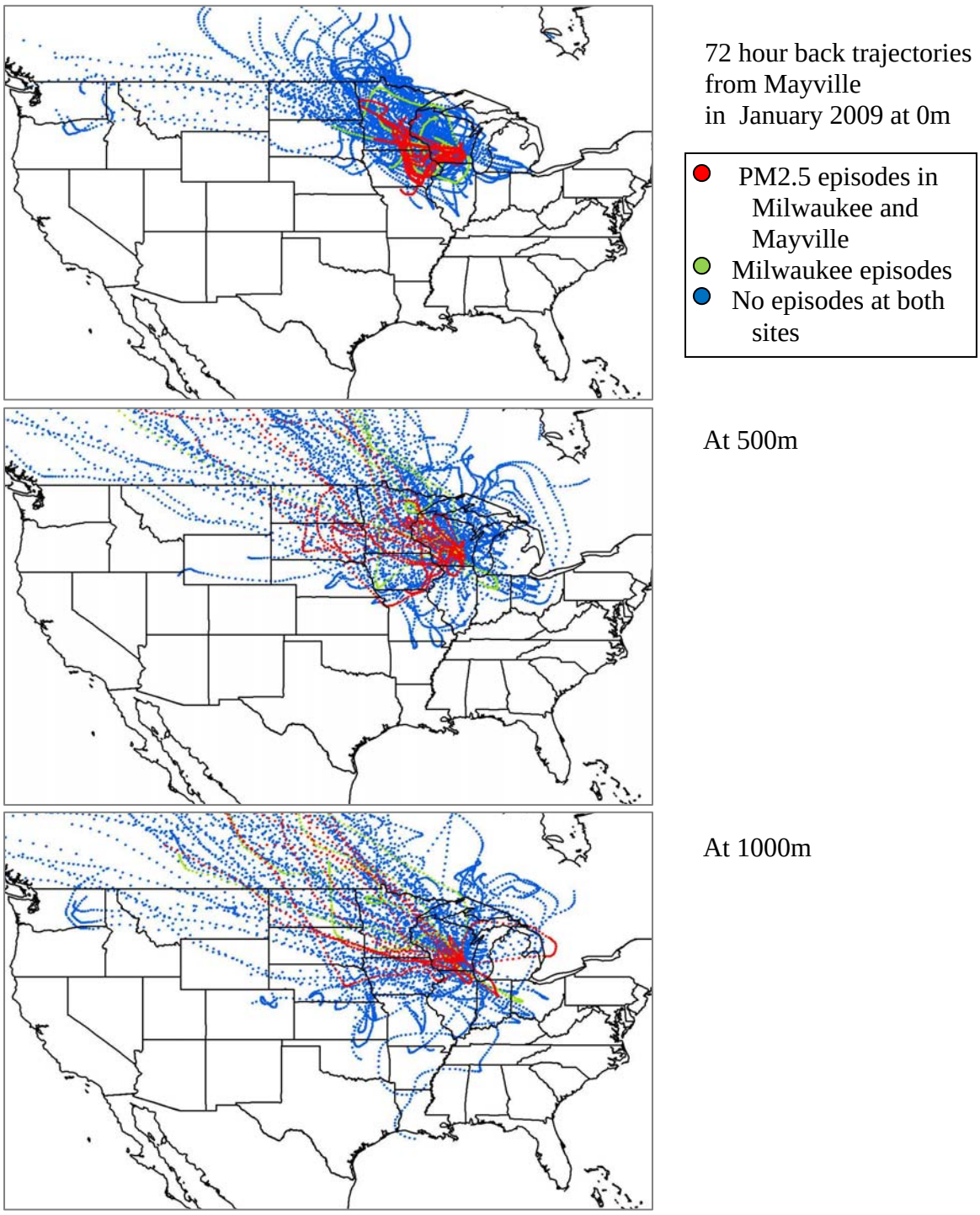

Figure 4-7. 72 hour back trajectories from the Mayville site in January 2009 at 0m, 500m, and 1000m. Back trajectories are analyzed at 6am, noon, 6pm and midnight every day.

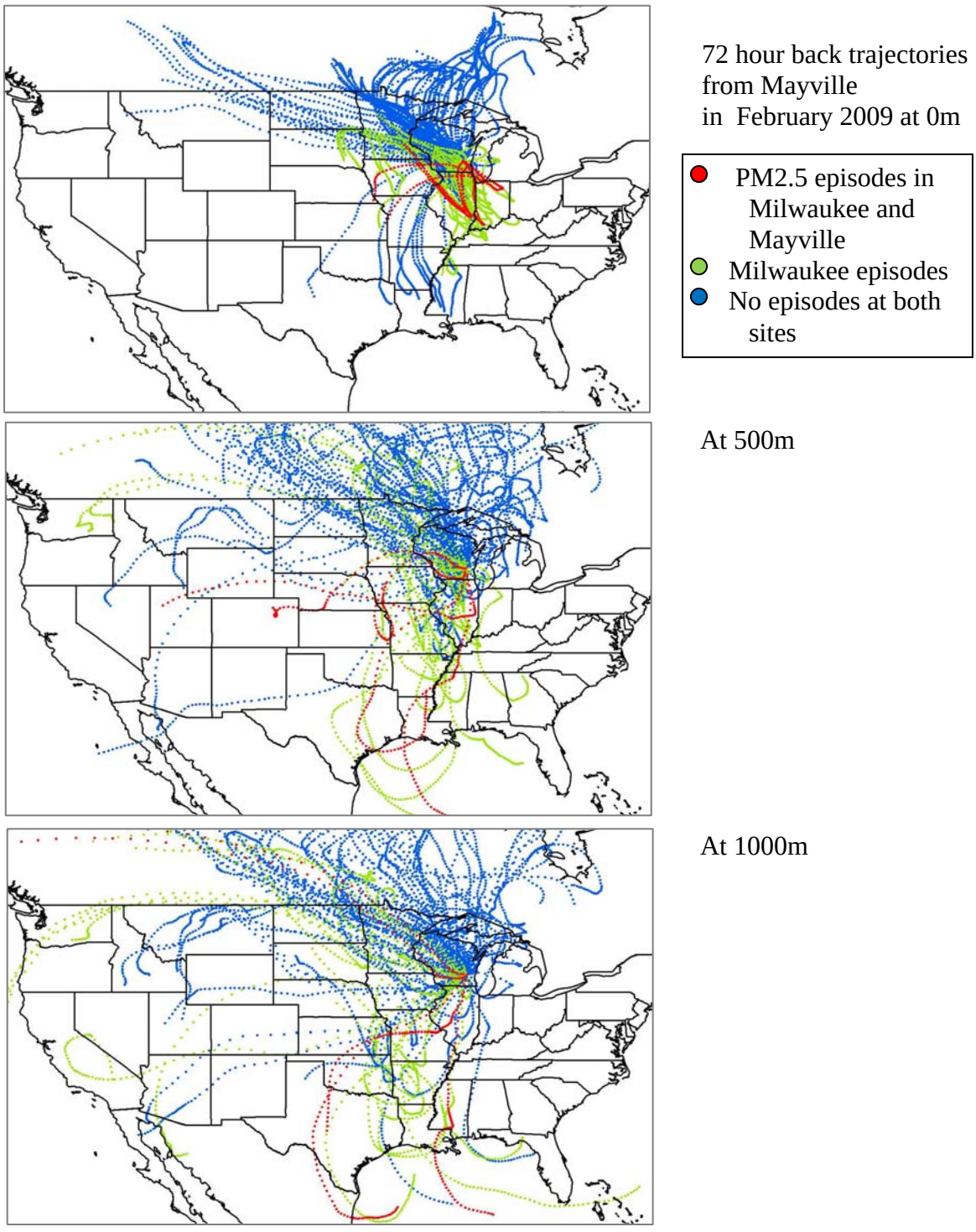

Figure 4-8. 72 hour back trajectories from the Mayville site in February 2009 at 0m, 500m, and 1000m. Back trajectories are analyzed at 6am, noon, 6pm and midnight every day.

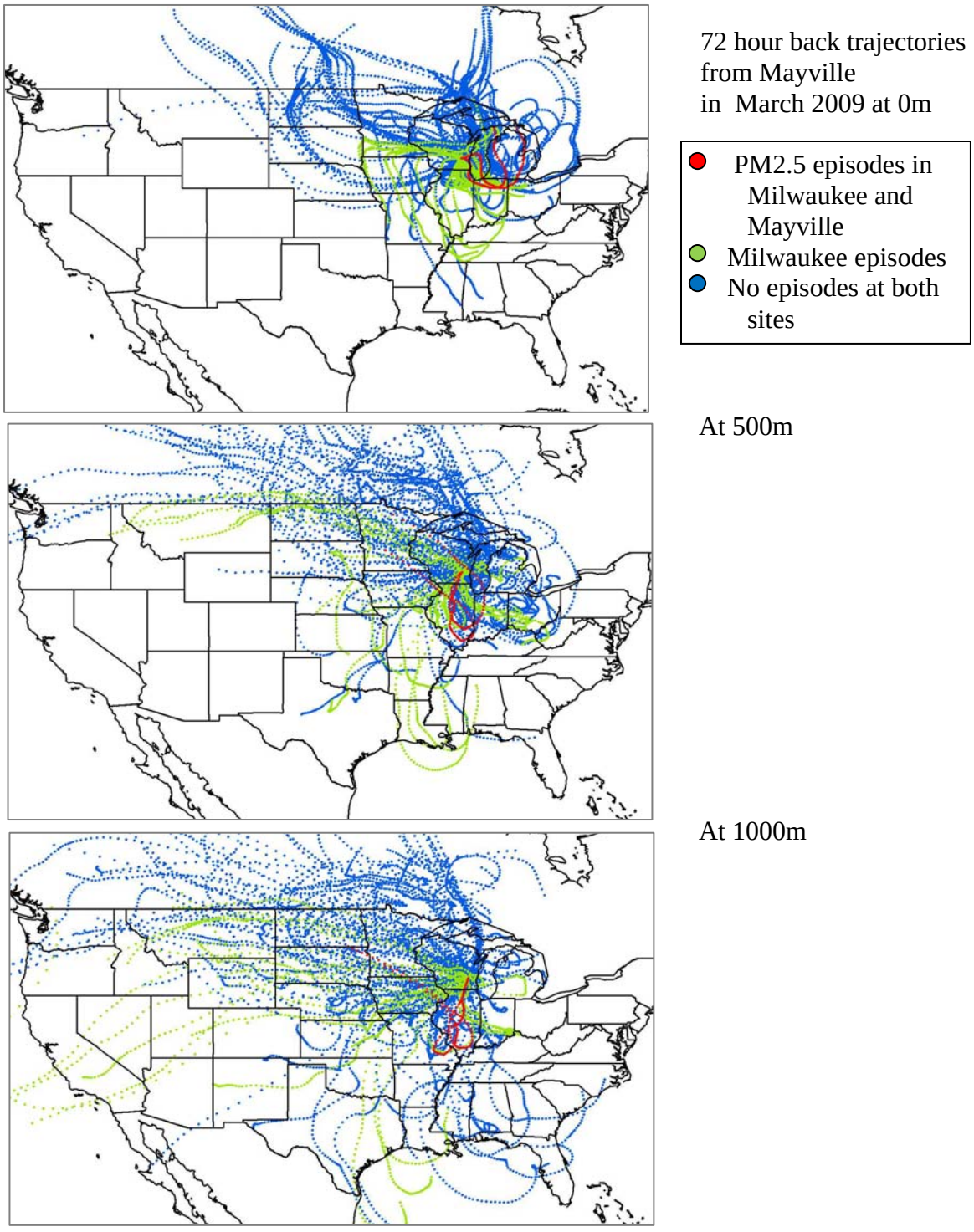

Figure 4-9. 72 hour back trajectories from the Mayville site in March 2009 at 0m, 500m, and 1000m. Back trajectories are analyzed at 6am, noon, 6pm and midnight every day.

Winds blew mostly from the west and northwest in January, and episodes typically occurred in airmasses originating to the west and west-southwest at low wind speeds. In February, winds from the south and north-northwest prevailed. Most episodes happened under southerly wind conditions. In March, wind most often blew from the north, but episodes were still defined by southerly winds.

The frequencies of airmass passage over neighboring states and regions (Figure 4-10) were analyzed for episode and non-episode periods in each month (Figures 4-11 and 4-12). Higher $PM_{2.5}$ concentration periods were associated with transport from regions located to the south, including southern Wisconsin, western Iowa, Illinois, and Indiana. Lower $PM_{2.5}$ concentration periods were associated with transport from regions to the west and north, including Minnesota and Canada. Based on trajectory analysis, there was no evidence that Mayville episodes were ever due directly to air polluted during passage over Milwaukee; these conditions occurred only eight times out of 1,030 cases for the three months, and never during episodes. However, we recognize that there are uncertainties in this conclusion due to the spatial resolution of the meteorological data as Milwaukee is only roughly one gridcell in the 40km NOAA EDAS model.

Figure 4-10. Regions to calculate frequency of air mass passage. States boundaries and US boundaries are used for the outside of the regions.

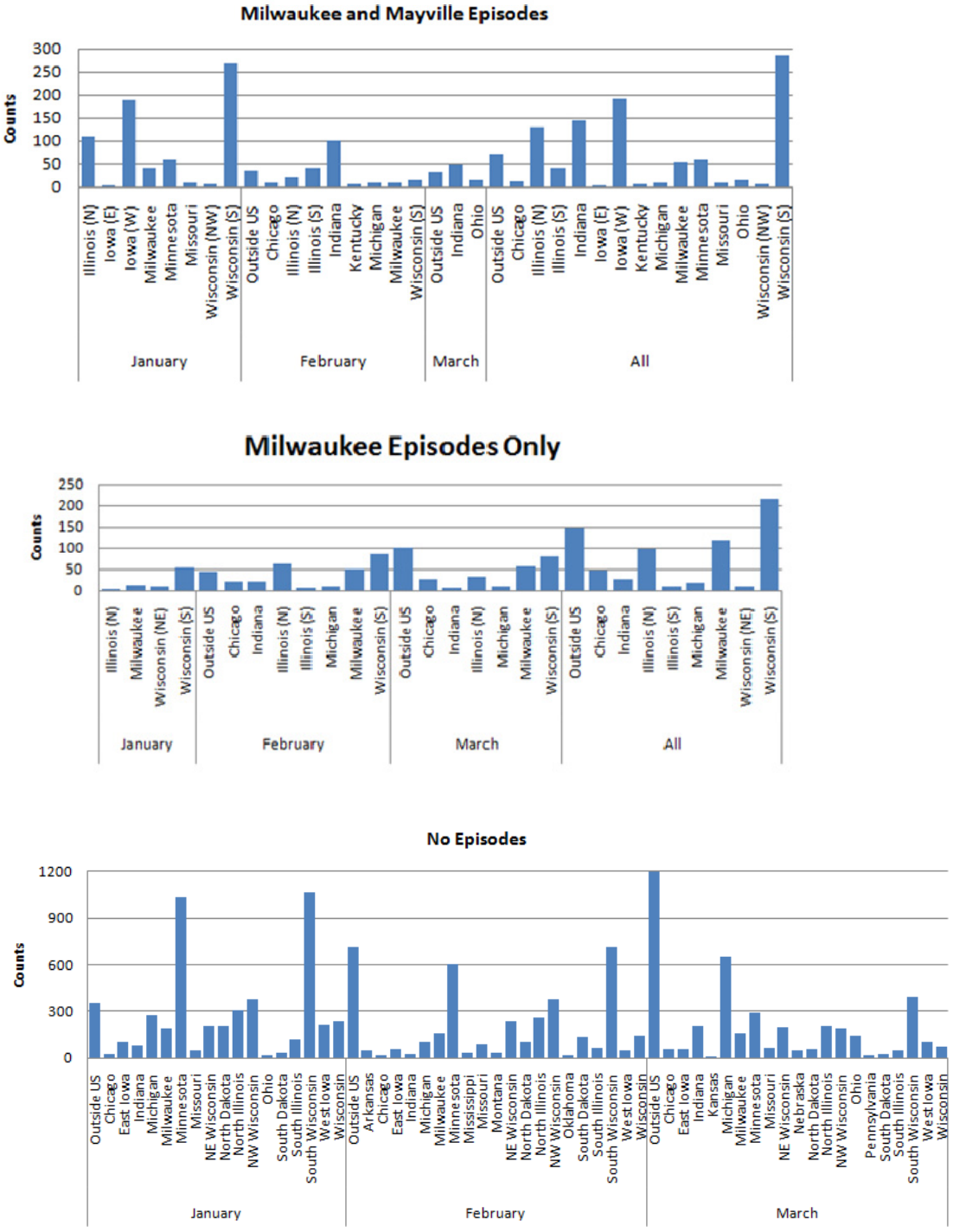

Figure 4-11. Histograms of air mass passages in the 48 hour back trajectories from Milwaukee at 0 m starting height. Histograms are plotted: 1) when there were PM2.5 episodes in both Milwaukee and Mayville; 2) only in Mayville; 3) only in Milwaukee; and 4) no episodes in both sites.

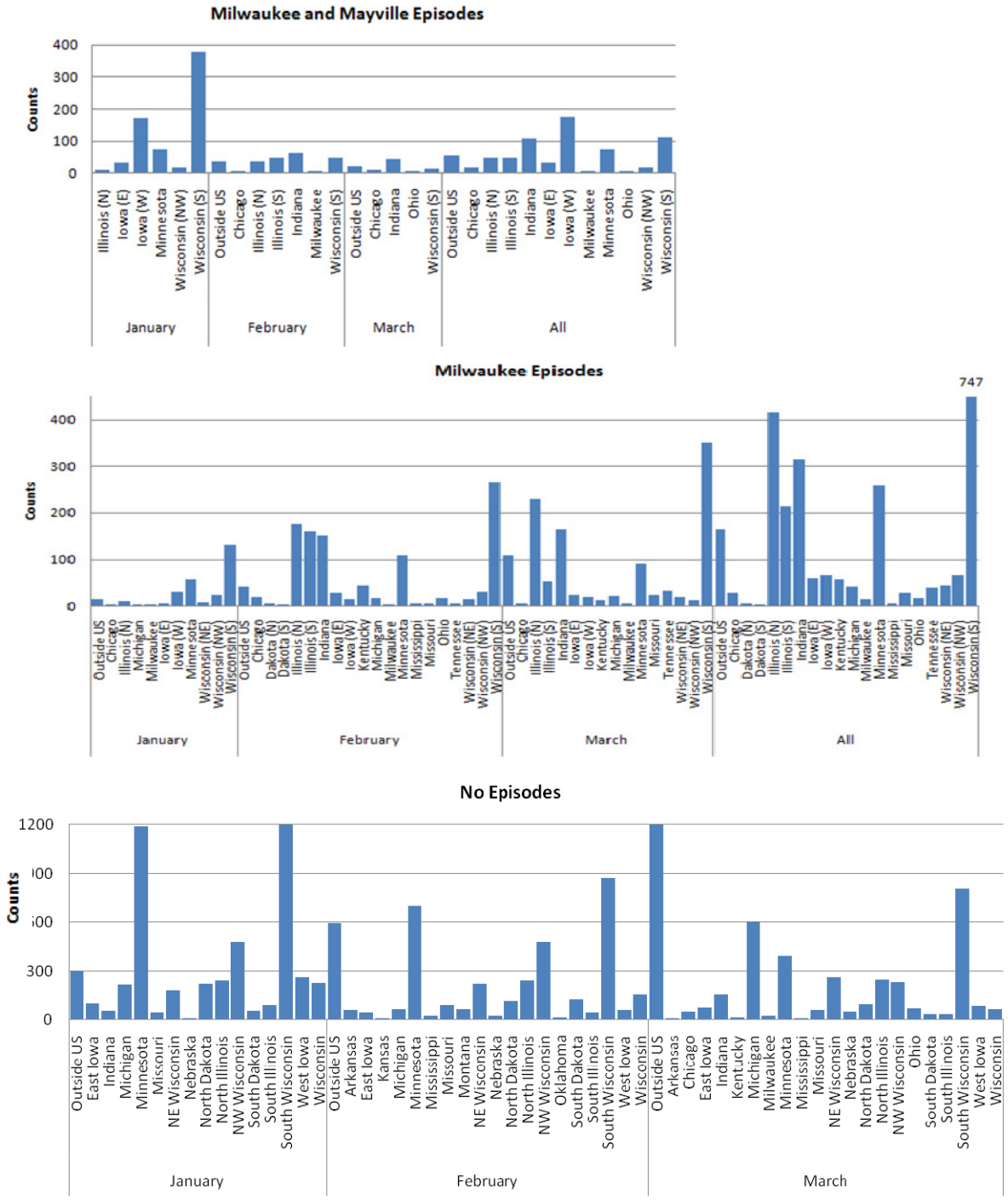

Figure 4-12. Histograms of air mass passages in the 48 hour back trajectories from Mayville at 0 m starting height. Histograms are plotted: 1) when there were PM2.5 episodes in both Milwaukee and Mayville; 2) only in Mayville; 3) only in Milwaukee; and 4) no episodes in both sites.

4.3 WINTER FINE PARTICLE EPISODES, 2002—2008

The level of episodic $PM_{2.5}$ particle pollution in Wisconsin during the WNS study period was above historical average levels. This has been investigated in three ways. First, a database of daily FRM and IMPROVE $PM_{2.5}$ mass values for the U.S. for the period Jan 2001 – Mar 2009 was assembled. This was then used to make a daily smoothed (kriged) $PM_{2.5}$ surface for the upper Midwest. Then on a pixel-by-pixel basis, this smoothed surface was used to calculate an episode index for the period. The episode index for a given cell is as follows:

INDEX = $\sum \max[0, (PM_{2.5} - 27)]$ where the sum is over multiple days and the units of this are in ug m^{-3} days. Accumulation of this quantity to 62 μg m^{-3} days is necessary (but not sufficient) for a 98^{th} percentile concentration of 35.5 μg m^{-3}. Figure 4-13 shows this index for the months of Jan-Mar for the years 2001-2009, and for the WNS study period. The black line shows the 62 μg m^{-3} day threshold, indicating how the strong 2009 WNS episodes were more localized and less regionally widespread than in prior years.

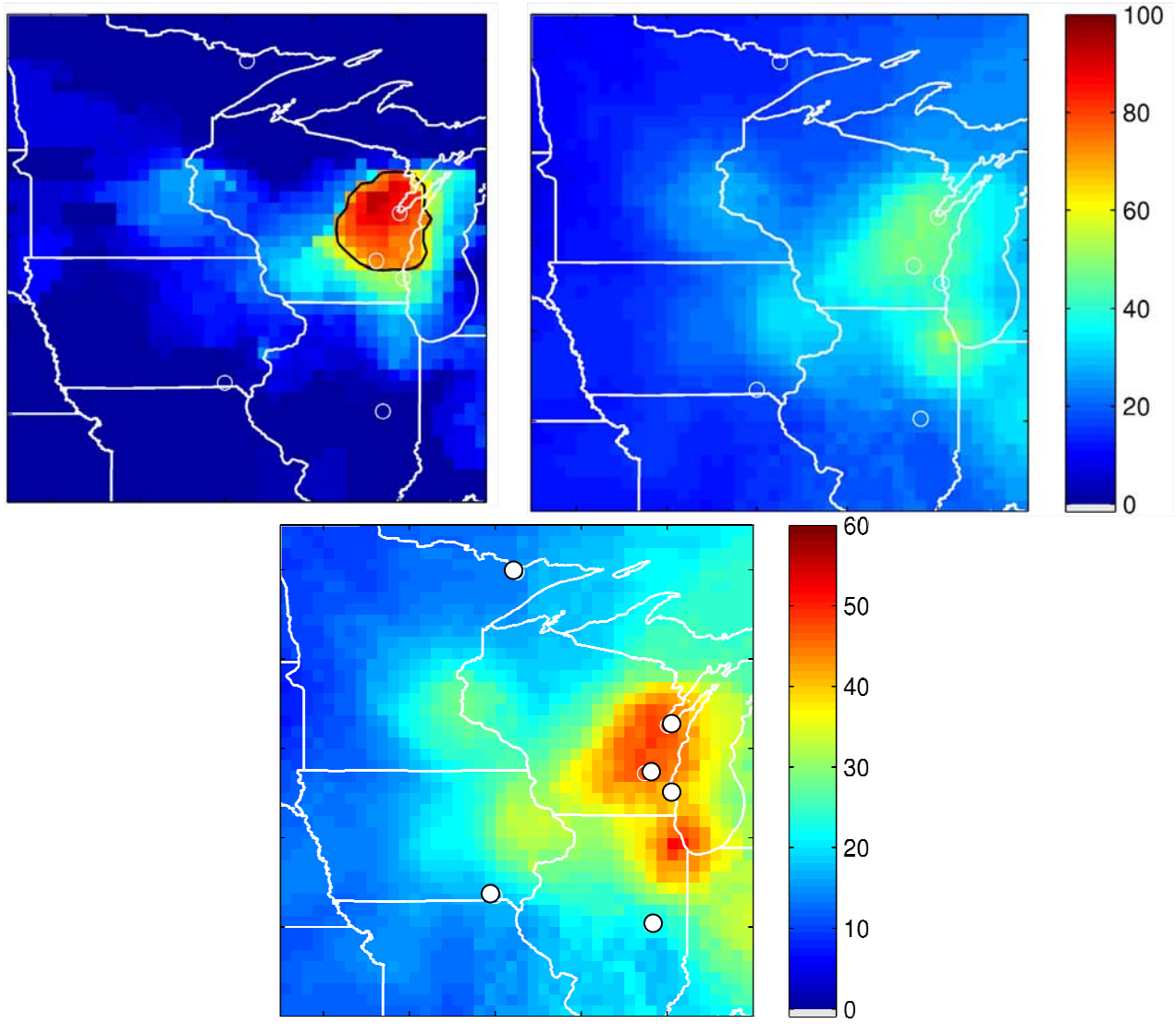

Figure 4-13. Historical average episode activity during January – March and the activity during the WNS period. Upper panels show 2009 JFM (left) and 2001-2009 JFM (right) using the same scale of 0-100 μg m^{-3} x day. Lower panel shows the long term 2001-2009 JFM average on a 0-60 μg m^{-3} x day scale so that the spatial structure can be seen. Black line shows a 62 μg m^{-3} x day threshold. Lower panel shows white dots for the five sites plotted in figure 4-15. From north to south, Boundary Waters; Green Bay; Mayville; Milwaukee; Lake Sugema IA; and Bondville IL.

A second way of looking at it is to use the same index, but to look at individual site concentrations. This avoids any artifacts that the spatial smoothing might impose on the data. On average, Jan-Mar episode activity is higher at Milwaukee than at Mayville (64 vs. 34), a ratio of 1.9:1. During the 2009 WNS, the ratio of the episode indicator was similar, but episode activity was elevated at both locations (151 at Milwaukee for 2009 and 80 for Mayville at 2009).

Figures 4-14 and 4-15 show that high episode activity years are 2009, 2005, and 2001. 2008 is moderate in Milwaukee but clean in Mayville. The kriged surfaces from Figure 4-13 are not in perfect agreement with the more accurate site-specific indices (The kriged surface has Mayville as more prone to episodes than Milwaukee when Figure 4-14 has the opposite). The kriging procedure tends to smooth out concentrations, lowering them at the edges of high concentration regions (such as in Milwaukee), and increasing concentrations at locations surrounded by polluted monitors (such as Mayville with Milwaukee, Green Bay, and Madison influencing it in the kriging process.

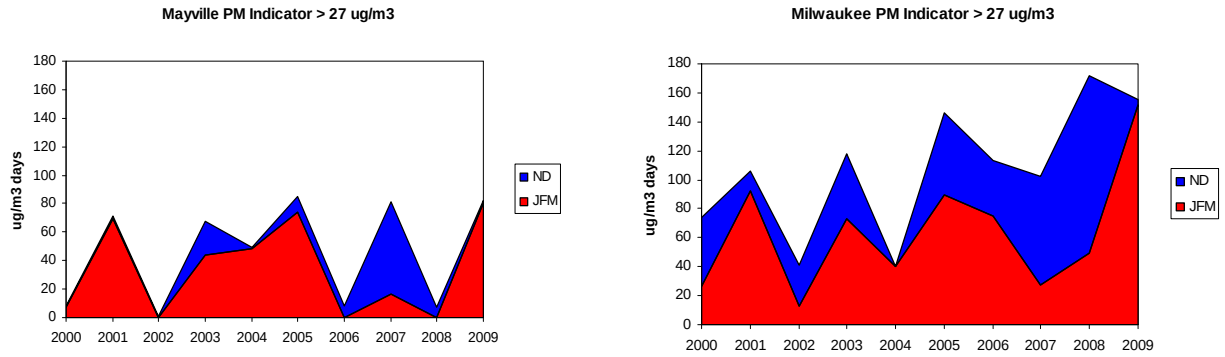

Figure 4-14. The episode indicator graphed on a year-by-year basis for Jan-Mar (red) and Nov&Dec (blue). November and December are offset by a year. For example, Nov08 and Dec08 are graphed at the 2009 tick to indicate the winter of 2008/2009. The LADCO WNS is characterized by the red area during year 2009. At Mayville, the episode indicator was 80 relative to its mean value of 34. At Milwaukee, the indicator was 151 versus an average value of 64. For reference, five episodes each with a single daily $PM_{2.5}$ reading of 37 μg m^{-3} would give an indicator value of 5x(37-27) or 50.

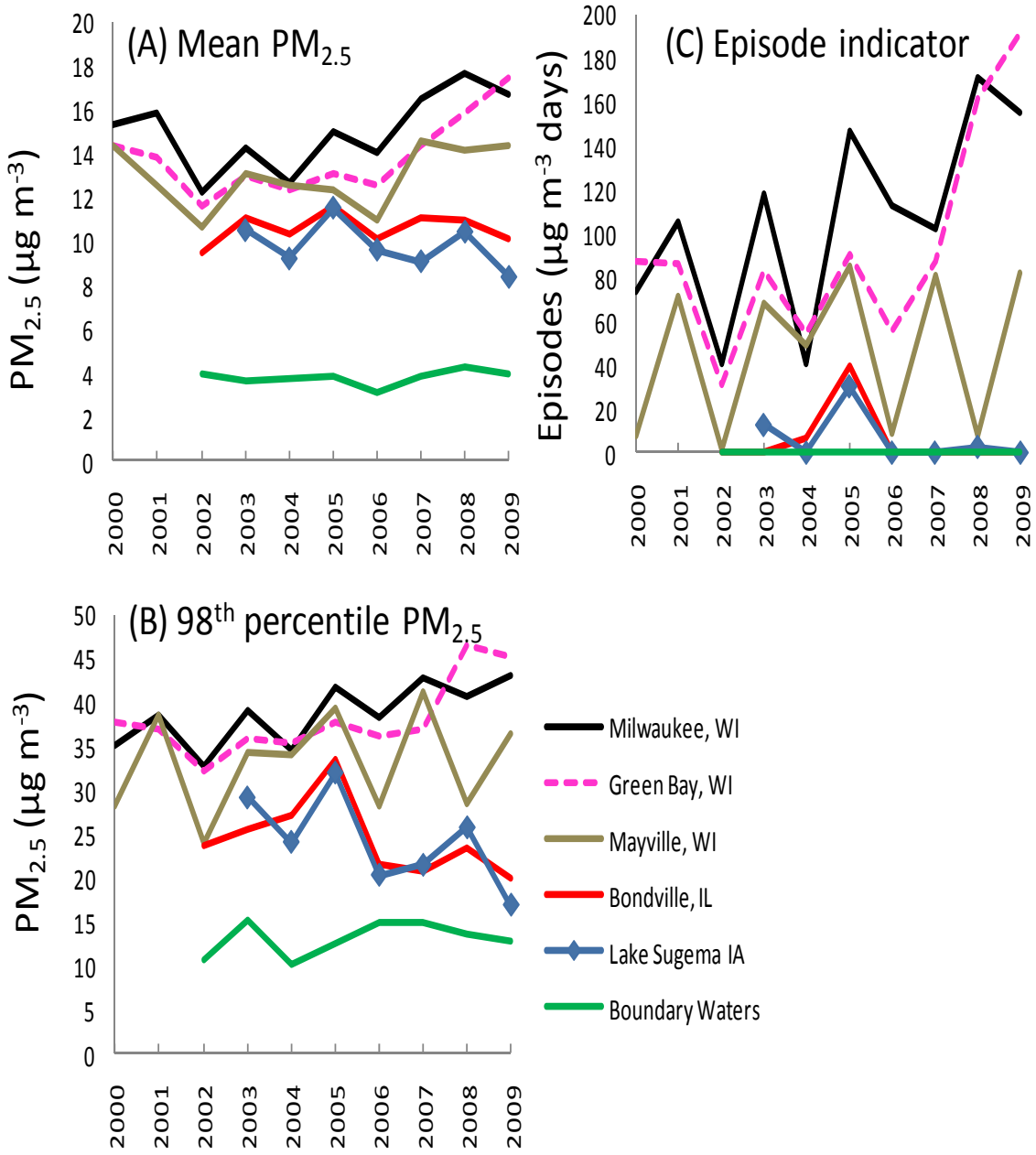

Figure 4-15. Panel A shows mean $PM_{2.5}$ for the cold winter season (Nov-Mar) of each year. Panel B shows the 98th percentile for each of these five month periods, and panel C shows the episode indicator variable in units of µg m^{-3} x days. For reference, five episodes each with a single daily $PM_{2.5}$ reading of 37 µg m^{-3} would give an indicator value of 5x(37-27) or 50. Map of these sites can be found in Figure 4-13.

Figure 4-15 shows that the Wisconsin sites were more polluted than IMPROVE sites at Bondville, IL, Lake Sugema, IA, and Boundary Waters MN, which are representative of regional background $PM_{2.5}$, and are locations that were identified through back trajectories as consistently

upwind of Milwaukee and Mayville during the winter. These sites are all shown together using actual IMPROVE or EPA $PM_{2.5}$ data (not Kriged data) for the entire cold weather season (Nov-Mar). There are sustained increasing trends in the episode indicator and 98^{th} percentile $PM_{2.5}$ at Milwaukee and Green Bay from 2004-2009 not seen at the other sites, which featured flat or decreasing concentrations and negligible episodes (Figures 4-14 and 4-15). An in-depth analysis of inter-annual climate and weather variability and trends in aerosol speciation and precursor emissions would identify potential source(s) of this localized increase in Milwaukee.

RFERENCES

Lake Michigan Air Directors Consortium (2009). Conceptual Model of PM2.5 Episodes in the Midwest.

National Operational Hydrologic Remote Sensing Center. 2009. Snow Data Assimilation System (SNODAS) Data Products at NSIDC. Boulder, Colorado USA: National Snow and Ice Data Center. Digital media.

5 URBAN AND DIRECTIONAL EXCESS CONCENTRATIONS

5.1 Urban Excess Calculations

Measured gas and $PM_{2.5}$ species at Milwaukee and Mayville were compared to determine differences in air mass composition during episode and non-episode periods. Specifically, measured gas and $PM_{2.5}$ species were averaged over the study period (from January to March) using all hourly observations, Milwaukee only episode hours, and both Mayville and Milwaukee episode hours. These urban excess calculations are shown in Table 5-1. Table 5-1a has values calculated using 24-hr samples. Table 5-1b has values calculated using hourly values. For example, all hours $PM_{2.5}$ values were 17.3 and 11.8 $\mu g\ m^{-3}$ at urban and rural sites respectively, a difference of 5.5 $\mu g\ m^{-3}$ or 46% of the rural aerosol concentration. Confining the analysis to hours identified as episode hours at both locations, then the mean $PM_{2.5}$ values were 42.9 and 33.6 at urban and rural sites respectively, a difference of 9.3 $\mu g\ m^{-3}$ or 28% of the rural aerosol concentration. Confining the analysis to hours identified as episode hour at only Milwaukee, then the mean $PM_{2.5}$ values were 32.5 and 18.9 at urban and rural sites respectively, a difference of 13.7 $\mu g\ m^{-3}$ or 73% of the rural aerosol concentration.

Averages of gas and $PM_{2.5}$ species over the study period using the hourly data are shown in Figure 5-1 (a-c). Since organic carbon and elemental carbon measurements were available only on a daily basis once every three days, the average of daily $PM_{2.5}$ measurements were analyzed and plotted separately (Figure 5-1 (d-f)). Mayville and Milwaukee showed typical urban-rural contrast; higher NO_y, organic carbon and elemental carbon levels in the urban area due to local sources, and higher ozone concentrations in the rural area. During the $PM_{2.5}$ episodes average concentrations of PM nitrate, OC and EC at both sites increased significantly, by ~6, 3, and 0.4 $\mu g\ m^{-3}$, respectively. The urban excess values during episodes of organic carbon and elemental carbon and total NO_y increased significantly (Table 5-1).

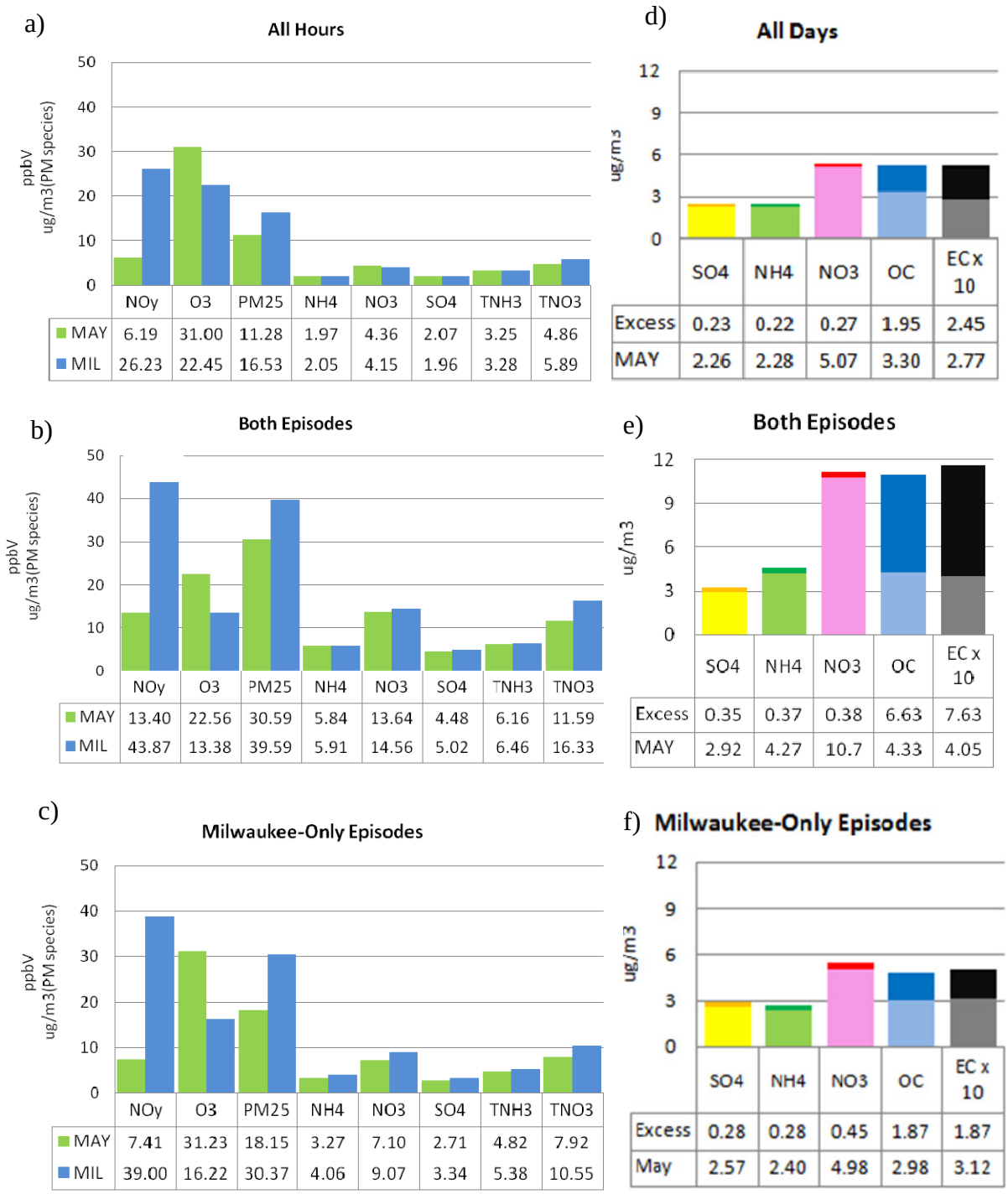

Figure 5-1. Averages of gas and $PM_{2.5}$ species over the study period. Panels a-c are averages of hourly measurements at Mayville (MAY) and Milwaukee (MIL). Panels d-f are averages of daily PM species concentrations at Mayville (MAY, bright colors) and urban excess at Milwaukee (Excess, dark colors). Daily PM measurements do not cover the all days in the study period since they are available every three days. EC values are multiplied by 10 for presentation.

Table 5-1a and table 5-1b lead to the same conclusion, that OC and EC dominate the urban excess, except perhaps during Milwaukee only episodes, when there is buildup of some excess inorganics.

Table 5-1a. Urban excess at Milwaukee in percentages of rural concentrations based on daily measurements.OC measurements on Jan 22 are excluded.

Species	All days	Milwaukee-Mayville episodes	Milwaukee only episodes
$PM_{2.5}$	14	18	4
Sulfate	10	12	11
Ammonium	9	9	11
Nitrate	5	4	9
OC	10	47	63
EC	41	16	60

Table 5-1b. Urban excess at Milwaukee in percentages of rural concentrations based on hourly measurements

Species	All days	Milwaukee-Mayville episodes	Milwaukee only episodes
$PM_{2.5}$	46	28	73
Sulfate	-8	-2	12
Ammonium	3	0	25
Nitrate	-5	5	31
NO_y	320	227	427

Daily averages of speciated $PM_{2.5}$, ozone and NO_y at Mayville and Milwaukee are plotted in Figure 5-2. Days when $PM_{2.5}$ episodes occurred are identified in green. Levels of ozone were higher at Mayville and NO_y was higher at Milwaukee throughout the study period. It is clear that "Other $PM_{2.5}$", which is unmeasured $PM_{2.5}$ species calculated by subtracting SO_4, NO_3 and NH_4 from the total $PM_{2.5}$ concentrations, is a major contributor to urban excess at Milwaukee. From figure 5-1e and 5-1f, it can be seen that the other $PM_{2.}5$ is primarily organic carbonaceous aerosol.

Figure 5-3 contains similar plots of the SEARCH monitoring sites for all hours, when $PM_{2.5}$ episodes were present and absent at Jefferson Street (Jefferson St. as an urban site and Yorkville as a rural site). At the SEARCH monitoring sites, hourly OC and EC measurements are available, so only plots using hourly averages are shown. NO_x and NO_y levels were higher at Jefferson St., and ozone and ammonia were higher at Yorkville. In contrast to Milwaukee-Mayville measurements, organic carbon was the major constituent that drove the $PM_{2.5}$ episodes,

higher than observations in the non-episode periods by 7 μg m^{-3}. Urban excess values were similar for episode and non-episodes periods for OC and EC concentrations, because the enhancements were the same at these sites during the $PM_{2.5}$ episodes.

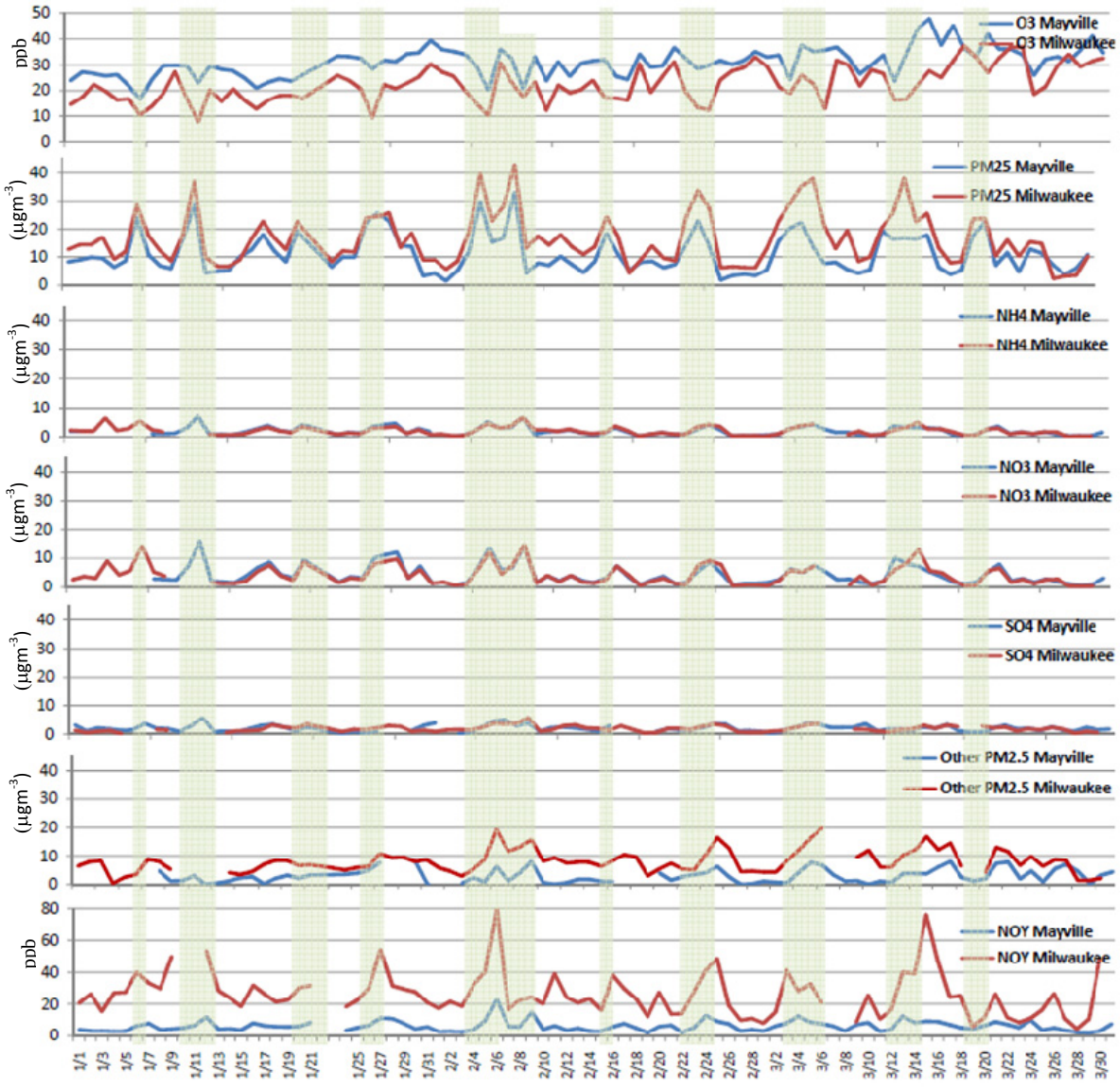

Figure 5-2. Daily averages of ozone, NO_y and $PM_{2.5}$ species over the study period at Mayville and Milwaukee. Green boxes indicate days when $PM_{2.5}$ episodes occurred.

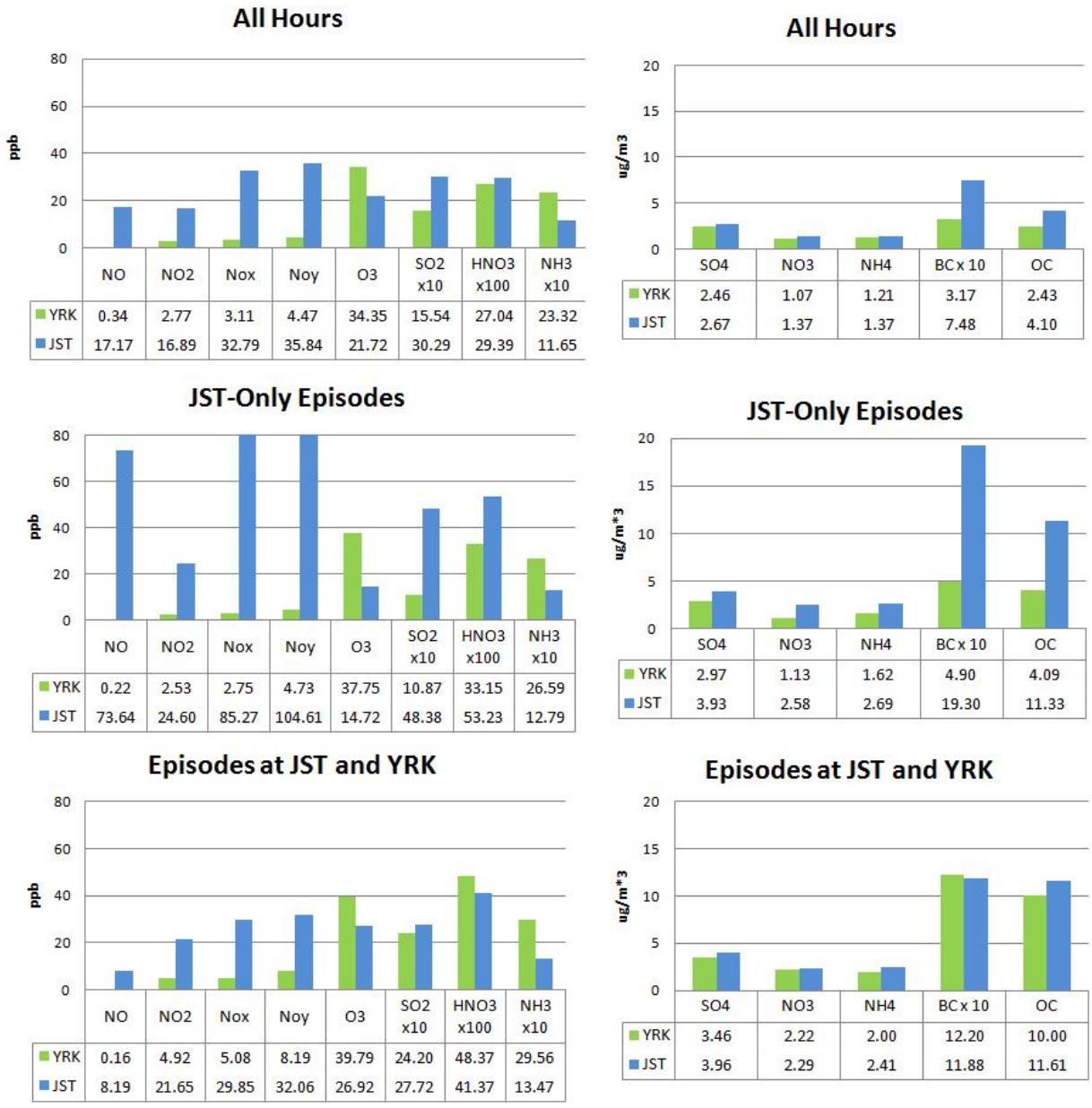

Figure 5-3. Averages of gas and $PM_{2.5}$ species measurements at the Yorkville (YRK, green bars) and Jefferson St. sites (JST, blue bars) from the SEARCH monitoring network (January 2009 to March 2009). All species were measured every hour. Note that BC, SO_2 and NH_3 measurements are multiplied by 10, and HNO_3 by 100 for presentation.

5.2 Directional Source Analysis

Directional analysis was performed for the period 01/01/2009 to 03/31/2009. Pollution roses, bivariate polar plots, and conditional probability function (CPF) plots were examined for all measured species at each site (summarized in Table 3-1). Pollution roses are wind rose plot with colored pollution concentration instead of wind speed. Bivariate polar plots graph measured concentrations (color) versus wind direction (angle) and wind speed (radius). CPF is probability of the measurement exceeding a threshold value relative to the total number of measurements at a specific wind angle. In other word, a CPF showing a value of 0.5 at the north direction means 50% of samples with wind from the north exceeded the threshold value. In the followings section, only species showing significant directionality are discussed.

5.2.1 Wisconsin Sites

Milwaukee: The Milwaukee site is located on a busy street (N. Martin Luther King Dr.), north of the downtown area, and is nearby to many local sources. As shown in Figure 5-4a, winds from the WNW, NW, and SE were dominant, while winds from the east and north (0 to 90^o) were infrequent. The mean wind speed was 3 ms^{-1}. As shown in figure 5-6a, higher $PM_{2.5}$ concentrations (yellow and red dots) are mostly shown in southern half. When the bivariate polar plot is drawn with $PM_{2.5}$ episodes only (Figure 5-6b), high concentrations were located in all directions. A CPF plot for $PM_{2.5}$ with a 15 $\mu g\ m^{-3}$ threshold shows highest probability with southern winds (150 to 240^o). However a CPF with a threshold value of 35 $\mu g\ m^{-3}$ shows very weak directionality (less than 0.2 for all directions). The $PM_{2.5}$ pollution rose (Figure 5-6d) also support this as it shows high concentration (>44 $\mu g\ m^{-3}$) in all direction. During episodes, the $PM_{2.5}$ concentrations do not show significant directional dependence which supports the conclusion that most $PM_{2.5}$ identified as episodic in this work is not from specific nearby sources. NO_x, a key indicator of primary emissions, showed strong directionality. Figure 5-7a shows that high concentrations were measured under southerly and westerly winds (160 to 240^o) with low wind speed (less than 2 ms^{-1}). The CPF of NO_x (Figure 5-7b) with a threshold value 53 ppb (annual NAAQS) and 100 ppb (hourly NAAQS) shows 0.2 and 0.1 respectively. However, when only low wind speed (less than 2 ms^{-1}) data are used (blue line) a much more prominent directional feature appears. As shown in Figure 5-5, interstate 43 is located 700 m to the west of the Milwaukee site and interstate 794 is located 2.8 km to the south. The CPF of NO_y (Figure 5-

7c) shows similar directionality. The CPF of NH_3 (figure 5-7d) shows SW-WSW (200 to 270^o) directionality.

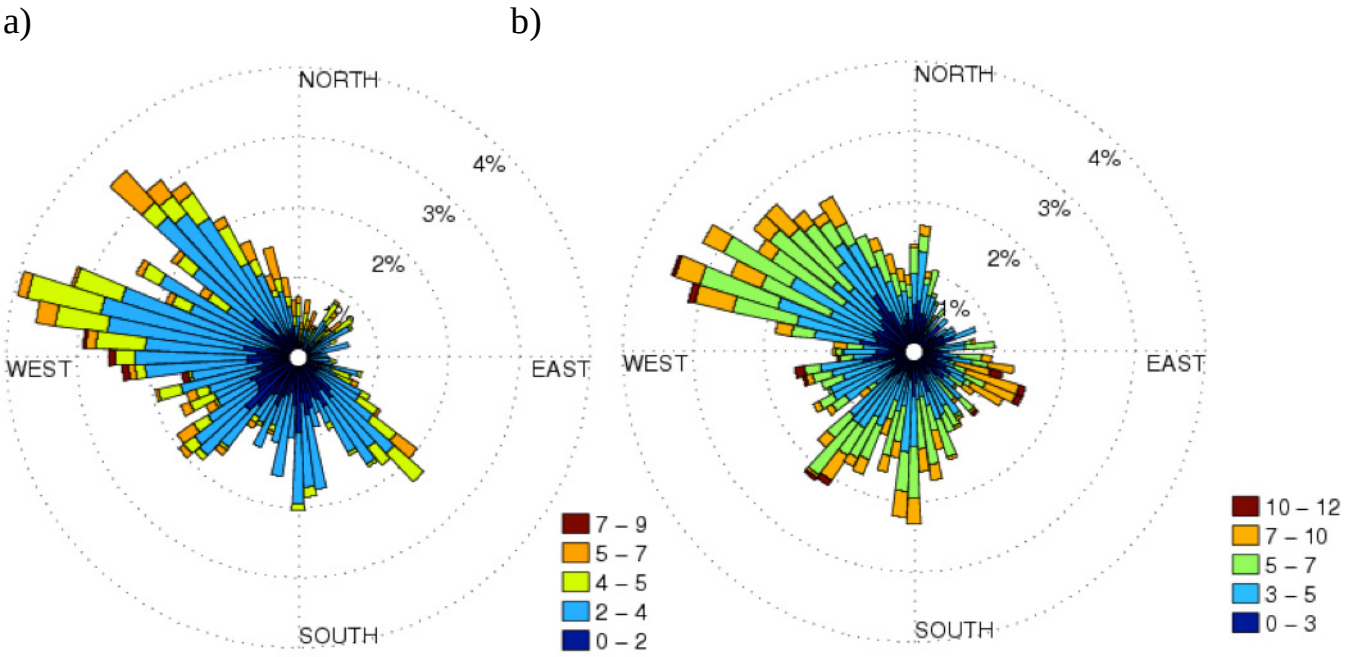

Figure 5-4. Wind roses for a) Milwaukee and b) Mayville.

Figure 5-5. Location of Milwaukee site (DNR SER HQRT) with surrounding highways.

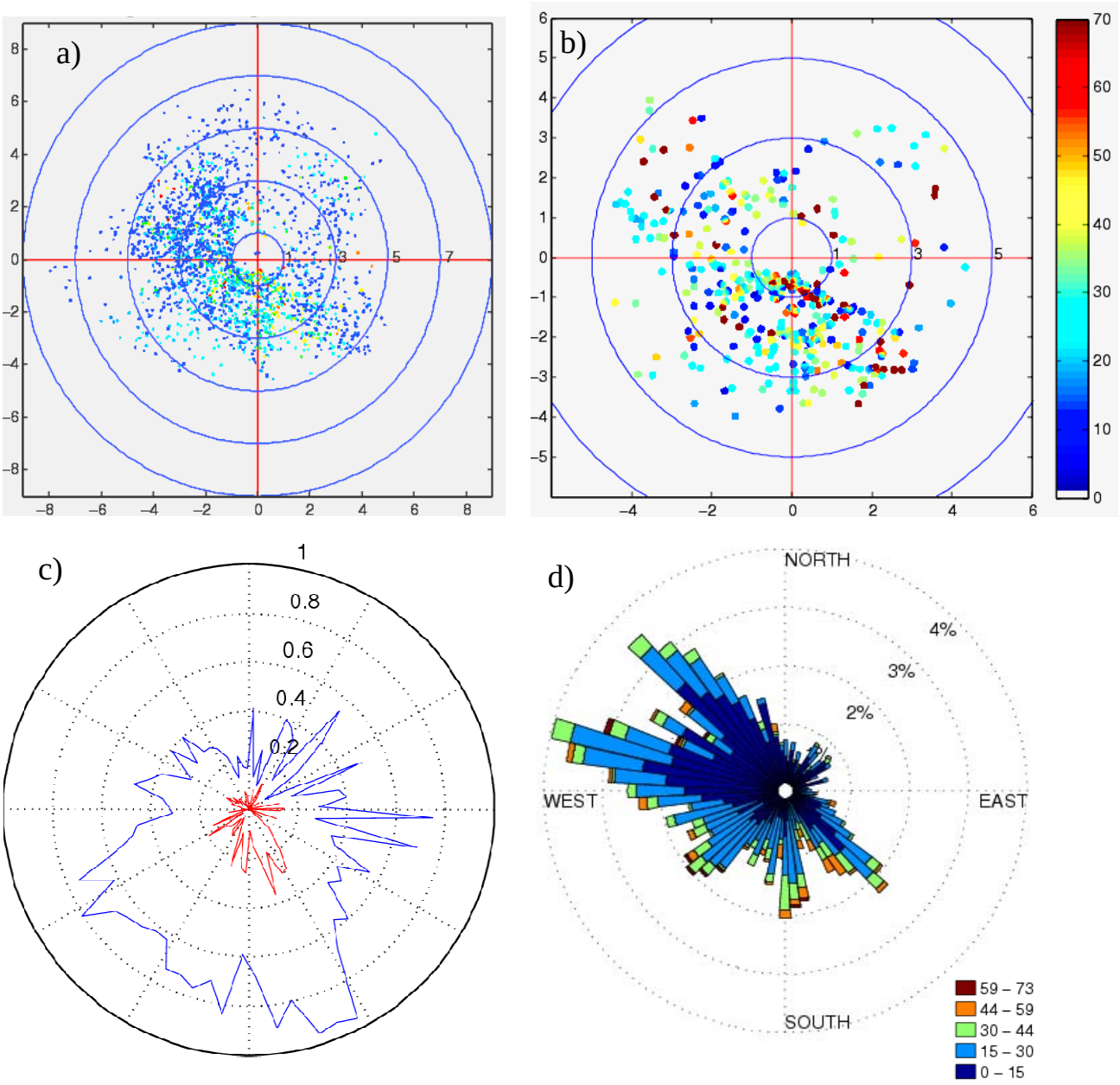

Figure 5-6. Directionality of $PM_{2.5}$ at Milwaukee. Bivariate polar plots $PM_{2.5}$ for (a) all hours and for (b) episode hours. Panel (c) shows the CPF of $PM_{2.5}$ with thresholds in blue (15 μg m^{-3}) and red (35 μg m^{-3}). Panel (d) is a pollution rose for $PM_{2.5}$ at Milwaukee. Threshold value of CPF is in parenthesis.

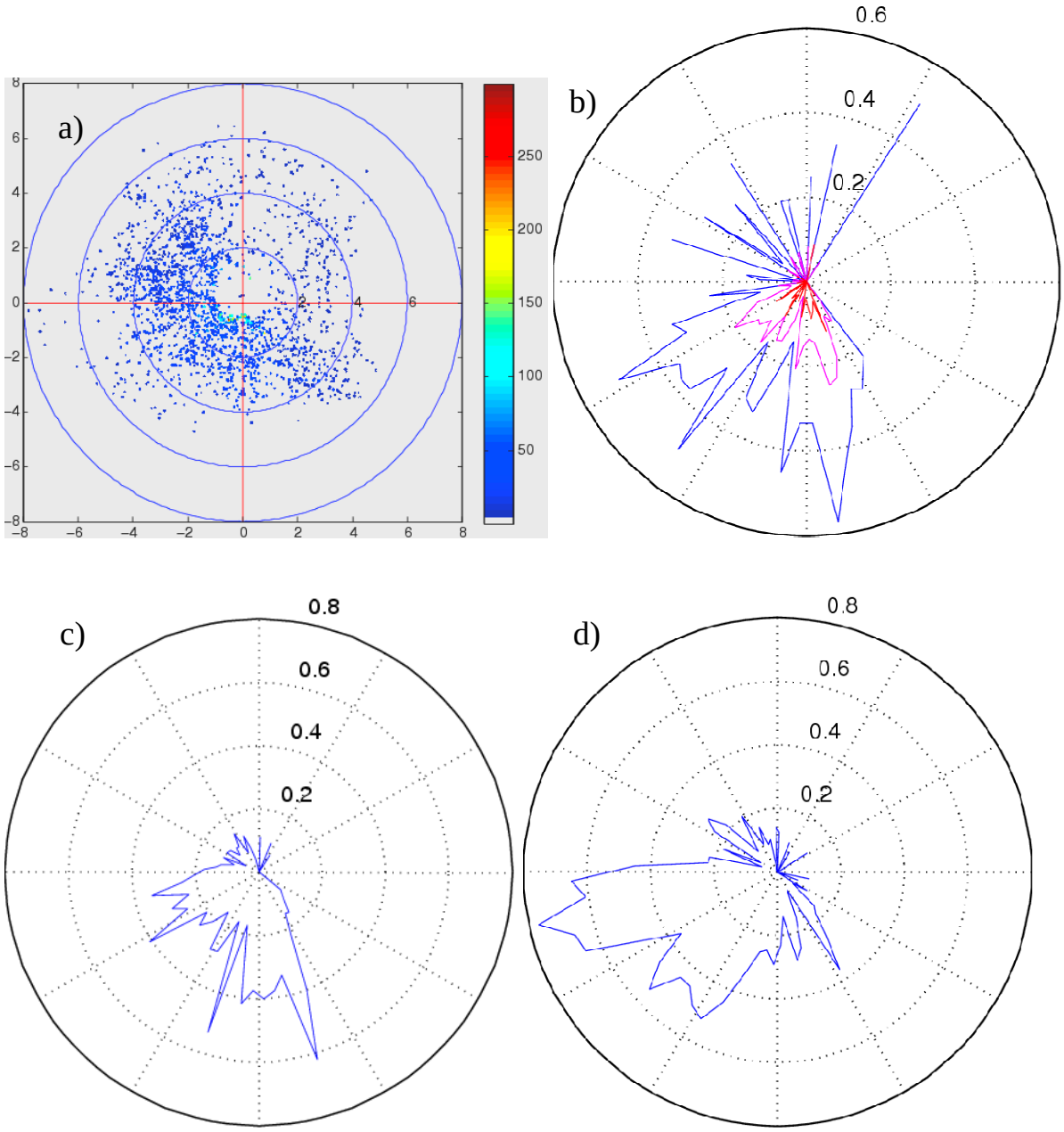

Figure 5-7. Directionality of NO_x, NO_y, and NH_3 in Milwaukee. The bivariate polar plot (a) of NOx can be compared to the CPF for NOx (b) with thresholds for wind speed less than 2 ms^{-1} in blue (53ppb), and for all wind speeds in magenta (53ppb) and red (100ppb). The CPF plots for NO_y (c, threshold of 40 ppb) and NH_3 (d, threshold of 3 ppb) are also shown.

Mayville: Mayville is a rural area and has a similar wind rose (Figure 5-4b) to Milwaukee's. Mean wind speeds were higher than Milwaukee (4 ms^{-1}) and winds from the northeast quadrant

were less frequent. As shown in Figure 5-8a (CPF of SO_2), when the conditional probability threshold is 1 ppb, there is no directionality (0.6 for all directions). When the threshold value is 3 ppb, the CPF is 0.3 for winds from the south. The pollution rose (Figure 5-8b) also shows high concentrations (>6 ppb) more frequently for southerly winds. There may be a directional source of SO_2 impacting Mayville; however, this is not expected to influence the representativeness of the site for characterization of regional episodes. NH_3 was elevated during periods of southwesterly winds (Figure 5-8c) and NO_y was elevated during periods of southeasterly winds (Figure 5-8d). The feature of elevated gas phase NH_3 under southwesterly winds is a feature at both Milwaukee and Mayville. $PM_{2.5}$ also did not show an overall directional source (Figure 5-9a). With data binned so that only episode hours are analyzed (Figure 5-9b), the most frequent direction for high $PM_{2.5}$ levels is to the southeast. This may imply urban-to-rural transport from Milwaukee, but that conclusion would require source fingerprinting using the aerosol and gas chemistry of distinct urban sources. The Milwaukee $PM_{2.5}$ CPF (Figure 5-9d) is similar, and this may mean that southeasterly winds are associated with episodes (rather than transport from Milwaukee to Mayville). The pollution rose (Figure 5-9c) also shows that concentrations higher than 26 μgm^{-3} were more frequently associated with SE and S wind directions. The CPF of $PM_{2.5}$ for a threshold value of 15 μgm^{-3} shows high directionality for southerly winds (140 to 210^o); however with a higher PM threshold (35 μgm^{-3}) CPF is about 0.2 for SE winds showing a weak directionality.

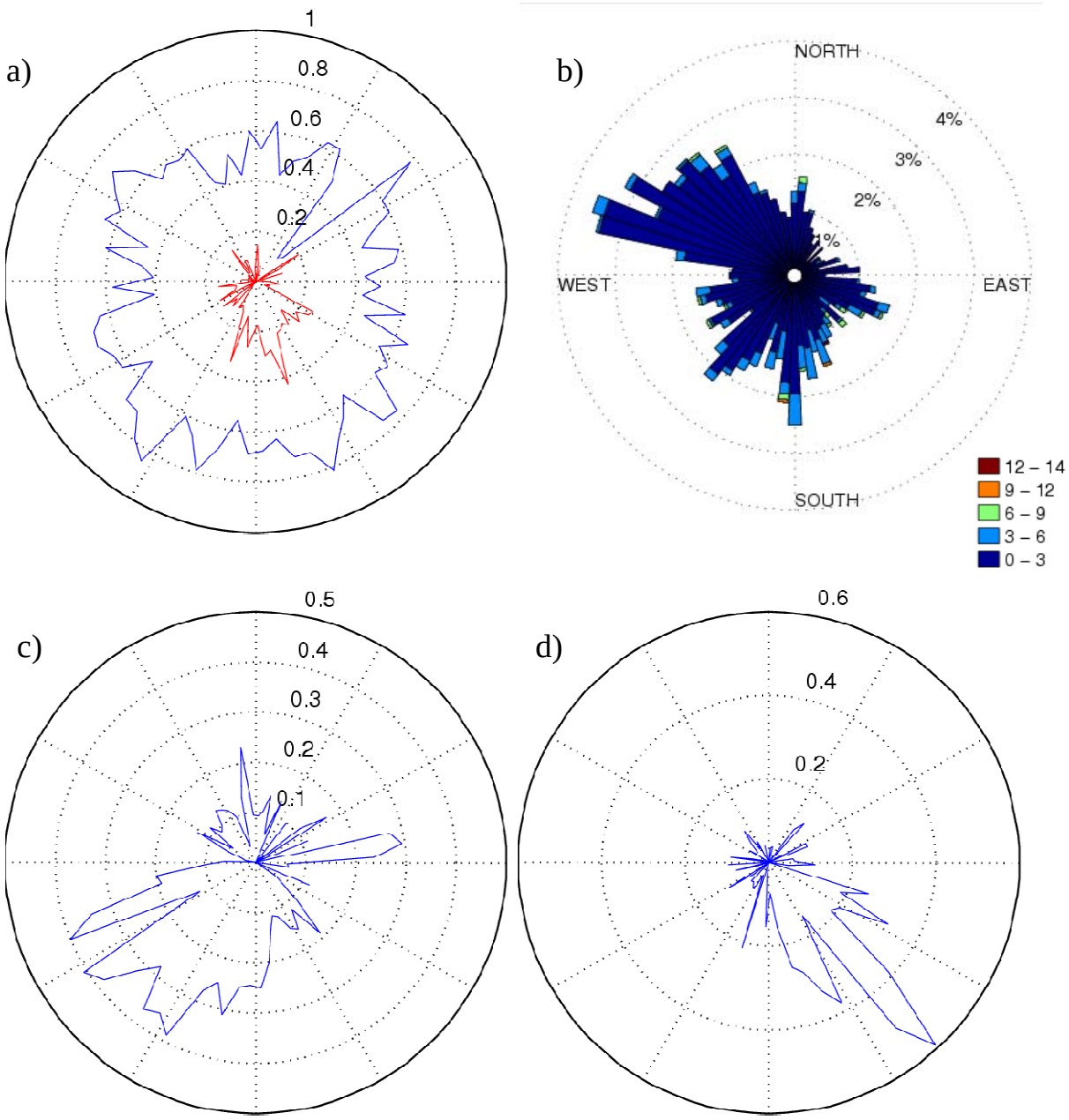

Figure 5-8. Directionality of SO_2, NH_3, and NO_y at Mayville. SO_2 directionality is shown by its (a) CPF with thresholds in blue (1 ppb) and red (3 ppb) and by (b) its pollution rose. CPF plots are shown for NH_3 (c, threshold of 3 ppb) and NO_y (d, threshold of 12 ppb).

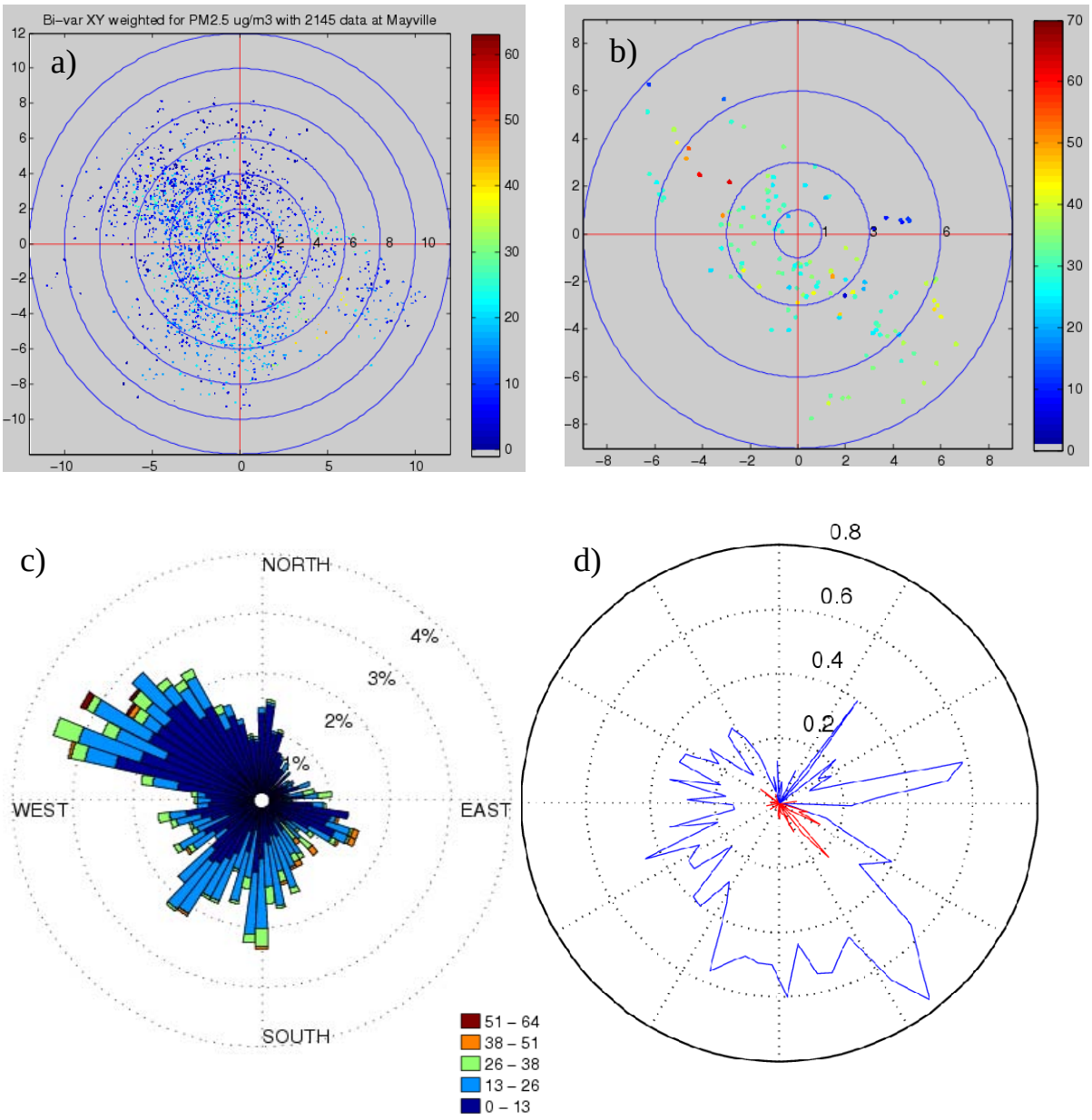

Figure 5-9. Directionality of $PM_{2.5}$ at Mayville by (a) bivariate polar plot during all hours; (b) bivariate polar plot during episode hours; (c) pollution rose; and (d) CPF with thresholds shown in blue (15 μg m^{-3}) and red (35 μg m^{-3}).

5.2.1 Georgia Sites

Jefferson St., Atlanta: The Jefferson St. site is located northwest of downtown Atlanta. As shown in figure 5-10a, the site is in an area of varied land use, including warehouses and factories with truck traffic very close to the sampling site, rail lines to the east and west within 2

km, and major interstates to the east. Approximately 4 km to the northwest is large rail transfer facility. The danger in interpreting episode $PM_{2.5}$ data and aerosol chemistry from this site is that local influences may be significant, and conclusions may or may not apply to the greater Atlanta urban area. Figure 5-10b shows the bivariate polar plot of NO_x overlaid on a map of the area. For this plot, wind speed (radius) is converted to distance by multiplying by 1 hour in order to help visualize possible local sources impacting the site. The most prominent grouping of high NO_x (red) data points are to the south and southeast. The source of this directional NO_x could be very local, or this could be associated with transport from more distant sources. The increase in frequency of high concentrations at low wind speeds (5-10b and 5-10c) perhaps suggests the former. Figure 5-10c shows the CPF of NO_x and the value is ~1 for 53 and 100 ppb thresholds when wind speeds were 0.56 m s^{-1} or less. When all wind speeds are included the CPF is ~0.4 for southerly winds (140 to 190^o). More comprehensive analysis using factor analysis tools and diurnal and weekend/weekday patterns could possibly pinpoint sources in this environment. In contrast to Milwaukee, the directional NO_x is not easily associated with large highways.

Figure 5-11a shows the bivariate polar for $PM_{2.5}$. Generally, high concentrations were measured with low wind speed (less than 1 ms^{-1}) and southerly winds, similar to the case for NO_x. However, several higher concentrations (>30 μgm^{-3}) were measured for SE winds (120^o) with speeds ~3 ms^{-1}. The CPF of $PM_{2.5}$ (15 μgm^{-3}) shows a southerly wind directionality (Figure 5-11b), however only a very weak directionality is seen with a 35 μgm^{-3} threshold.

The clearest directional signals at the Jefferson St. location were for ammonia and SO_2. The bivariate polar plot for ammonia (Figure 5-12a) shows high concentrations for NW winds and higher values as the wind speed increases to the 2-4 ms^{-1}. The CPF for ammonia (Figure 5-12b) supports a source to the northwest. Figure 5-13a shows the CPF for SO_2 with 1 and 5 ppb threshold values. The lower threshold value does not show directionality, while the higher threshold value shows NW directionality and the pollution rose (Figure 5-13b) show frequent winds from the NW during periods with high concentrations. There is a large rail facility about 4 km NW of Jefferson St. and this may be a relevant source.

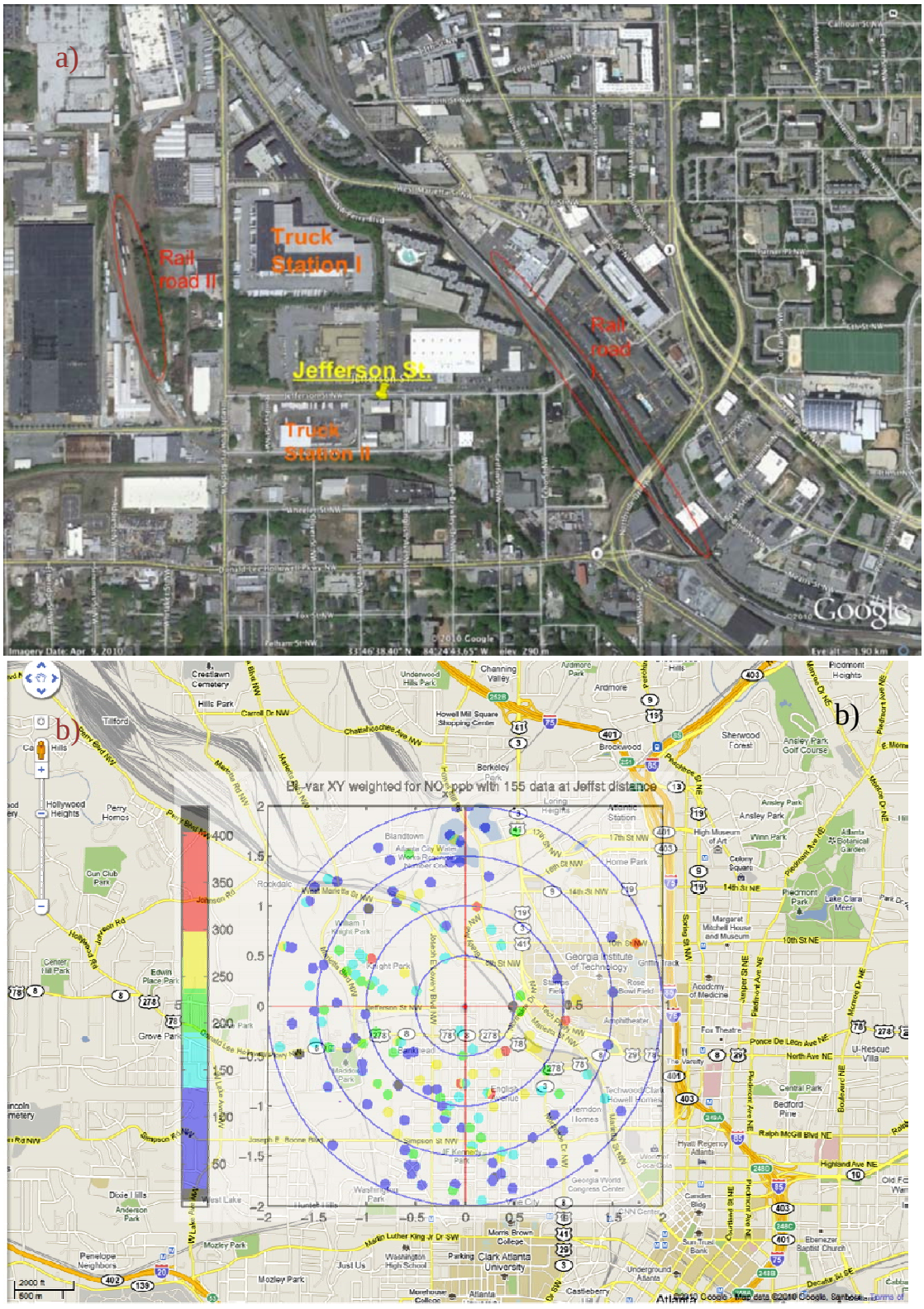

Figure 5-10. Land use and directionality of NO_x around the Jefferson St. site. (a) satellite image; (b) overlay of NO_x bivariate plot of local map.

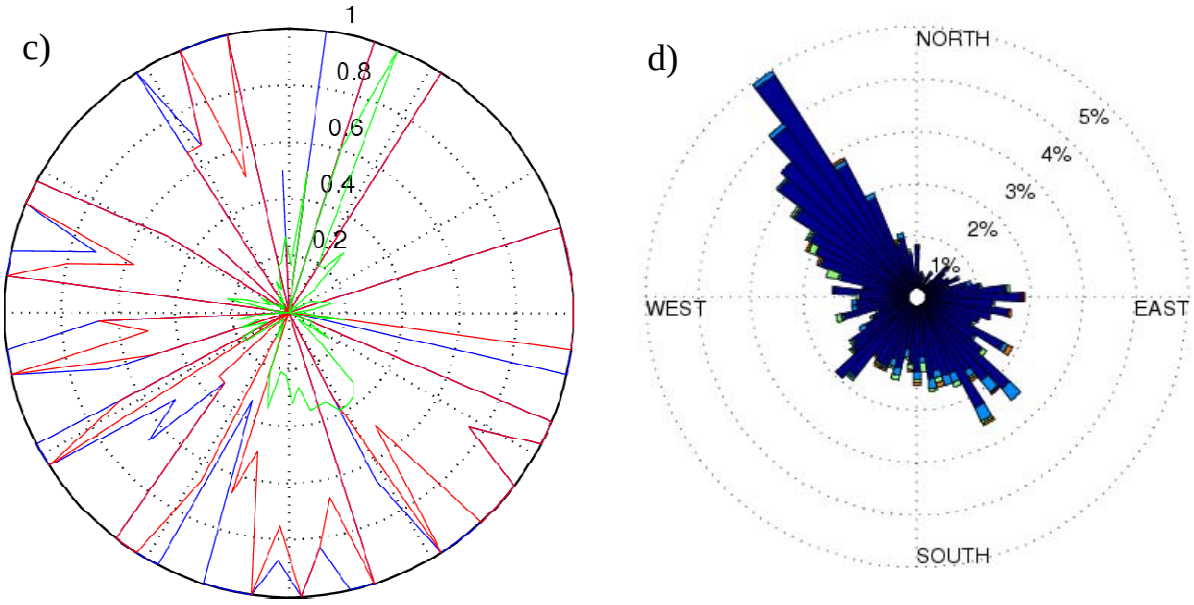

Figure 5-10 continued. Land use and directionality of NO_x around the Jefferson St. site. (c) CPF of NO_x with wind speed less than 0.56 ms^{-1} (blue 53 ppb threshold; red 100 ppb threshold) and with all data (green 53 ppb); (d) pollution rose of NO_x.

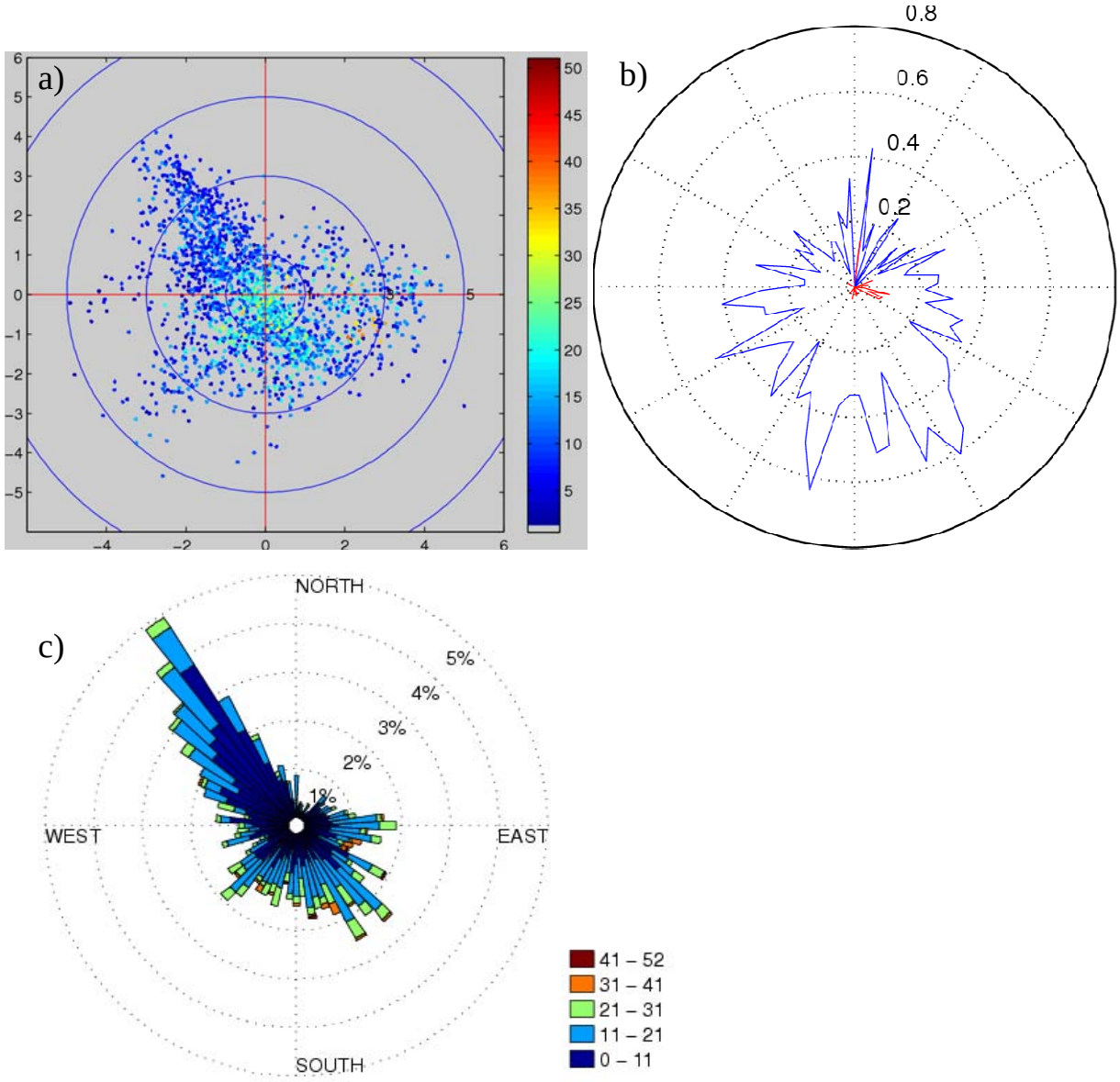

Figure 5-11. Directionality of $PM_{2.5}$ at Jefferson St. as shown by (a) bivariate polar, (b) CPF (blue for 15 μgm^{-3} threshold, red for 35 $\mu g\ m^{-3}$ threshold) and (c) pollution rose.

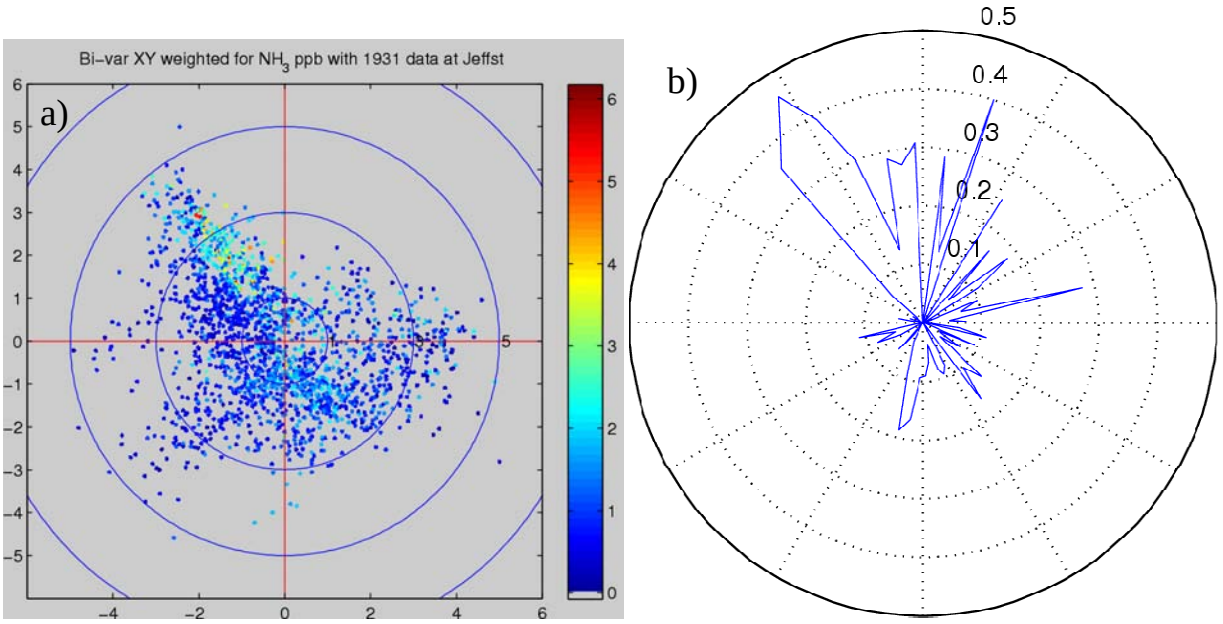

Figure 5-12. Directionality of ammonia at Jefferson St. by (a) bivariate polar plot and (b) CPF of NH_3 (2 ppb threshold).

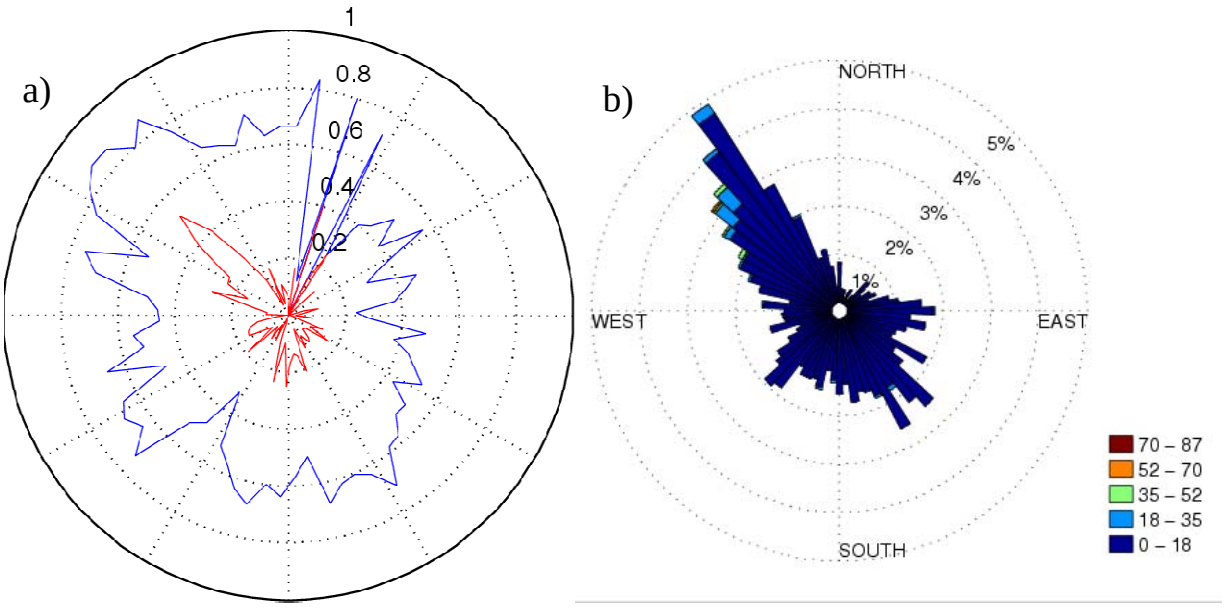

Figure 5-13. Directionality of SO_2 at Jefferson St. by (a) CPF of SO_2 (blue 1 ppb threshold, red 5 ppb threshold) and (b) pollution rose of SO_2.

Yorkville: Yorkville is a rural site about 65 km to the NW of the Jefferson St. station (Figure 2-2). Yorkville does not have nearby anthropogenic emission sources, hence the NO_x concentrations are much lower than at Jefferson St. (mean is 3 ppb). Directional sources of ammonia from poultry processing have previously been identified. As shown in Figure 5-14a, high concentrations of NO_x were measured when winds were from the SE, where Atlanta is located. The green line in the CPF (Figure 5-14b) is for data for which the wind speed is less than 4 ms^{-1} and the blue line is for winds faster than 4 ms^{-1}. Both have the same threshold value (10 ppb). The higher wind speeds show higher SE directionality. The CPF of NH_3 (Figure 5-15a) shows southerly directionality for a threshold value of 2 ppb, and a weak, southerly directionality for a threshold value of 5 ppb. The ammonia sources to the southeast and east have previously been identified as from confined poultry facilities. The source of the directional ammonia feature to the southwest is not known. The pollution rose for ammonia (Figure 5-15b) shows most concentrations measured were less than 14 ppb, although high concentrations (28 ppb and up) were occasionally measured. The CPF of SO_2 (Figure 5-16a) for 1 ppb shows no directionality, while the 3ppb threshold shows a weak SE-SW directionality. As shown in pollution rose (Figure 5-16b) for SO_2, the concentrations were mostly less than 12 ppb.

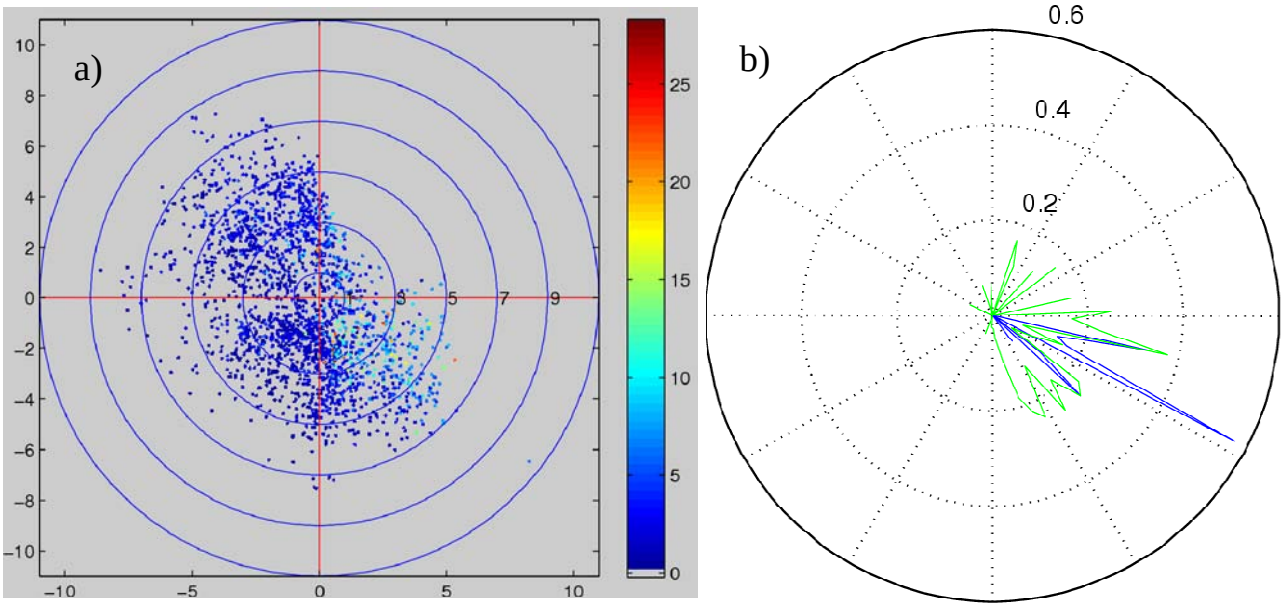

Figure 5-14. Directionality of NO_x at Yorkville by (a) bivariate polar plot and (b) CPF. CPF is segregated into high wind speeds (blue, wind speed faster than 4 ms^{-1} and 10 ppb threshold), and low/moderate wind speeds (green, wind speed less than 4 ms^{-1} and 10 ppb threshold).

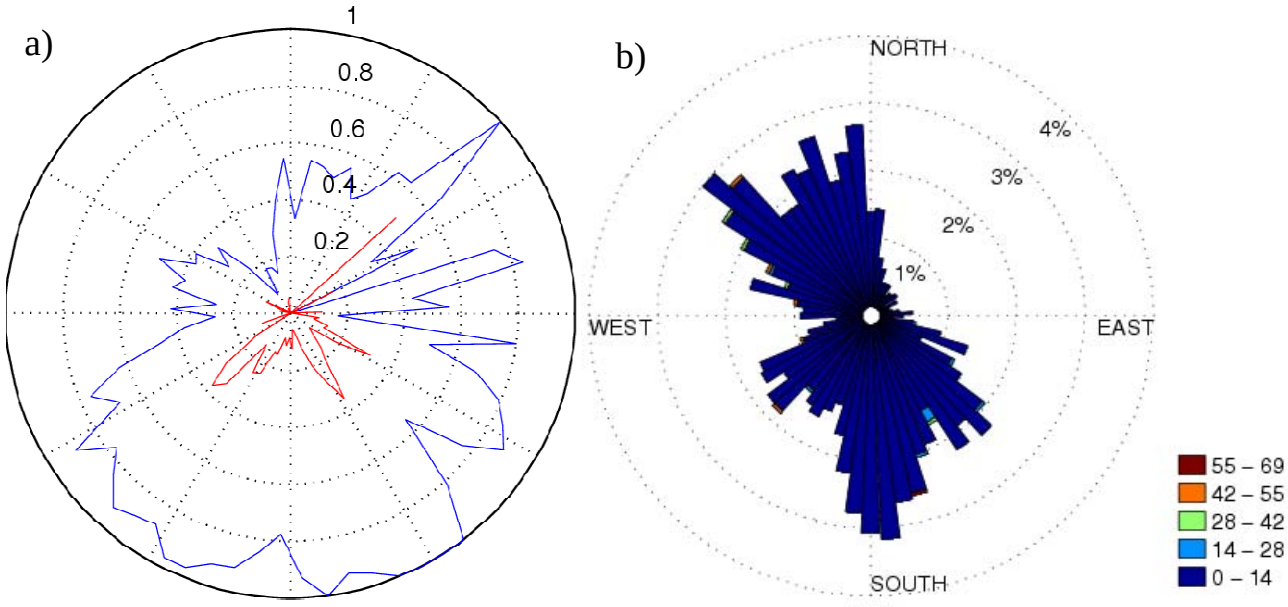

Figure 5-15. Directionality of NH_3 at Yorkville by (a) CPF (blue, 2 ppb threshold; red, 5 ppb threshold) and (b) pollution rose.

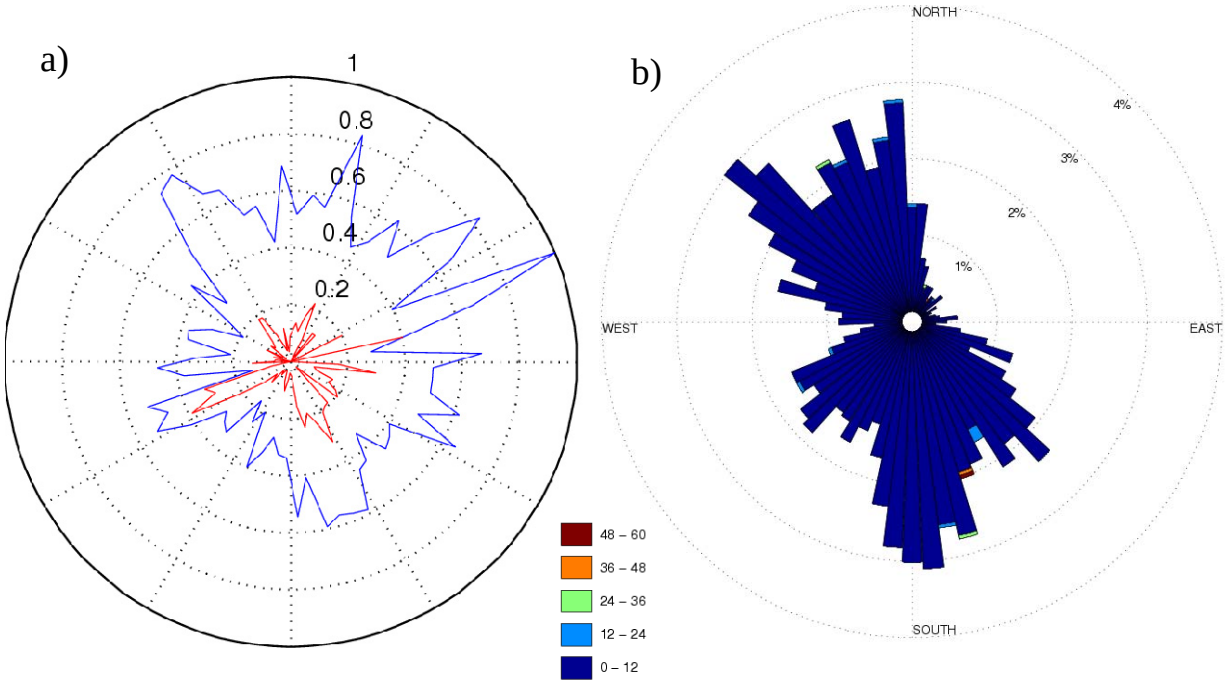

Figure 5-16. Directionality of SO_2 at Yorkville by (a) CPF (blue, 1 ppb threshold; red, 3 ppb threshold) and (b) pollution rose.

5.3 Summary and synthesis

The primary goal of directional analysis was to confirm some spatial representativeness for the four sampling sites. The sites have fairly good representativeness, although the Jefferson St. site with clear NO_x sources to the south, sulfur dioxide source(s) to the northwest, and ammonia source(s) to the northwest, may register some pollution events that are not representative of the overall urban airshed. The Milwaukee site also may be prone to some nonrepresentative sampling due to the strong NO_x impact to the south under low wind speeds, presumably from vehicles. Secondary goals of the directional analysis were to (1) gain confidence in the measurements when known directional sources such as NO_x in Milwaukee can be identified; and (2) to find similarities in directional source signatures, either at one site (for example similar CPF features for SO_2, NO_y and $PM_{2.5}$ at Mayville), or across sites (similar CPF features for NH_3 at both Mayville and Milwaukee).

Once sites are thought to be representative, the urban excess calculation can be used to understand the regional versus urban contribution to episodes. The urban excess calculations in this work establish that in the Wisconsin urban-rural pair, aerosol nitrate, ammonia aerosol, and total ammonia are not associated with the urban center but are rather regional. Total nitrate has a small urban excess, possibly indicating faster formation rates of nitrate in the urban center. NO_x, NO_y, OC, and EC have substantial urban excess and reductions in OC are likely to impact urban episode frequency. The urban-excess calculation for the Georgia sites confirms the strong role of primary pollutants (including OC as the important $PM_{2.5}$ species) in episodes.

6.0 THERMODYNAMIC SENSITIVITY

Establishing the thermodynamic sensitivities of aerosol concentrations during episodes is a key scientific goal of the study. This work builds on previous work in the Midwest and at larger regional modeling scales, but focuses on episode-specific thermodynamic sensitivity and in trying to use the full information in the hourly iCAMS measurements. To the extent possible, the LADCO WNS results are compared with the Midwest Ammonia Monitoring Project as reported by "Analysis of Inorganic PM Formation in the Midwestern United States – Final Report" (Blanchard 2008).

6.1 Models used and assumptions regarding aerosol hydration

Two thermodynamic box models were selected for use in this project: ISORROPIA version 1.7 and GFEMN (Gibbs Free Energy Minimization) version 2.2. ISORROPIA (Nenes, Pandis et al. 1998) was employed because of (1) computational efficiency; (2) the fact that it is used within CMAQ; and (3) it was used, in addition to SCAPE, in previous LADCO analyses for the region (Blanchard and Tanenbaum 2008). GFEMN was used because of familiarity with this model at the University of Iowa, and because of its ability to successfully simulate both crystallized and hydrated aerosols during the Pittsburgh Air Quality study (Khlystov, Stanier et al. 2005). Furthermore, GFEMN has been used in other thermodynamic sensitivity studies (Takahama, Wittig et al. 2004; Vayenas, Takahama et al. 2005).

These models were validated against previous simulations and experimental data, and against one another. These are discussed in Appendix 11. Minor differences were identified between the models, but these were small compared to measurement uncertainty. Data-model agreement was much better under the assumption of hydrated metastable aerosols than under the assumption of aerosols on the deliquescence branch. Therefore, all simulations in this section are done with ISORROPIA on the efflorescence branch.

6.2 Background and selection of metrics of sensitivity quantification

Thermodynamic sensitivity of the nitrate-sulfate-ammonia system has been quantified in a large number of ways. Perhaps the most widely used metrics of characterizing the inorganic system are the degree of sulfate neutralization and the gas ratio. The gas ratio (GR) (defined in Table 6-1) is a measure of ammonia availability (Ansari and Pandis 1998), with gas ratio values

above one indicating free gas phase ammonia). The adjusted gas ratio AdjGR (which does not assume full neutralization of sulfate) was introduced by Pinder et al. (2008) to more accurately reflect the true amount available gas phase ammonia. Pinder et al. also showed that reductions in nitrate concentrations in 3D model runs were more tightly correlated with AdjGr than with the gas ratio. However, this effect was most pronounced at gas ratios below about 0.8, which are important in the eastern U.S. but not in the Midwest in winter.

A key study of thermodynamic sensitivity influencing the design of this analysis was "*Analysis of Inorganic PM Formation in the Midwestern United States – Final Report*" (Blanchard 2008). This report analyzed data from the Midwest Ammonia Monitoring Project and included analysis of data from Mayville, WI. The main analysis tool in that work was the production of isopleths plots showing the effects on mean $PM_{2.5}$ concentrations from changes in total sulfate, total nitrate, and total ammonia. These plots (and the corresponding tables) are measures of the fractional sensitivity of aerosol concentrations to percentage reductions in precursors. The all-site / all-sample mode in the gas ratio was around 1.8. A previous LADCO study, "*The Effects of Changes in Sulfate, Ammonia, and Nitric Acid on Fine PM Composition at Monitoring Sites in Illinois, Indiana, Michigan, Missouri, Ohio, and Wisconsin,* 2000-2002" (Blanchard and Tanenbaum, 2004) was less relevant to the current work because very few ammonia measurements were available and the report focused on nitrate replacement in the aerosol under anticipated sulfate reductions.

Similar to the approach of Blanchard 2008, thermodynamic sensitivity contour plots were generated by running ISORROPIA. Because of the time resolved data, the thermodynamic model could be run on each hour of the study. This was repeated for 400 separate sensitivity cases. 10 levels of total ammonia (30%, 40%, …, 90%, 100%, 110%, 120% of measured levels), 10 levels of total nitrate (30%, 40%, …, 90%, 100%, 110%, 120% of measured levels), and 4 levels of total sulfate (50%, 75%, 100%, and 120% of measured levels) were used. Contour plots were generated for total $PM_{2.5}$ with x axis of fraction of measured nitrate, y axis of fraction of measured ammonia, and z axis of $PM_{2.5}$ concentration.

Since the model only addressed changes in inorganic constituents, the following formula was used to convert changes in inorganic mass to changes in total $PM_{2.5}$.

$$PM_{2.5,TOT}^{\text{control scenario i}} = PM_{2.5,TOT}\left[1 - f_{inorg}\left(1 - \frac{PMmodel_{2.5,inorg}^{\text{control scenario i}}}{PMmodel_{2.5,inorg}^{\text{no controls}}}\right)\right]$$

While these graphical representations of sensitivity are useful, a visual point of reference for ammonia limited and nitric acid limited regimes is helpful. Therefore, on each contour plot, a ridgeline is drawn, corresponding to points on the graph where equal fractional reductions (relative to the base case, i.e. 1.0x TNH_3, 1.0x TNO_3) give equal response for reduction in $PM_{2.5}$.

The main measure of ammonia availability used in this work is the gas ratio (Blanchard Roth et al. 2000). Other measures of ammonia availability or sensitivity indicators include the adjusted gas ratio, excess ammonia, and nitrate relative response. Formulae for these are given in Table 6-1. While in principle the adjusted gas ratio is more informative, the advantages of the adjusted gas ratio are most important when the gas ratio is less than 0.8. The disadvantage of the adjusted gas ratio is that it requires accurate measurement of total nitrate, total ammonia, and nitrate and ammonia partitioning. The gas ratio requires only measurement of the total amounts. As shown in Appendix 2, the measurement suite deployed often measured the total inorganic species with more confidence than the gas / aerosol partitioning. Therefore, gas ratio is used in this work rather than adjusted gas ratio.

A choice was made to develop a new measure of aerosol sensitivity for this work, called the mass-based relative sensitivity RS_M. This variable is helpful to use in conjunction with the relative sensitivity metric used in previous LADCO works. Both relative sensitivities are defined in Table 6-1. The interconversion formula are:

$$RS_f = RS_M \frac{TNO3}{TNH3} \quad \text{and} \quad RS_M = RS_f \frac{TNH3}{TNO3}$$

Both RS_f and RS_M are needed. RS_f has the advantages that it is easily compared to previous work and is shown directly on isopleth diagrams with fractional TNO_3 and TNH_3 as the x and y axes. The main disadvantage of RS_f is that it can remain constant while the actual mass or mole-based sensitivity of the inorganic aerosol system is changing. For example, imagine that during period A the TNO_3 to TNH_3 mass ratio is 1.2 : 1 and 20% reductions in each precursor have an equal effect on PM2.5. Then during period B the TNO_3 to TNH_3 ratio shifts to 2:1 and the effect of a 20% reduction in each still have an equal effect. In this case, the RS_f would be 1.0 in both cases, but the gas ratio and the true thermodynamic balance between the species has changed. The RS_M would be 0.83 (1 / 1.2) and in the second case 0.5.

Table 6-1. Definitions of sensitivity variables

Symbol in this work	Name	Formula
DSN	Degree of Sulfate Neutralization	$\frac{[NH_4^+](mol)-[NO_3^-](mol)}{[SO_4^-](mol)}$
GR	Gas Ratio	$\frac{TA-2xTS}{TN}$
AdjGR	Adjusted Gas Ratio	$\frac{TA-DSNxTS}{TN}$
EA	Excess Ammonia	$TA-2xTS-TN-[HCl(g)]+2[Ca^{2+}]+2[Mg^{2+}]+[Na^+]+[K^+]-[Cl^-]$
$S_{NO3\text{-}f}$	Sensitivity to a fractional reduction in total nitrate	$\frac{\Delta PM_{2.5,inorg}/PM_{2.5,inorg}}{\Delta TNO3/TNO3}$
$S_{NH3\text{-}f}$	Sensitivity to a fractional reduction in total ammonia	$\frac{\Delta PM_{2.5,inorg}/PM_{2.5,inorg}}{\Delta TNH3/TNH3}$
RS_f	Relative sensitivity (on fractional basis)	$S_{NO3\text{-}f} / S_{NH3\text{-}f}$
$S_{NO3\text{-}M}$	Sensitivity to a mass reduction in total nitrate	$\frac{\Delta PM_{2.5,inorg}}{\Delta TNO3}$
$S_{NH3\text{-}M}$	Sensitivity to a mass reduction in total ammonia	$\frac{\Delta PM_{2.5,inorg}}{\Delta TNH3}$
RS_M	Relative sensitivity (on mass basis)	$S_{NO3\text{-}M} / S_{NH3\text{-}M}$

6.3 Properties of the relative sensitivity mass (RS_M) variable

The properties of RS_f and RS_M as a function of GR were explored with pseudodata. For readers only interested in the field study results, section 6.3 can be skipped. Pseudodata for Figure 6-1 were generated for mean temperature and RH for Milwaukee episodes and typical concentrations for the LADCO WNS. Total sulfate, total nitrate, and total ammonia were sampled from uniform distributions running from 1-6, 1-21, and 1-9 μg m^{-3}, respectively. Input concentrations of sodium and chloride were zero. The size of the perturbation used to calculate the ΔTNO_3, ΔTNH_3, and $\Delta PM_{2.5}$ values was a 5% reduction from base case in TNO_3 or TNH_3. At gas ratios between 1 and 2, the RS_M is slightly more predictable as a function of GR than the RS_f. Furthermore, the $S_{NO3\text{-}f}$ variable exhibits a high level of scatter at gas ratios greater than 1.

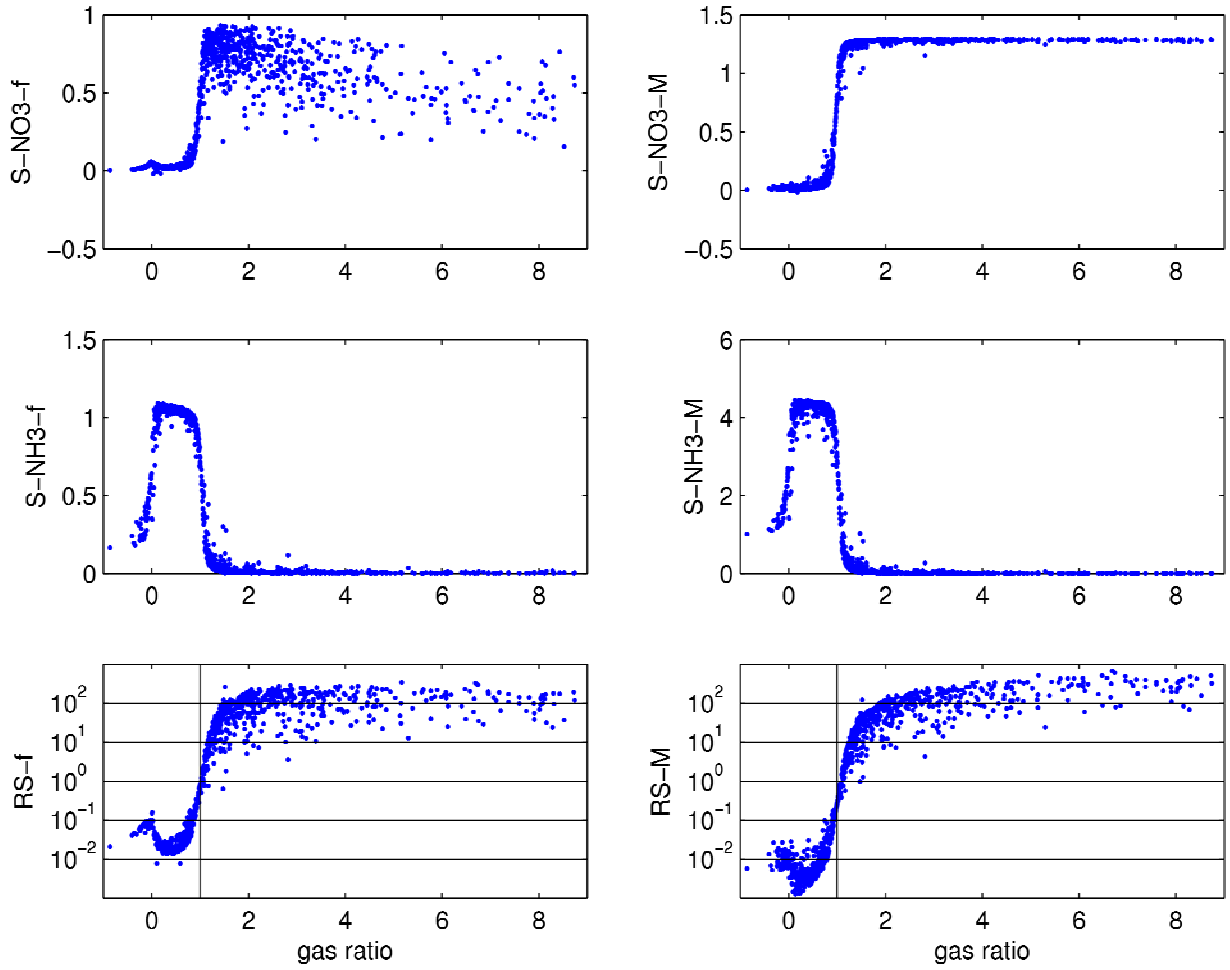

Figure 6-1. Properties of the 6 sensitivity variables in Table 6-1 with respect to gas ratio. Blue dots correspond to pseudodata as described in the text modeled in ISORROPIA. All cases are fixed at 79% RH, 0°C (the mean conditions for Milwaukee episodes). Fractional sensitivity variables are on the left, mass-based sensitivity variables are on the right. $S_{NO3\text{-}M}$ has an upper limit of (62+18)/62 (molecular weight ratios of ammonium nitrate and nitrate) while $S_{NH3\text{-}M}$ has an upper limit of (62+18)/18.

Because of the advantages of RS_M described above, we use it as the primary variable for quantification of thermodynamic sensitivity in this work, and for intercomparison of results between time periods and between sites. Qualitative regimes of sensitivity are avoided in this work. However, we note that a gas ratio of 1.0 is traditionally used as the threshold for ammonia sensitivity (Ansari and Pandis 1998; Pinder et al., 2008). This corresponds to a mass-based sensitivity of ~0.29 (the molecular weight ratio of ammonium to nitrate). All RS_M values from the LADCO winter nitrate study are greater than 0.29 except for a few specific episodes. Rather than focusing on arbitrary labels for the RS_M values, this report instead focuses on quantification

in a way that enables intercomparisons between measurements and models, between time periods, and between sites.

By varying parameters in the pseudodata simulation shown in Figure 6-1, the sensitivity of the shape of the RS_M vs. gas ratio curve to variation in temperature, relative humidity, size of nitrate or ammonia reduction, and inorganic species concentrations was determined. The most important result is that the shape of the relationship between RS_M and gas ratio is sensitive to the size of the fractional cuts in inorganic precursors. Figure 6-1 was developed using 5% fractional reductions. Figure 6-2 contrasts the 5% reductions with 30% reductions. Other factors noted in the pseudodata simulations are that temperatures influence the RS_M values at gas ratios above 1 (with increasing temperatures decreasing the values of RS_M at GR > 1, and decreasing temperatures having the opposite effect). Shifting the TNH_3 values higher had the same effect as decreasing temperature, and shifting TNH_3 lower had a similar effect as increased temperatures. Adjusting total sulfate and changing the relative humidity between 69% and 89% (79% was the average for Milwaukee episodes) did not have much influence on the shape of the curve.

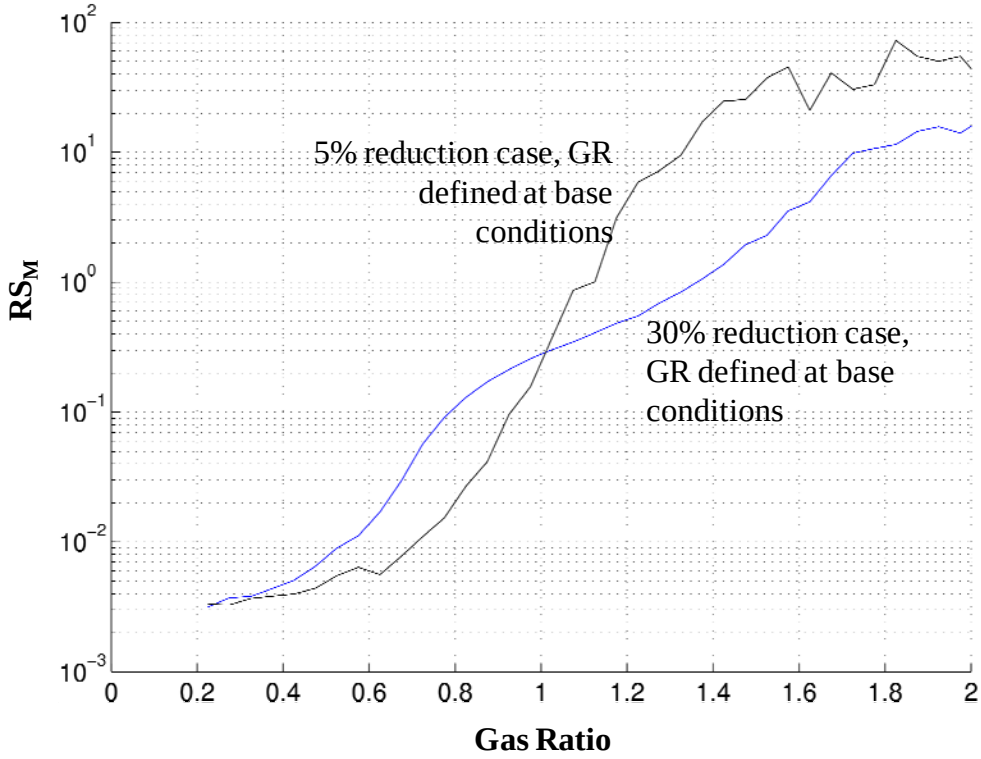

Figure 6-2. RS_M as a function of gas ratio for a small change (5%) in TNH_3 or TNO_3 from baseline, and a 30% reduction case. Lines show the median of RS_M values binned by gas ratio with a bin width of 0.05 and a total of 10,000 pseudodata cases.

The ratios of total nitrate to total ammonia are necessary for conversion between the RS_f and RS_M variables. These values can be found in Table 6-2. The number of hours figured into the calculations in Table 2 can be found in Appendix 4, and are ~1300 for all hours columns, ~49 for Mayville episodes, ~202 for Milwaukee episodes, and ~1100 for non-episode hours. While relative sensitivity on a mass basis is proposed as a useful variable for data analysis, two important caveats are necessary:

1. There is no single relationship between gas ratio and RS_M. While the gas ratio is an indicator of ammonia availability, the RS_M (or RS_f) variables are quantitative determinations of sensitivity of $PM_{2.5}$ to precursor reductions.
2. For certain applications, the molar based sensitivity (RS_M x 3.71) may be more applicable. The molar-based sensitivity takes on a value of ~1 at a gas ratio of 1.0. For other applications, the fractional sensitivity may be the most intuitive. For emissions reductions, this is the traditional approach. Using RS_M values for anticipating the impacts of emissions reductions is straightforward. From an emissions scenario, the change in precursor levels (TNO_3 or TNH_3) during the time period of interest (e.g. an episode) must be estimated. Then this can be propagated to the anticipated $\Delta PM_{2.5}$ value during the same period using the period-specific value of RS_M.

Table 6-2 – TNO_3 and TNH_3 values and indicator ratios for Mayville and Milwaukee

	Mayville			Milwaukee		
	no episodes	all hours	episode hours	no episodes	all hours	episode hours
TNO_3 concentration (mass, µg m^{-3})	4.52	4.79	12.35	4.55	5.62	12.04
TNH_3 concentration (mass, µg m^{-3})	3.15	3.24	5.79	2.77	3.30	6.24
TNO_3/TNH_3	1.44	1.48	2.13	1.64	1.70	1.93
DSN	1.74	1.76	2.03	1.94	1.93	1.88
Gas Ratio	1.69	1.66	0.98	1.59	1.50	1.35
Adjusted Gas Ratio	2.43	2.39	1.33	2.29	2.09	1.54

6.4 Thermodynamic Sensitivity Results

6.4.1 Concentration isopleths based on fractional sensitivity

A more complete set of contour diagrams can be found in Appendix 10. The following figures are the "all study hours" contour plot for Milwaukee (Figure 6-3), the "all study hours" plot for Mayville (Figure 6-4), the "episode only" plot of Milwaukee (Figure 6-5), and the

"episode only" plot for Mayville (Figure 6-6).

Using Figure 6-3 as an example, it can be seen that the base case $PM_{2.5}$ concentration (at x=1, y=1) is 16.8 μg m^{-3}. A 30% reduction in nitrate with no ammonia reduction results in a modeled mean concentration of 15.4 μg m^{-3}. A 30% reduction in ammonia with no nitric acid reduction results in a modeled mean concentration of 15.5 μg m^{-3}. The ridgeline is just below the x=1, y=1 point. The ratio of $\Delta PM_{2.5}$ for a 30% nitrate only reduction to the $\Delta PM_{2.5}$ for a 30% ammonia only reduction is RS_f and is equal to 1.04. To convert the RS_f to RS_M, the ratio of total ammonia to total nitrate is needed from Table 6-2 (TNO_3 = 5.62; TNH_3 = 3.30). RS_M is then 1.04 x 3.30 / 5.62 or 0.61.

Figure 6-4 (all hours, Mayville) is qualitatively similar to Figure 6-3. The PM2.5 concentrations are lower reflecting the urban excess of PM2.5. Figure 6-5 (episode hours, Milwaukee) is also qualitatively similar. Figure 6-6 (episode hours, Mayville) is qualitatively different. In that case, the ridgeline is above the 1:1 point, an indication that episode hours at Mayville are more sensitive to ammonia reductions that the other 3 cases.

Figures 6-3 through 6-6 are for sulfate levels at 100% of current levels. A more realistic scenario is that proposed under the Transport Rule. EPA projects emissions from power plants in the eastern half of the U.S. to decrease by 71% for SO_2 and by 52% for NOx from 2005 levels. These are also the approximate reductions expected in the five LADCO States plus Minnesota, Iowa, and Missouri. Taking into account reductions in other sectors, a relevant future year control scenario is on the order of -55% SO_2 and -35% NOx (for these eight states). Most results in this section are for a 30% reduction in TNO_3, a 30% reduction in TNH_3, and results are presented for the measured sulfate levels, and for 50% of measured sulfate levels. It should be noted that fractional reductions in NOx are unlikely to result in the same fractional reductions in TNO_3. In general, reductions in total sulfate free up ammonia, and thus shift the systems toward higher gas ratios, higher RS_M values, increased ammonia availability, and decreased nitric acid availability.

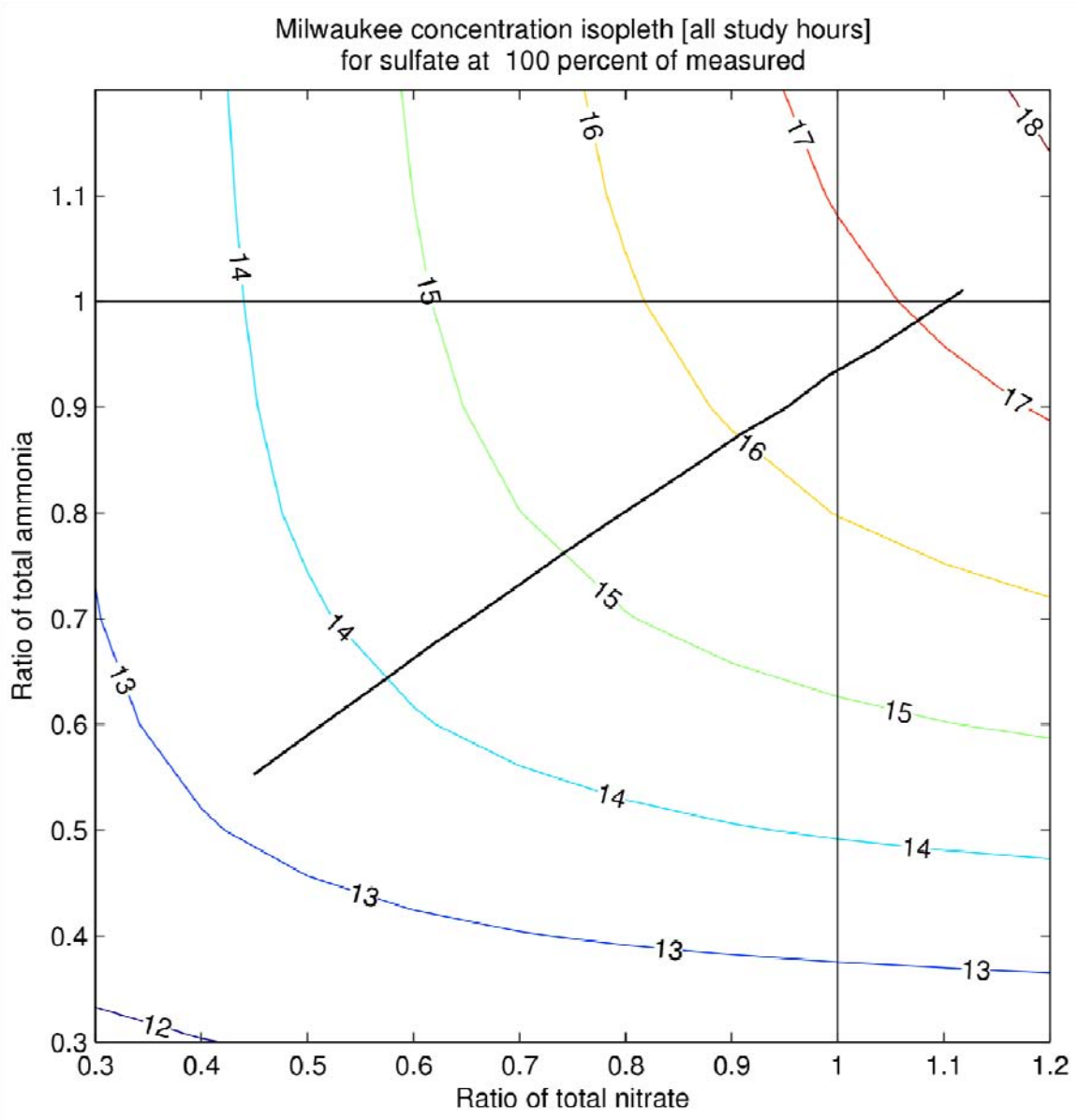

SITE: MILWAUKEE
PERIOD: ALL STUDY HOURS
SULFATE LEVEL: 100% OF MEASURED VALUE

Figure 6-3. Sensitivity of $PM_{2.5}$ to reductions in total nitrate and total ammonia.

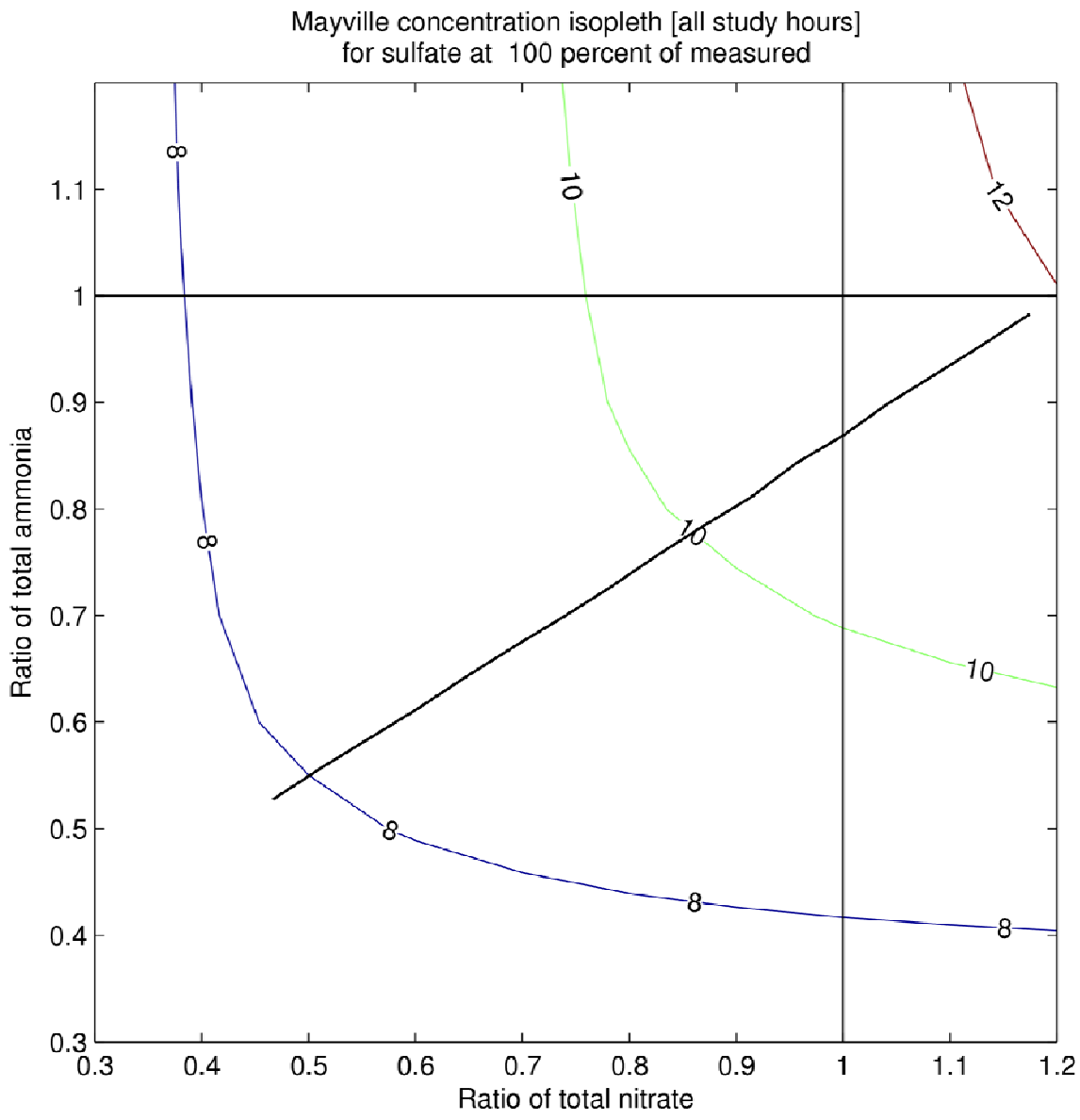

Figure 6-4. Sensitivity of $PM_{2.5}$ to reductions in total nitrate and total ammonia.

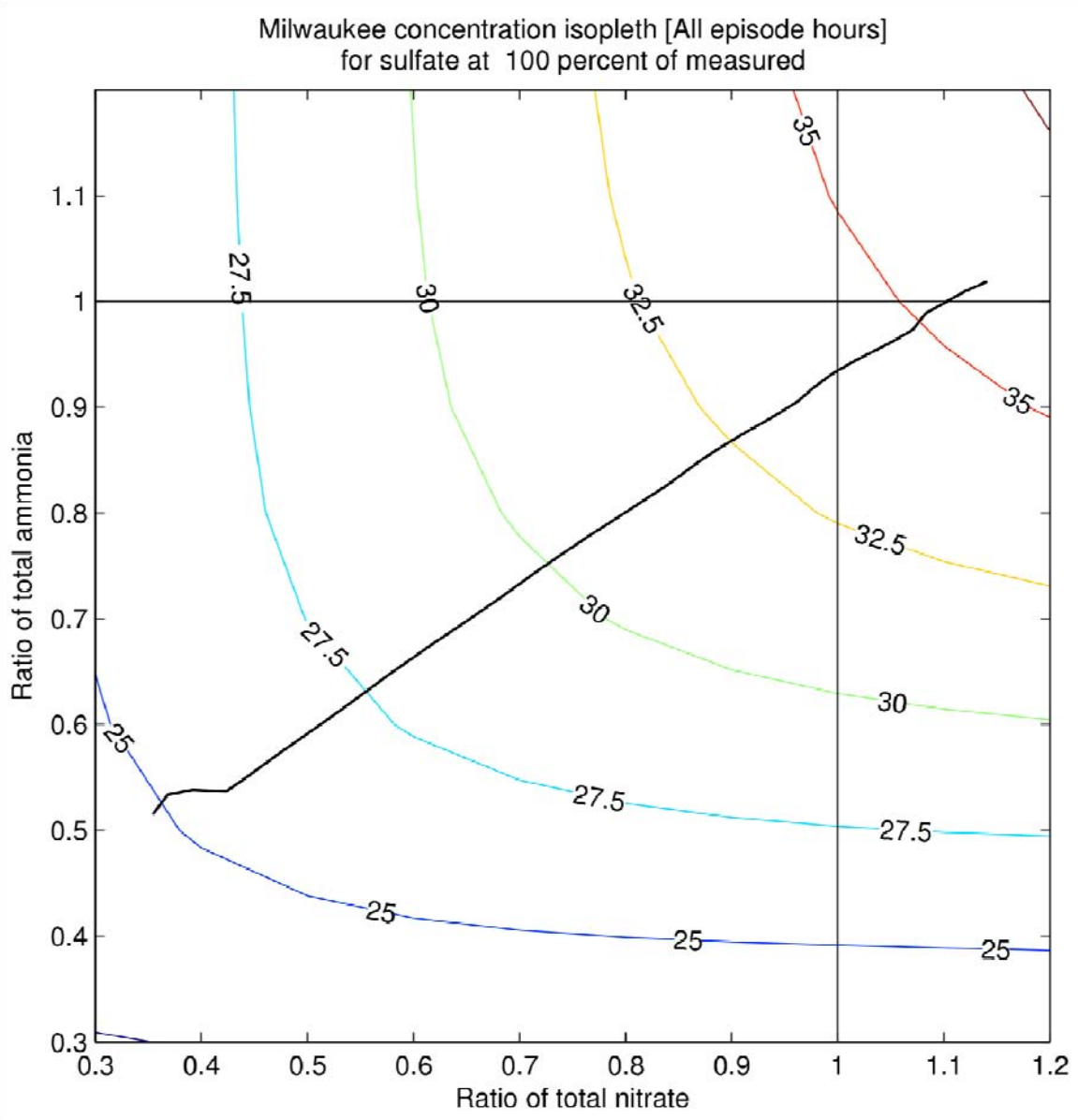

SITE: MILWAUKEE
PERIOD: ALL EPISODE HOURS ONLY
SULFATE LEVEL: 100% OF MEASURED VALUE

Figure 6-5. Sensitivity of $PM_{2.5}$ to reductions in total nitrate and total ammonia.

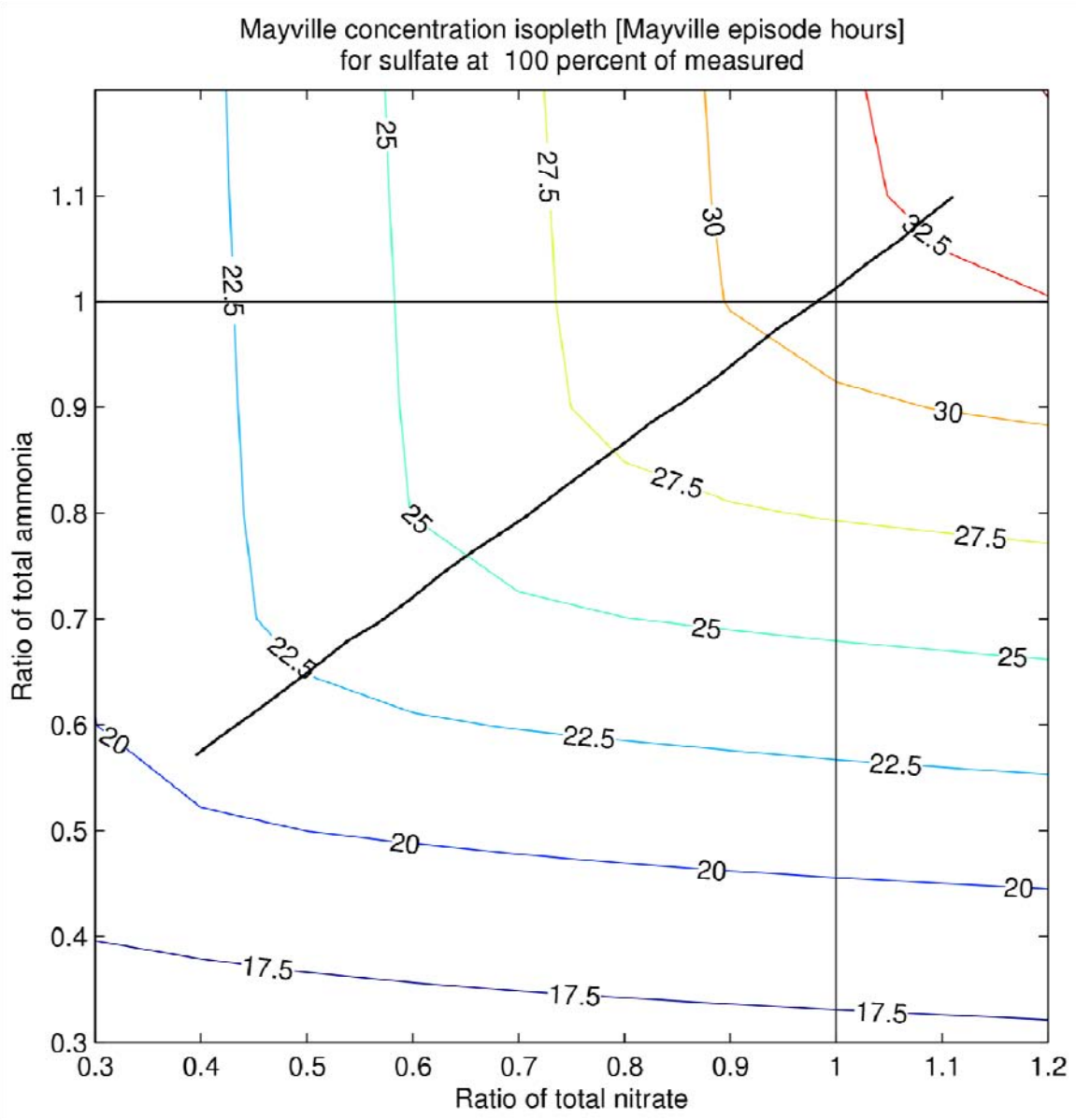

SITE: MAYVILLE
PERIOD: ALL EPISODE HOURS ONLY
SULFATE LEVEL: 100% OF MEASURED VALUE

Figure 6-6. Sensitivity of $PM_{2.5}$ to reductions in total nitrate and total ammonia.

Figure 6-7 illustrates the importance of the sulfate levels as shifting the sensitivity of the system.

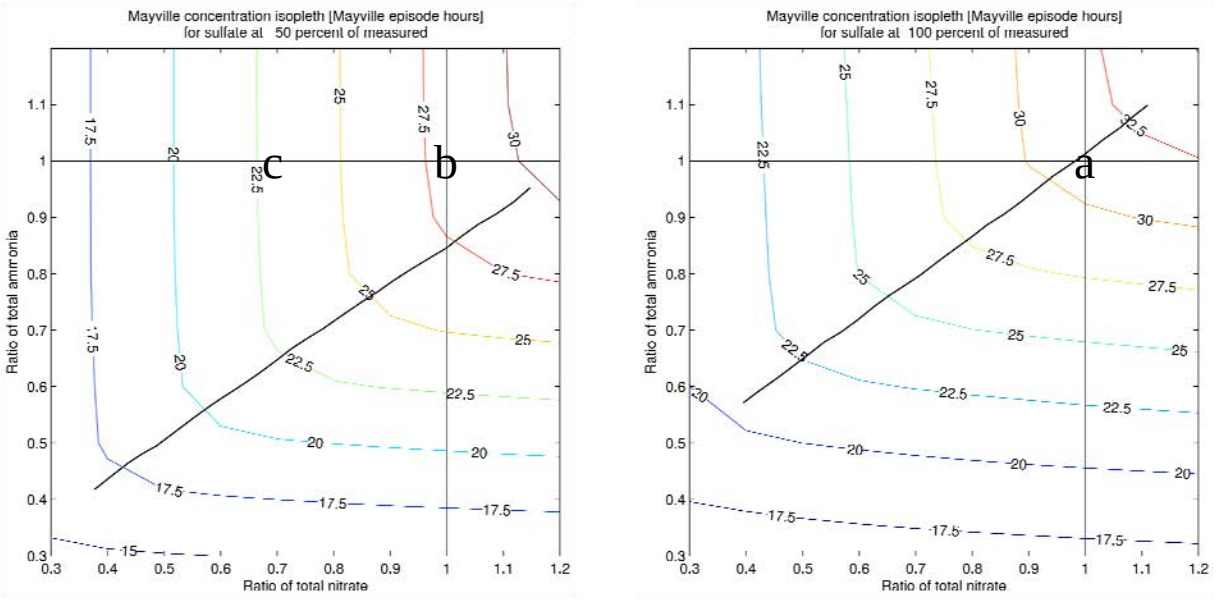

Figure 6-7. Thermodynamic sensitivity contours for 2 levels of sulfate **during episodes** at Mayville. Diagonal black line is ridge line. Above the ridge line nitrate reductions are more effective (on a basis of ΔPM/ [Δtotal precursor / base case precursor concentration]). Below the ridgeline ammonia reductions are more effective. Sulfate scenarios are 50% (left), and 100% (right) of measured values. Point a indicates the base case that is used to calculate the sensitivities in Table 6-3a. Point b is the base case for Table 6-3b. Point c is the base case for Table 6-3c.

As the figure shows, moving from point a to point b the sensitivity shifts considerably due to the availability of NH_3 from decreased sulfate. Point c represents a future base case after 30% nitrate reductions and 50% sulfate reductions. At point c, the system is strongly nitrate sensitive. In other words, if the initial reductions are from nitrate and sulfate rather than ammonia, ammonia will cease to be limiting.

Many of the values from Figures 6-3 to 6-7 are tabulated in Tables 6-3a, b, and c. Each table lists slightly different cases, and uses a different base case from which sensitivities are calculated. The effect of controls on acidic species is strongly evident, as RS_M values shift from 0.35-1.03 in table a (base case = measured values), to 0.8-2.0 in table b (50% sulfate reduction), to 5-22 (base case = 50% sulfate reduction and 30% nitrate reduction). Figure 6-8 summarizes the thermodynamic sensitivity result for the episode hours for two of the cases (base case, measured sulfate levels; and 50% sulfate reduction case). Figure 6-8 shows that the ammonia

sensitivity is greatest at Mayville under current sulfate levels.

Table 6-3a. Sensitivities to 30% total nitrate reductions, 30% total ammonia reductions, and combined 30/30 nitrate and ammonia reductions with base case as 100% measured nitrate, 100% measured ammonia, and 100% of measured sulfate levels.

	Mayville			Milwaukee		
Variable or Case	Hours with no episode	All study hours	All episode hours	Hours with no episode	All study hours	All episode hours
BASE CASE a - ISORROPIA $PM_{2.5}$ with 0% / 0% reductions in TNO_3 and TNH_3 ($\mu g\ m^{-3}$)	10.4	11.2	31.2	13.5	16.8	34.5
Values at base case conditions or sensitivities evaluated at the base case						
Total nitrate ($\mu g\ m^{-3}$)	4.52	4.79	12.35	4.55	5.62	12.04
Total ammonia ($\mu g\ m^{-3}$)	3.15	3.24	5.79	2.77	3.30	6.24
Median gas ratio (from section 4)	1.69	1.66	0.98	1.59	1.50	1.35
RS_f	1.47	1.34	0.74	1.04	1.04	1.03
RS_M	1.03	0.91	0.35	0.63	0.61	0.54
ISORROPIA $PM_{2.5}$ with 30% / 0% reductions in TNO_3 and TNH_3 ($\mu g\ m^{-3}$)	9.1	9.7	26.9	12.6	15.4	31.1
ISORROPIA $PM_{2.5}$ with 30% / 30% reductions in TNO_3 and TNH_3 ($\mu g\ m^{-3}$)	8.6	9.2	24.6	12.0	14.7	29.4
ISORROPIA $PM_{2.5}$ with 0% / 30% reductions in TNO_3 and TNH_3 ($\mu g\ m^{-3}$)	9.5	10.1	25.5	12.6	15.5	31.3

Table 6-3b. Sensitivities to 30% total nitrate reductions, 30% total ammonia reductions, and combined 30/30 nitrate and ammonia reductions at with base case as 100% measured nitrate, 100% measured ammonia, and 50% sulfate of measured sulfate levels.

	Mayville			Milwaukee		
Variable or Case	Hours with no episode	All study hours	All episode hours	Hours with no episode	All study hours	All episode hours
BASE CASE b - ISORROPIA $PM_{2.5}$ with 0% / 0% reductions in TNO_3 and TNH_3 ($\mu g\ m^{-3}$)	9.5	10.1	28.1	12.8	15.9	32.7
Values at base case conditions or sensitivities evaluated at the base case						
Total nitrate ($\mu g\ m^{-3}$)	4.52	4.79	12.35	4.55	5.62	12.04
Total ammonia ($\mu g\ m^{-3}$)	3.15	3.24	5.79	2.77	3.30	6.24
RS_f	2.82	2.62	1.65	1.59	1.65	1.75
RS_M	1.97	1.77	0.77	0.97	0.97	0.91
ISORROPIA $PM_{2.5}$ with 30% / 0% reductions in TNO_3 and TNH_3 ($\mu g\ m^{-3}$)	8.0	8.5	23.1	11.6	14.3	28.7
ISORROPIA $PM_{2.5}$ with 30% / 30% reductions in TNO_3 and TNH_3 ($\mu g\ m^{-3}$)	7.8	8.3	22.9	11.3	13.8	27.8
ISORROPIA $PM_{2.5}$ with 0% / 30% reductions in TNO_3 and TNH_3 ($\mu g\ m^{-3}$)	8.9	9.5	25.5	12.1	14.9	30.4

Table 6-3c. Sensitivities to additional 20% cuts in total nitrate and total ammonia, starting from a hypothetical future policy-relevant base case with 70% measured nitrate, 100% measured ammonia, and 50% of measured sulfate levels.

	Mayville			Milwaukee		
Variable or Case	Hours with no episode	All study hours	All episode hours	Hours with no episode	All study hours	All episode hours
BASE CASE c - Future base case with 30% TNO_3 reduction, 0% TNH_3 reduction, and 50% sulfate reduction ($\mu g\ m^{-3}$)	8.0	8.5	23.1	11.6	14.3	28.7
Values at base case conditions or sensitivities evaluated at the base case						
Total nitrate ($\mu g\ m^{-3}$)	3.16	3.35	8.65	3.19	3.93	8.43
Total ammonia ($\mu g\ m^{-3}$)	3.15	3.24	5.79	2.77	3.30	6.24
RS_f	11.8	12.6	31.6	3.97	4.75	6.97
RS_M	11.8	12.2	21.2	3.45	3.98	5.16
Future sensitivity case with 50% TNO_3 reduction, 0% TNH_3 reduction, and 50% sulfate reduction ($\mu g\ m^{-3}$)	6.9	7.4	19.7	10.8	13.1	25.8
Future sensitivity case with 50% TNO_3 reduction, 20% TNH_3 reduction, and 50% sulfate reduction ($\mu g\ m^{-3}$)	6.9	7.3	19.7	10.7	13.0	25.6
Future sensitivity case with 30% TNO_3 reduction, 20% TNH_3 reduction, and 50% sulfate reduction ($\mu g\ m^{-3}$)	7.9	8.4	23.0	11.4	14.0	28.3

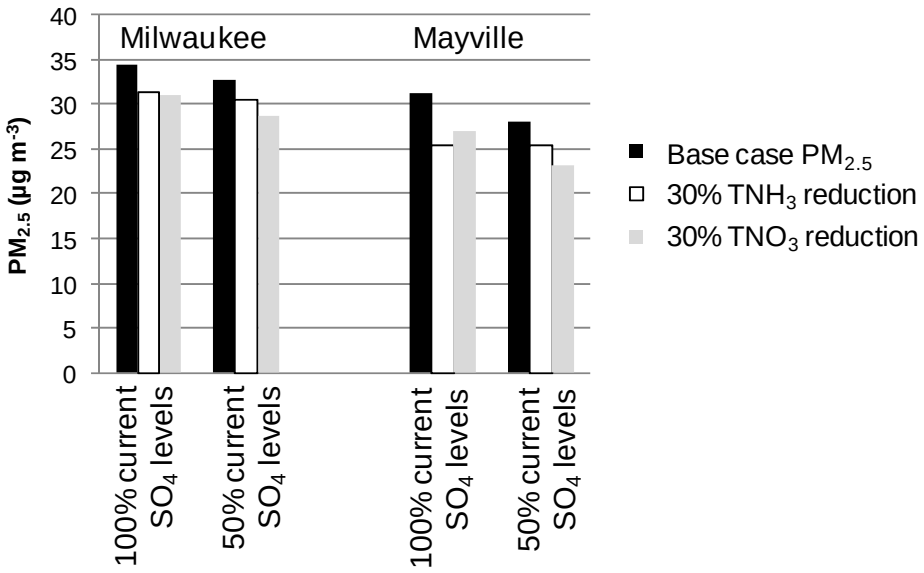

Figure 6-8. Summary of thermodynamic modeling results for all episode hours. Values graphed from Tables 6-3a and 6-3b.

6.4.2 Episode indicator isopleths

While analysis of changes in average $PM_{2.5}$ concentrations (possibly during special periods such as episodes) due to aerosol precursor controls as presented above is the type of analysis that has been done in the past, this analysis may be misleading with respect to guiding policy aimed specifically at eliminating episodes. The reason for this is that while all reductions factor into calculating the average, reductions to levels already below the episode threshold have no bearing on controlling episodes. In other words, reduction of concentrations already above the 35 µg m^{-3} threshold are critical, while reductions to concentrations already below the 35 µg m^{-3} level have no additional benefit on compliance. Therefore, this section looks at the sensitivity of metrics other than average $PM_{2.5}$ concentration. Contour plots of the episode indicator metric (with thresholds of 27 and 35 µg m^{-3}) are shown in Figure 6-9. Larger versions of these figures can be found in Appendix 10. Figure 6-9 confirms that sensitivity analysis using the episode indicators rather than using mean concentrations during episodes gives a similar result. For example, fractional reductions in TNH_3 and TNO_3 at Milwaukee give equal reductions in the episode indicator metrics. This can be compared to the RS_f value at Milwaukee from Table 6-3a of 1.03. For Mayville, 30% reductions in TNH_3 are more effective than TNO_3 at reducing the episode indicator metric using the 35 µg m^{-3} threshold. This agrees with the RSf

value of 0.74 for Mayville episodes. Also figure 6-9 can be used to see what level of reduction would be required to reduce episode occurrence (as defined by the episode indicator variables) in half, and this is not something that can be discerned using contour maps based on average concentration. Finally, the figure also shows that much larger fractional reductions in TNO_3 and/or TNH_3 are required at Milwaukee to equalize the episode indicators between the two sites.

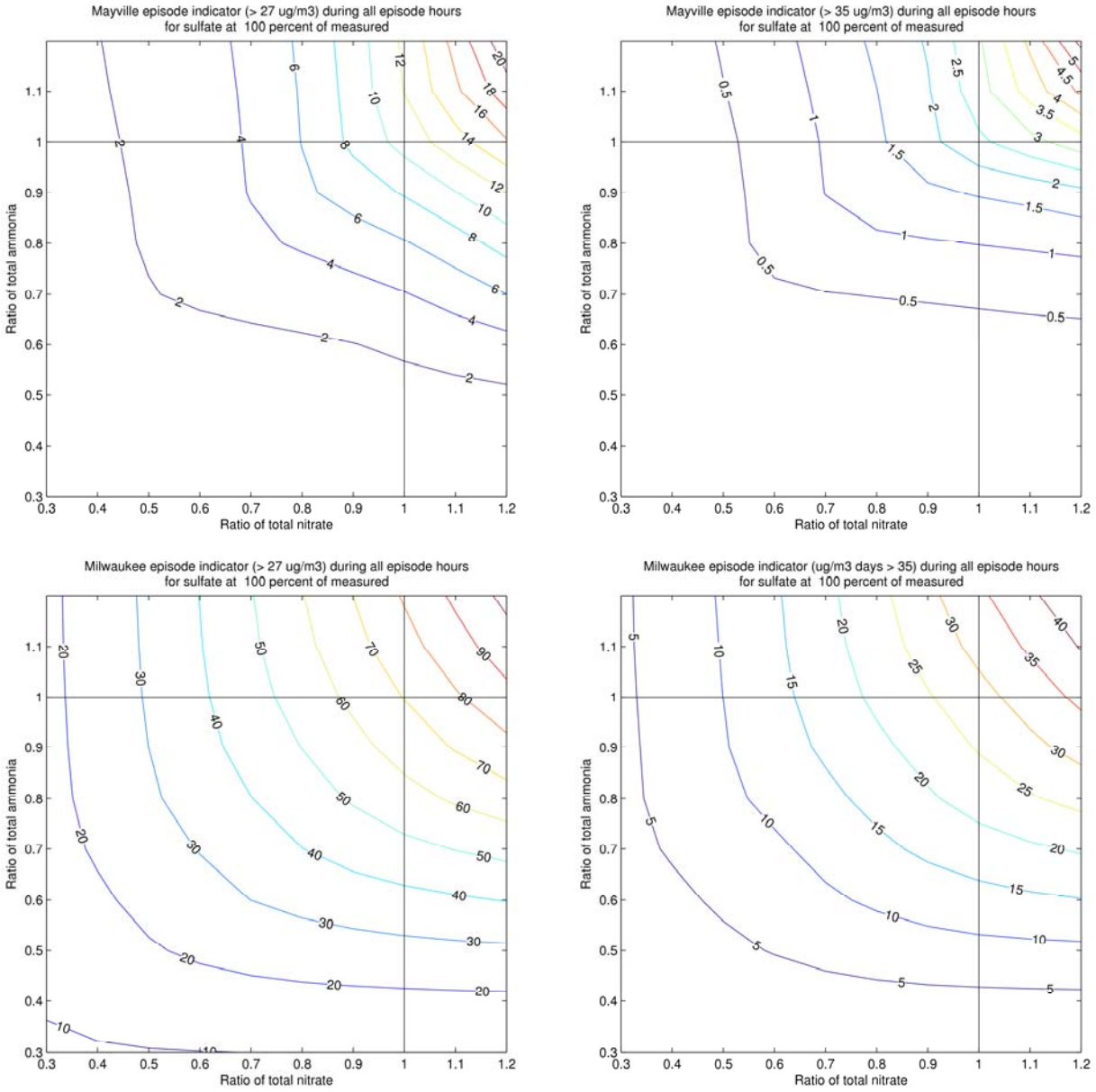

Figure 6-9. Relative sensitivity (fractional) plots with the z axis as an episode indicator with sulfate at 100% of measured values.

6.4.3 Shifting of sensitivity with $PM_{2.5}$ concentrations and gas ratio

In the previous sections, we established that (1) we expect RS_M to increase as the gas ratio increases, and (2) as we move from non-episode to "all hour" to episode sets of Milwaukee and Mayville data, the gas ratio drops, the ammonia sensitivity increases, and the PM concentration increases. However, this has all been based on analysis using time averaged data. If instead hour-by-hour sensitivities are examined, the question is whether the same relationships are demonstrated.

Figure 6-10, instead of binning into long periods, calculates the sensitivity for each hour of the study at the Mayville site. Therefore, no averaging is required. Comparing the Mayville hourly RS_M figure to the same figures with pseudodata (Figures 6-1 and 6-2) shows strong similarities. The effect of the size of the perturbation in TNO_3 and TNH_3 on the shape of the RS_M versus GR curve (shown in Figure 6-2) is consistent with the differences between Figure 6-1 (5% changes) and Figure 6-10 (30% changes).

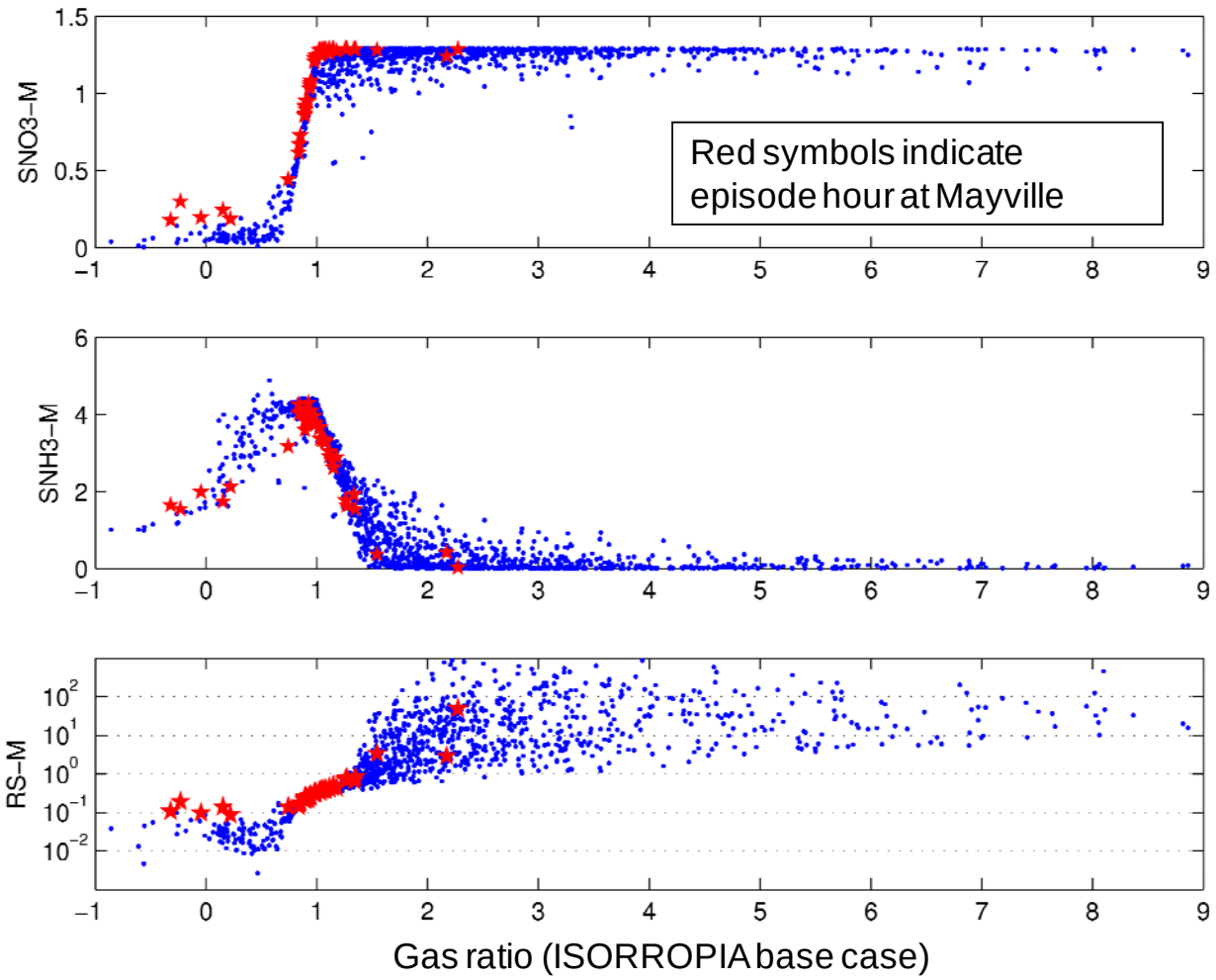

Figure 6-10. Use of gas ratio as a controlling variable on nitrate sensitivity (Mayville). Compare to same graph with pseudodata (fig 6-1). Red symbols indicate episode hours at Mayville.

Figure 6-11 is very similar to Figure 6-10, except the x axis is $PM_{2.5}$ concentration rather than gas ratio.

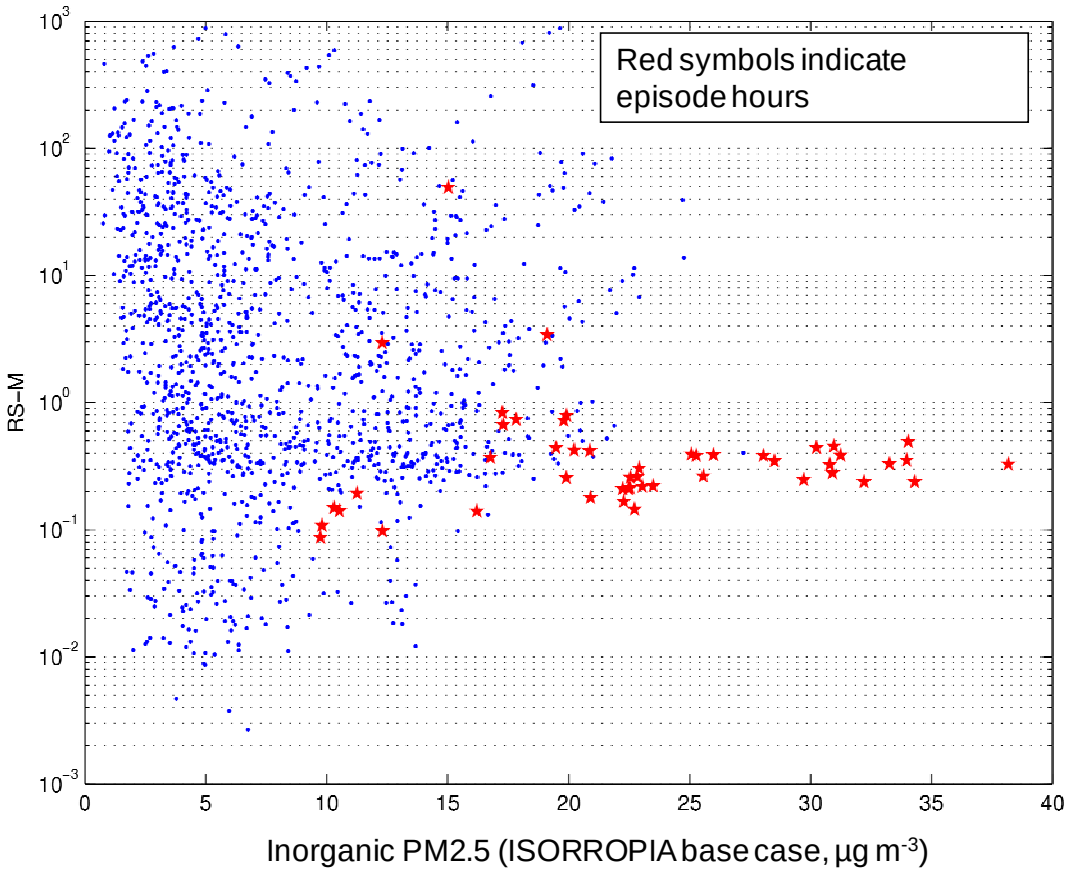

Figure 6-11. Mayville nitrate sensitivity as a function of $PM_{2.5}$ concentration.

Figure 6-11 shows that for the Mayville episodes, the nitrate sensitivity seems to reach an approximately constant value of around 0.4 during the episodes. The same phenomenon (convergence of RS_M at high $PM_{2.5}$ values) is not seen for Milwaukee (Figure 6-12). This is true for "both site" episode hours and for Milwaukee only episode hours, as shown in Figures 6-12 and 6-13.

In Figure 6-12 the cloud of points is the same shape as for Mayville (Figure 6-10) as expected since this is a feature of the thermodynamics of the system. The difference is that the episode gas ratios (in red) are much more variable, and a median value is not that informative. There are at least four possible explanations for this: (1) higher measurement variability (perhaps from higher NOy influencing TNO_3 or TNH_3 measurement) such that the actual variability in gas ratio and sensitivity is more like that of Mayville; (2) TNO_3 and TNH_3 sources and sinks

(emissions or chemical) may not be applicable in Mayville;[1] (3) Mayville did not have a sufficient number of episodes to exhibit its true range of variability; and (4) Milwaukee only episodes contribute to the variability while regional episodes have a tighter range of thermodynamic sensitivity.

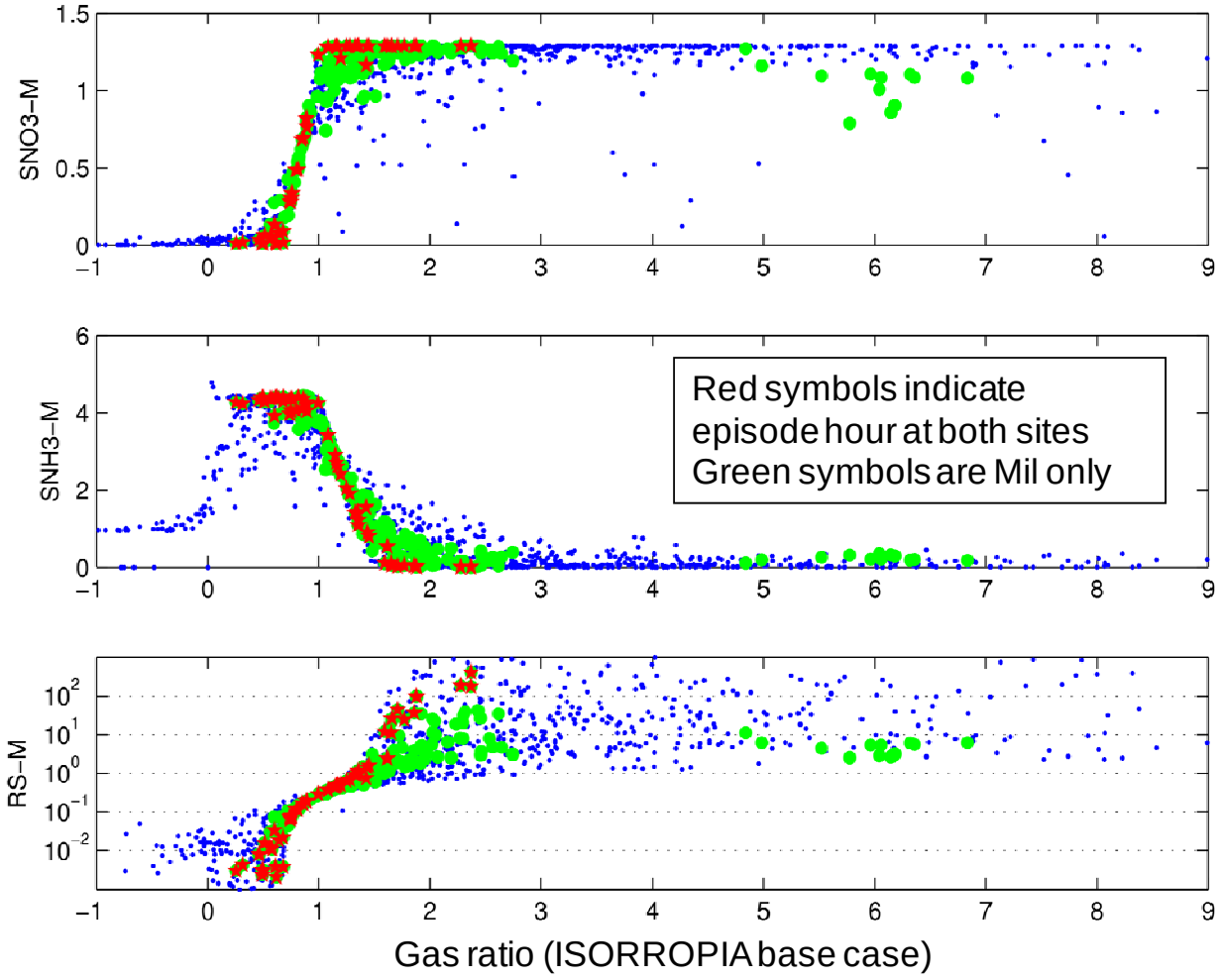

Figure 6-12. Milwaukee nitrate sensitivity as a function of gas ratio.

[1] for example, one hypothesis is that during snowmelt volatilization of inorganic compounds may be enhanced due to impervious surfaces such as concrete, roofs, and pavement found near one site but not the other; other hypotheses are that Milwaukee may have urban NH_3 emissions or that nighttime nitric acid production may be more variable (relative to TNH_3) in Milwaukee than in Mayville, etc.

Of these, one thru three are difficult to test with the available data. The 4th hypothesis, concerning Milwaukee only versus episodes shared across the sites, is investigated using Figure 6-13. Separating episodes into "both sites" and "Milwaukee only" sites does not explain the variability in nitrate sensitivity.

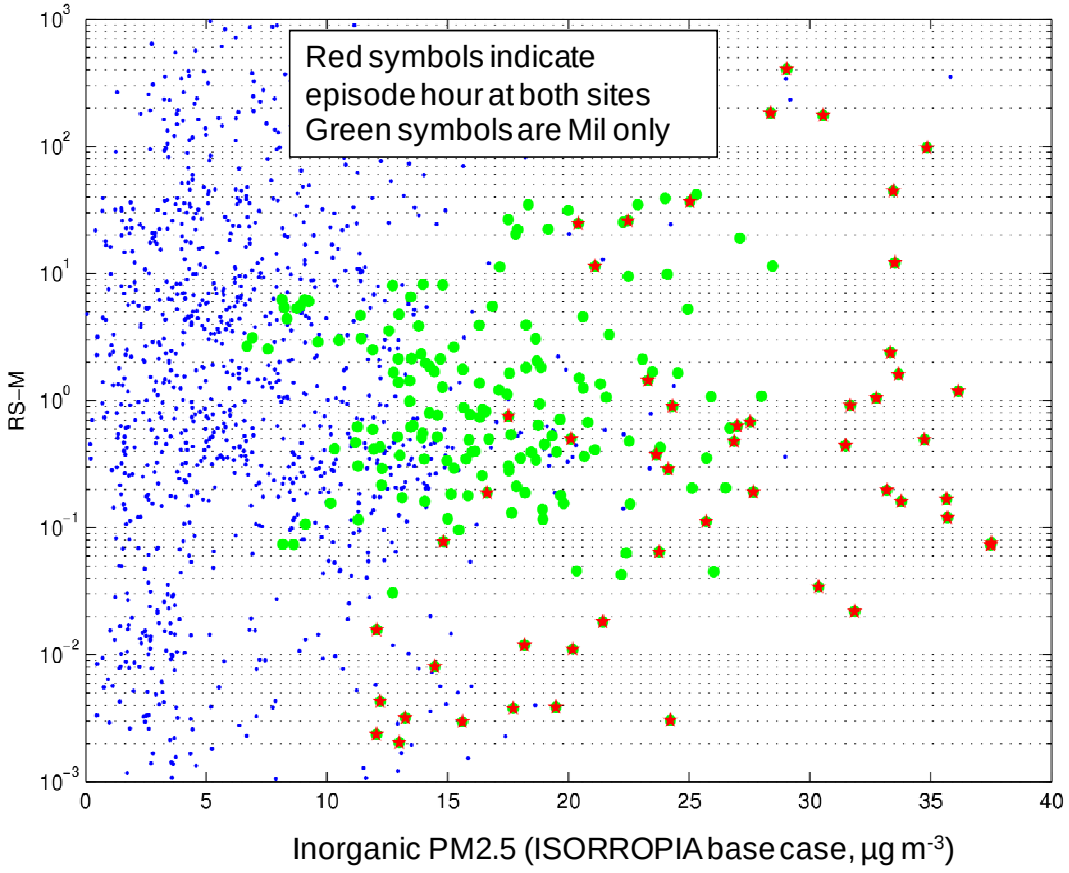

Figure 6-13. Milwaukee nitrate sensitivity as a function of PM2.5

6.4.4 Relation to previous studies

The report "*Analysis of Inorganic PM Formation in the Midwestern United States – Final Report*" (Blanchard 2008) is highly relevant to this work because of the use of similar methods and overlap between monitoring sites. The Midwest Ammonia Monitoring Project included analysis of data from Mayville, WI. Results from Bondville, IL, Great River Bluffs, MN (southeastern MN), Lake Sugema, IA (southeastern IA), and Allen Park, MI (Detroit area) will also be discussed here. Except for Mayville, these sites had samples in all months of the year, and a total of 28-46 samples for each site. 13 winter samples (presumably from Dec 2005) were

analyzed for Mayville. Mayville had samples only during May – December 2005. Therefore, no samples were taken in the months Jan-Mar. The all-site / all-sample mode in the gas ratio was around 1.8. Isopleths similar to this work are done for each site and season, and direct comparison is possible. A separate analysis is done for a high PM episode on Feb 3, 2005.

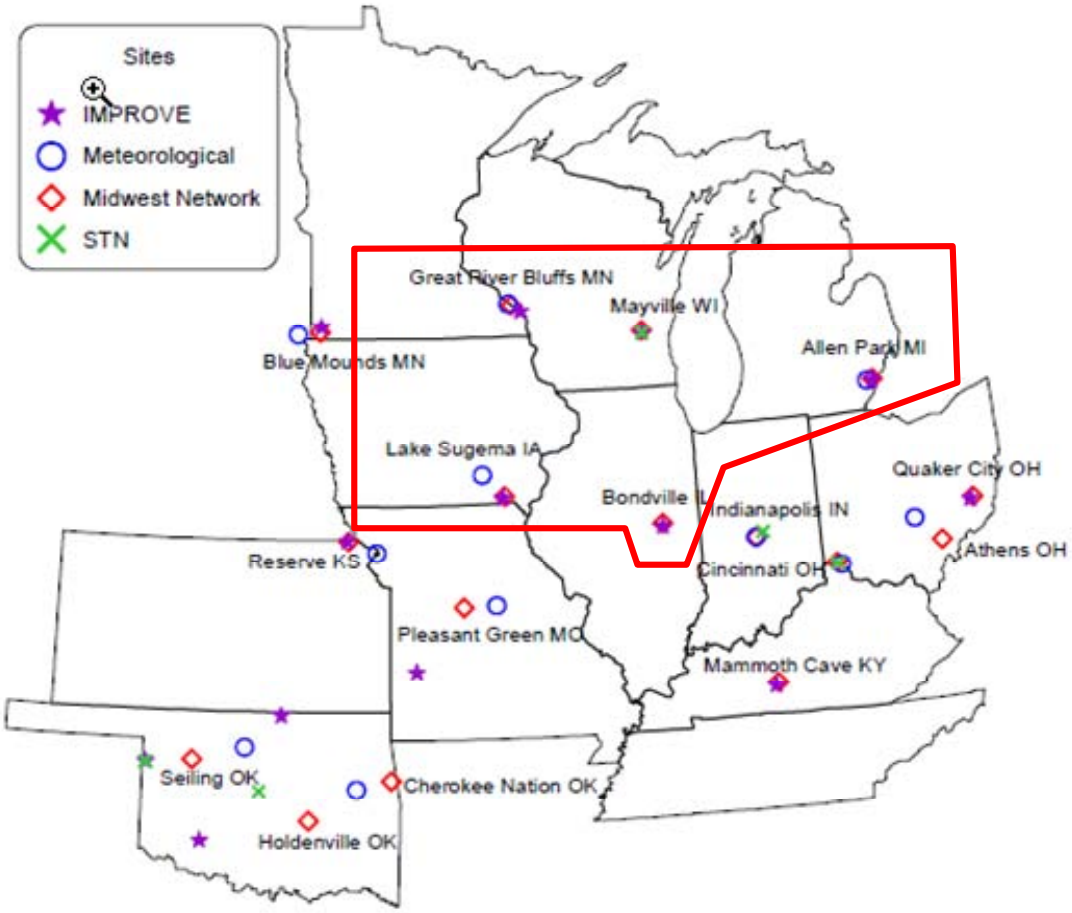

Figure 6-14. Map of LADCO Midwestern Ammonia Network Sites. Sites analyzed in this work are within the red box.

Figure 6-15 explores whether, and to what extent, the relationship between $PM_{2.5}$ and nitrate sensitivity overlaps for wintertime in Blanchard 2008 and this work. There is a suggestion of a decrease in the RS_M as $PM_{2.5}$ values increase in both works. The one overlapping datapoint between the two studies is point 2 and point b. However, these have very different sensitivities. A possible cause of this difference is the smaller number of datapoints used in the Blanchard analysis. A further possibility is that the winter datapoints for Mayville, WI in

Blanchard (2008) were all from December 2005 (rather than an average of December, January and February that was the case for most sites). Therefore, there was not overlap in terms of the exact month of sampling.

Table 6-4 Comparison of values from Blanchard 2008 versus this study. Values for this study use 30% TNO_3 and TNH_3 reductions. Values from Blanchard are December-February averages (taken from 1 in 3 day sampling) and are calculated based on extraction of 30% reduction from concentration isopleths. Values from Blanchard 2008 for episode are for 50% controls on Feb 3, 2005.

	Milwaukee (this study, all hours)	Milwaukee (this study, episode hours)	Mayville (this study, all hours)	Mayville, WI (Blanchard 2008 DJF avg)[i]	Mayville (this study, all episode hours)
Base case	16.8	34.5	11.2	10.9	31.2
only TNO_3 red.	15.4	31.1	9.7	9.35	26.9
only TNH_3 red.	15.5	31.3	10.1	10.45	25.5
fraction remaining with only TNO_3 red.	0.92	0.90	0.87	0.86	0.86
fraction remaining with only TNH_3 red.	0.92	0.91	0.90	0.96	0.82
Relative sensitivity (fractional) RS_{frac}	1.04	1.03	1.34	3.44	0.74
TNO_3 (μg m^{-3} for this study; mass % for Blanchard sites)	4.55	12.04	3.78	61	12.35
TNH_3 (μg m^{-3} for this study; mass % for Blanchard sites)	2.77	6.24	2.72	39	5.79
Relative sensitivity (mass) RS_{mass}	0.63	0.54	1.06	2.2	0.35

Table 6-4 continued

	Great River Bluffs (DJF)	Great River Bluffs Epi.	Allen Park (Detroit) MI (DJF)	Allen Park, MI Epi.	Lake Sugema, IA (DJF)	Lake Sugema, IA Epi.	Bondville, IL (DJF)	Bondville, IL Epi.
Base case	10.5	24.7	14.8	54.9	13.15	30.6	13.7	32.4
only TNO_3 red.	9.1	17.6	13.4	44.9	11.5	22.5	12.45	23.2
only TNH_3 red.	10.3	17.2	13.3	38.8	11.25	19.5	11.8	18.9
fraction remaining with only TNO_3 red.	0.87	0.71	0.91	0.82	0.87	0.74	0.91	0.72
fraction remaining with only TNH_3 red.	0.98	0.70	0.90	0.71	0.86	0.64	0.86	0.58
Relative sensitivity (fractional) RS_{frac}	7.00	0.95	0.93	0.62	0.87	0.73	0.66	0.68
TNO_3 (μg m^{-3} for this study; mass % for Blanchard sites)	65.00	70	64	70	67	70	67	70
TNH_3 (μg m^{-3} for this study; mass % for Blanchard sites)	35.00	30	36	30	33	30	33	30
Relative sensitivity (mass) RS_{mass}	3.77	0.41	0.52	0.27	0.43	0.31	0.33	0.29

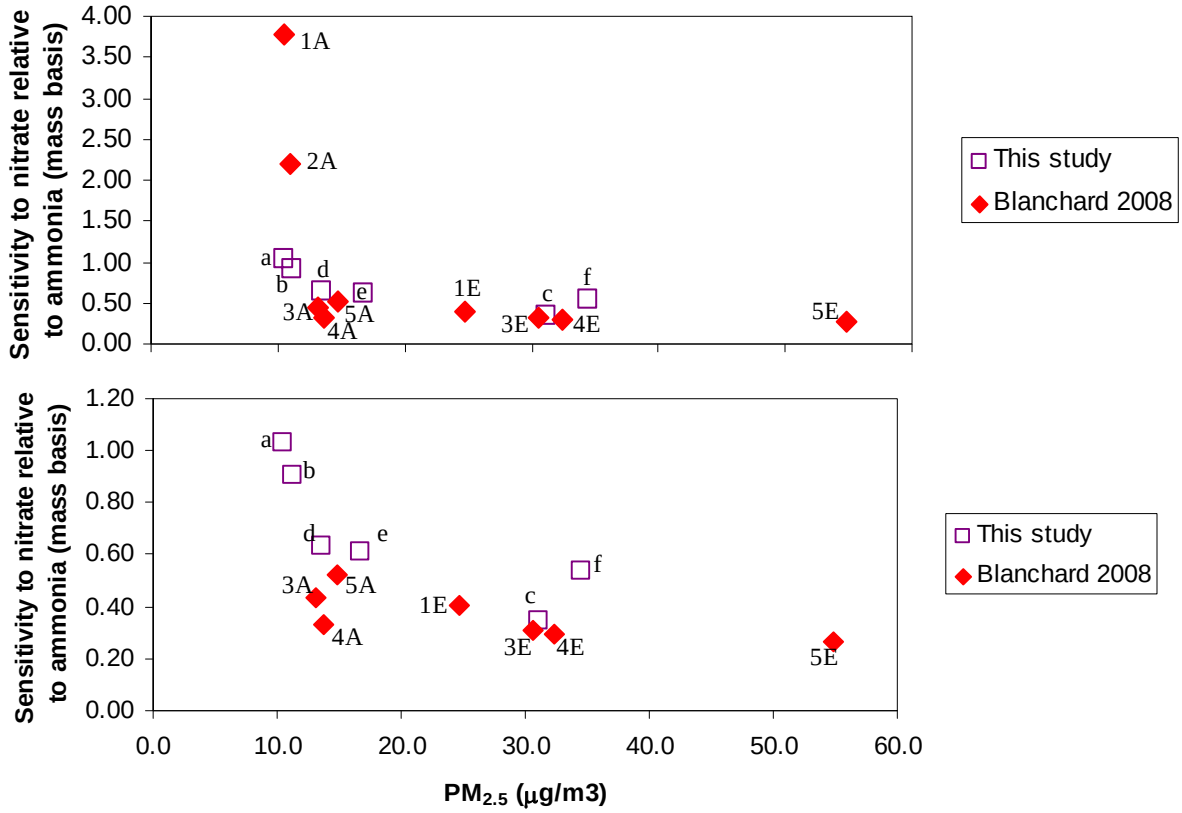

1 Great River Bluffs MN (A=DJF avg; E=Feb 3, 2005 episode)
2 Mayville WI (A=Dec avg)[i]
3 Lake Sugema IA (A=DJF avg; E=Feb 3, 2005 episode)
4 Bondville IL (A=DJF avg; E=Feb 3, 2005 episode)
5 Allen Park MI (A=DJF avg; E=Feb 3, 2005 episode)
a Mayville (JFM avg; no episodes)
b Mayville (JFM avg; all hours)
c Mayville (JFM avg; episodes)
d Milwaukee (JFM avg; no episodes)
e Milwaukee (JFM avg; all hours)
f Milwaukee (JFM avg; episodes)

Figure 6-15. Comparison of nitrate sensitivities in winter between this study and Blanchard (2008). Top panel shows all sites. Bottom panel excludes two sites with $RS_M > 1.2$. Blanchard DJF averages are 30% sensitivities. Blanchard episodes are 50% sensitivities. Sensitivities from this study are 30% sensitivities. Points 2 and b are for the same site and season. The value from this study is based on a large number of hours, while the value from Blanchard is based on a relatively small number of 24 hour samples.

[i] The winter (DJF) average for Mayville is based on 13 samples from Dec 2005. See pages 8 and 13 of Blanchard (2008).

REFERENCES

Ansari, A. S. and S. N. Pandis (1998). "Response of inorganic PM to precursor concentrations." Environmental Science & Technology **32**(18): 2706-2714.

Blanchard, C. L. and S. Tanenbaum (2008). Analysis of Inorganic Particulate Matter Formation in the Midwestern United States, Final Report. Prepared for Lake Michigan Air Directors Consortium. Albany, CA.

Khlystov, A., C. O. Stanier, et al. (2005). "Water content of ambient aerosol during the Pittsburgh Air Quality Study." Journal of Geophysical Research-Atmospheres **110**(D7): D07S10, doi:10.1029/2004JD004707.

Nenes, A., S. Pandis, et al. (1998). "ISORROPIA: A new thermodynamic equilibrium model for multiphase multicomponent inorganic aerosols." AQUATIC GEOCHEMISTRY **4**(1): 123-152.

Takahama, S., A. E. Wittig, et al. (2004). "Modeling the diurnal variation of nitrate during the Pittsburgh Air Quality Study." Journal Of Geophysical Research-Atmospheres **109**(D16).

Vayenas, D. V., S. Takahama, et al. (2005). "Simulation of the thermodynamics and removal processes in the sulfate-ammonia-nitric acid system during winter: Implications for PM2.5 control strategies." Journal of Geophysical Research-Atmospheres **110**(D7): -.

7.0 NITRATE FORMATION

In this Section we first discuss the average diurnal patters (episodes versus non-episodes) of total nitrate contrasting the Wisconsin sites and the SEARCH sites (Section 7.1). We then present a back-of-the-envelope calculation to estimate the daytime and nighttime nitrate formation rates for Milwaukee and Mayville (Section 7.2). Section 7.3 presents an analysis of the diurnal patterns of weekends versus weekdays. We close with Section 7.4 by giving a brief summary of the literature review on nitrate formation. The bulk of the literature review with a full list of references is contained in Appendix A13.

7.1 Average diurnal patterns

A typical diurnal cycle of total nitrate (TNO_3) during wintertime exhibits an increase of TNO_3 concentration during the night with a maximum in the early morning and a decrease during the day with a minimum in the early afternoon. Moreover most of TNO_3 is usually found in the aerosol phase (see Figure 13-2 in the Appendix 13 by Wittig et al. (2004) for an example).

The averaged diurnal cycle for TNO_3 at Milwaukee followed this pattern as shown in Figure 7.1 (top) with a diurnal variation (max to min) of a few micrograms per cubic meter. About 80% of total nitrate existed in the aerosol phase. The diurnal cycle was less pronounced at Mayville (Fig. 7.1, bottom), but the partitioning of total nitrate towards the aerosol phase was even stronger with about 90%. Comparing the averaged cycles including all data (green line) to those that only include the data during the episodes (blue line), we found that the total nitrate concentrations were about doubled at Milwaukee and tripled at Mayville when only episodes were considered. During episodes the total nitrate existed almost exclusively as aerosol nitrate. Total ammonia was increased during episodes by a factor of 2. This increase can be attributed almost entirely to an increase in ammonium in the aerosol phase while gas phase ammonia stayed about at the same level during episodes (Milwaukee) or even decreased (Mayville). The corresponding Figures for the averaged diurnal patterns for aerosol nitrate, ammonium and ammonia can be found in the Appendix 3.

Figure 7-2 shows the corresponding averaged diurnal cycles for TNO_3 for the SEARCH sites in

Atlanta. This data set provides data from a winter environment with higher temperatures and

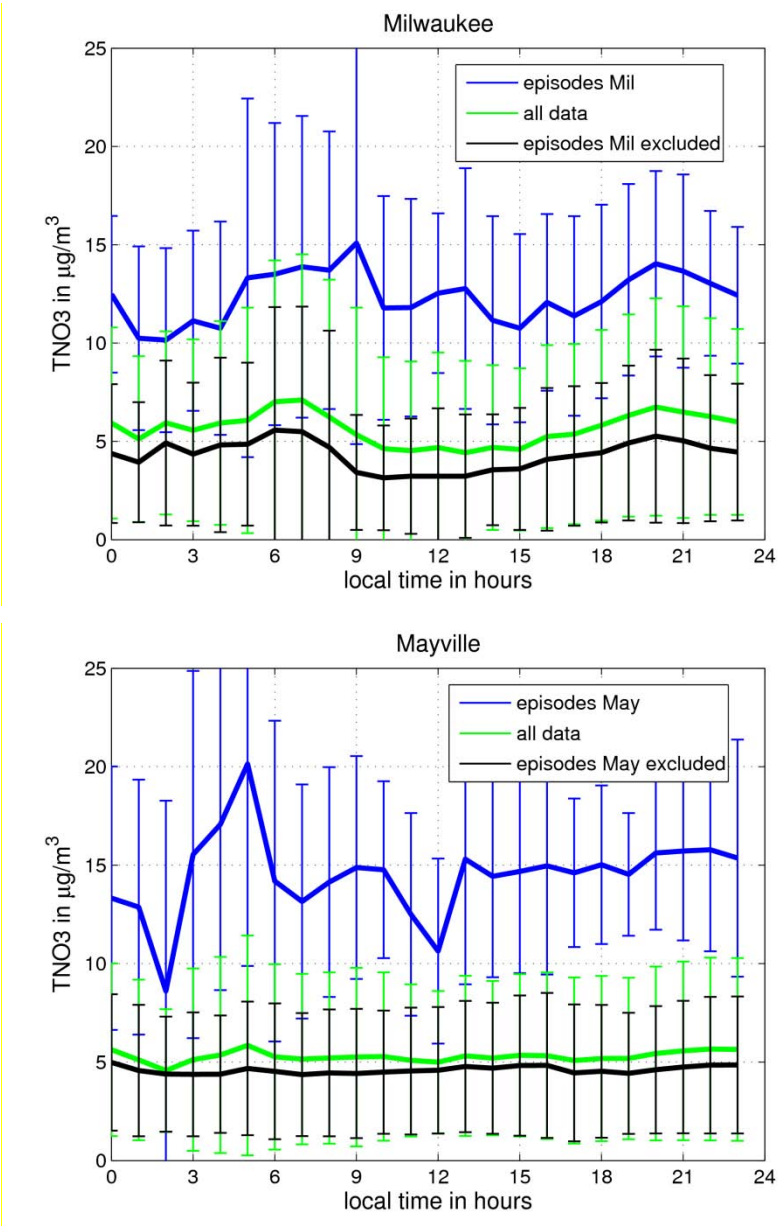

Figure 7-1. Averaged diurnal cycle for total nitrate for the Wisconsin sites. Top: Milwaukee; Bottom Mayville; Three different data collectives are shown: The green line represents the average including all data during the measurement period; The blue line is the average based on data that only includes the episode hours at the respective site; The black line is the average based on data that excludes the episode hours at the respective site. Also shown are the corresponding standard deviations.

different relative contributions of individual constituent species to total $PM_{2.5}$. In particular, nitrate pollution is less important in Georgia compared to Wisconsin, and its relative contribution

decreased in Georgia during episodes whereas it increased in Wisconsin as we saw in Figure 3-9.

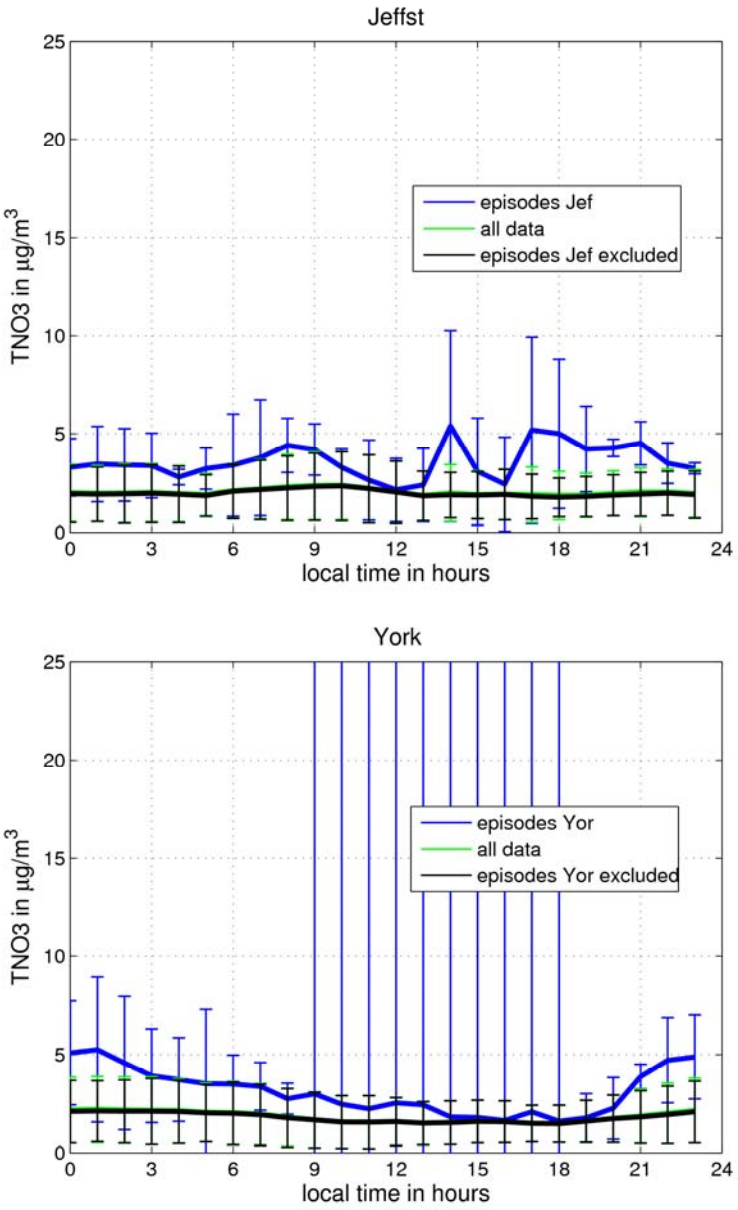

Figure 7-2. Averaged diurnal cycle for total nitrate for the SEARCH sites. Top: Jefferson Street, Atlanta, GA; Bottom: Yorkville; Three different data collectives are shown: The green line represents the average including all data during the measurement period; The blue line is the average based on data that only includes the episode hours at the respective site; The black line is the average based on data that excludes the episode hours at the respective site. Also shown are the corresponding standard deviations.

Comparing Figure 7-1 and 7-2 we see that the total nitrate levels in Atlanta were on average 2.5 times lower than in Milwaukee. This is despite the fact that O_3 levels are comparable (22 ppb

mean in Milwaukee, 20 ppb mean in Atlanta) and NO_2 levels are comparable (16 ppb in Milwaukee, 17 ppb in Atlanta). A possible explanation for this difference in nitrate formation is a more favorable nighttime conversion from NO_2 to nitrate in Milwaukee: Lower temperatures favor the formation of N_2O_5 and the subsequent formation of HNO_3 as explained in more detail in Section 7.2 below and in Appendix 13.3.1. Lower temperatures also favor the partitioning of HNO_3 into the aerosol phase (on average 91% aerosol fraction for nitrate in Milwaukee, versus 62% aerosol fraction in Atlanta). Aerosol nitrate, in turn, has a longer lifetime compared to nitric acid gas.

7.2 Nitrate production pathways during daytime versus during nighttime at Milwaukee and Mayville

There are two primary pathways producing nitric acid, a nighttime pathway and a daytime pathway. Knowledge about the relative magnitude of these pathways is important for the fundamental understanding of the processes that determine the nitrate budget and their accurate representation in models. This in turn is crucial for improving nitrate predictions and for capturing adequately the sensitivity of those predictions towards control strategies.

The chemical formation rates of nitric acid and the relative importance of nighttime versus daytime pathways can be estimated from the available dataset. In the absence of sunlight, the following reaction initiates the formation of HNO_3:

$$NO_2 + O_3 \rightarrow NO_3 + O_2 \qquad \text{(R1)}$$

This reaction is followed by the conversion of NO_3 to N_2O_5 and eventually to HNO_3. The last step involves the heterogeneous hydrolysis of N2O5 on or in aqueous aerosol particles (see Appendix A13, Section A13.3 for a more detailed discussion). Assuming that all NO_3 radicals produced by reaction (R1) yield HNO_3, we can calculate the HNO_3 production rate using the observed NO_2 and O_3 measurements and a rate constant recommended by JPL (Sander et al., 2003). Reactions of NO_3 with NO and VOC result in a lower production rate, hence the rate of reaction R1 represents an upper limit. As a lower limit we estimate an efficiency of this

conversion of 30% according to Vayenas et al. (2005).

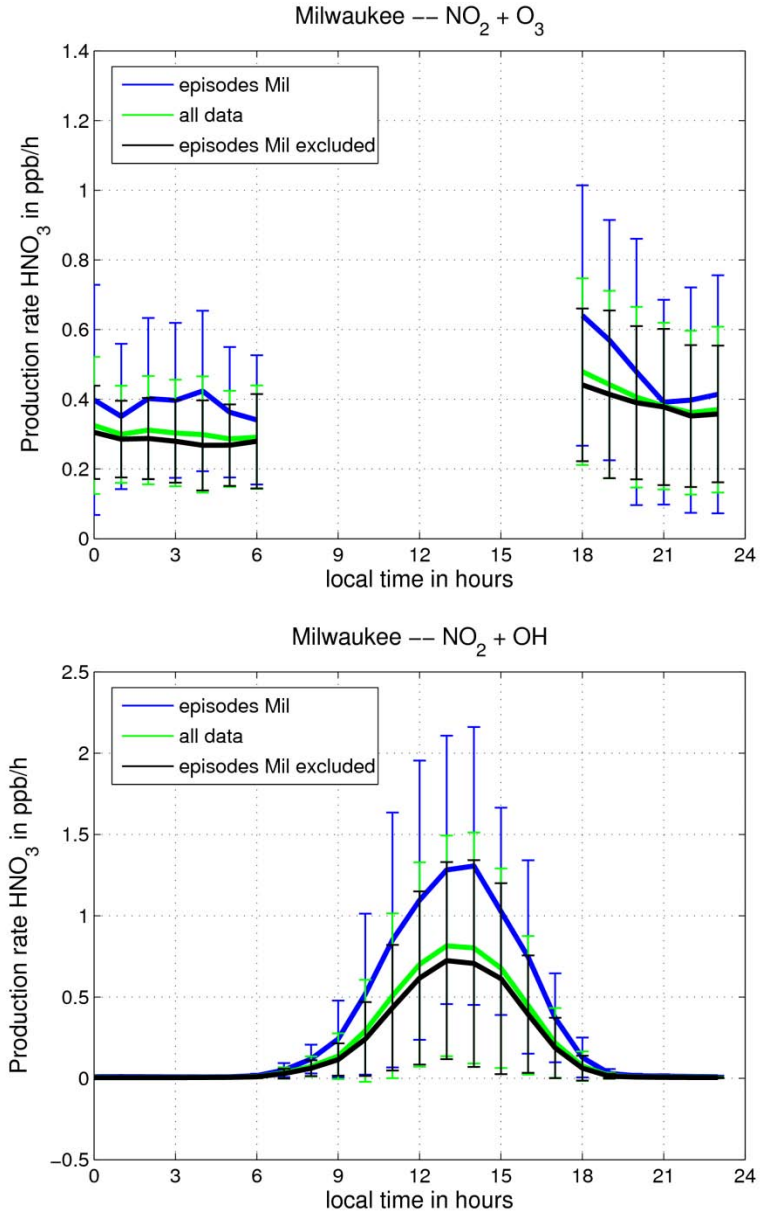

Figure 7-3. Diurnal averages of the estimated production rates of HNO_3 for Milwaukee. Top: nighttime pathway; Bottom: daytime pathway. Three different data collectives are shown: The green line represents the average including all data during the measurement period; The blue line is the average based on data that only includes the episode hours at the respective site; The black line is the average based on data that excludes the episode hours at the respective site. Also shown are the corresponding standard deviations.

Since NO_3 is rapidly photolyzed, the dominant pathway for HNO_3 production during daytime is:

$NO_2 + OH \rightarrow HNO_3$. (R2)

Since the OH radical was not directly measured during the LADCO study, we used representative OH concentrations from CMAQ modeling results to estimate the corresponding reaction rates.

The averaged OH concentrations for January, February, and March at Mayville were $3.3 \cdot 10^{-3}$ ppt, $8.1 \cdot 10^{-3}$ ppt, and $2.4 \cdot 10^{-2}$ ppt, respectively. The averages for the maximum daytime concentrations at Mayville were $1.6 \cdot 10^{-2}$ ppt, $3.7 \cdot 10^{-2}$ ppt , and $1.0 \cdot 10^{-1}$ ppt. For Milwaukee the averaged OH concentrations were $3.5 \cdot 10^{-3}$ ppt, $1.1 \cdot 10^{-2}$ ppt, and $2.8 \cdot 10^{-2}$ ppt, respectively. The averages for the maximum daytime values were $1.7 \cdot 10^{-2}$ ppt, $5.1 \cdot 10^{-2}$ ppt , and $1.2 \cdot 10^{-1}$ ppt, respectively. We have to keep in mind that the modeled OH concentrations are uncertain and will introduce corresponding uncertainties in the estimate of the reaction rate for (R2) that we are not able to quantify further. Measurements by Ren et al. (2006) for January and February 2004 in New York City show maximum daytime concentrations of 0.05 ppt, which is on the same order of magnitude than the modeled values.

Figure 7-3 and 7-4 show the diurnal averages of the estimated production rates of HNO_3 for Milwaukee and Mayville, respectively. As in Section 7.1 we grouped the data in three different data collectives: The green line represents the average including all data during the measurement period; The blue line is the average based on data that only includes the episode hours at the respective site; The black line is the average based on data that excludes the episode hours at the respective site. Also shown are the corresponding standard deviations.

When using all data, we found that the rates during night were of comparable magnitude to the rates during day for both Milwaukee and Mayville. However they were generally at a higher level in Milwaukee, approx. 0.4 ppb/h compared to 0.15 ppb/h at Mayville, due to the higher NO_2 concentrations. Note that we used the upper limit estimate for the nighttime rates assuming that all NO_3 radicals produced by reaction R1 form HNO_3.

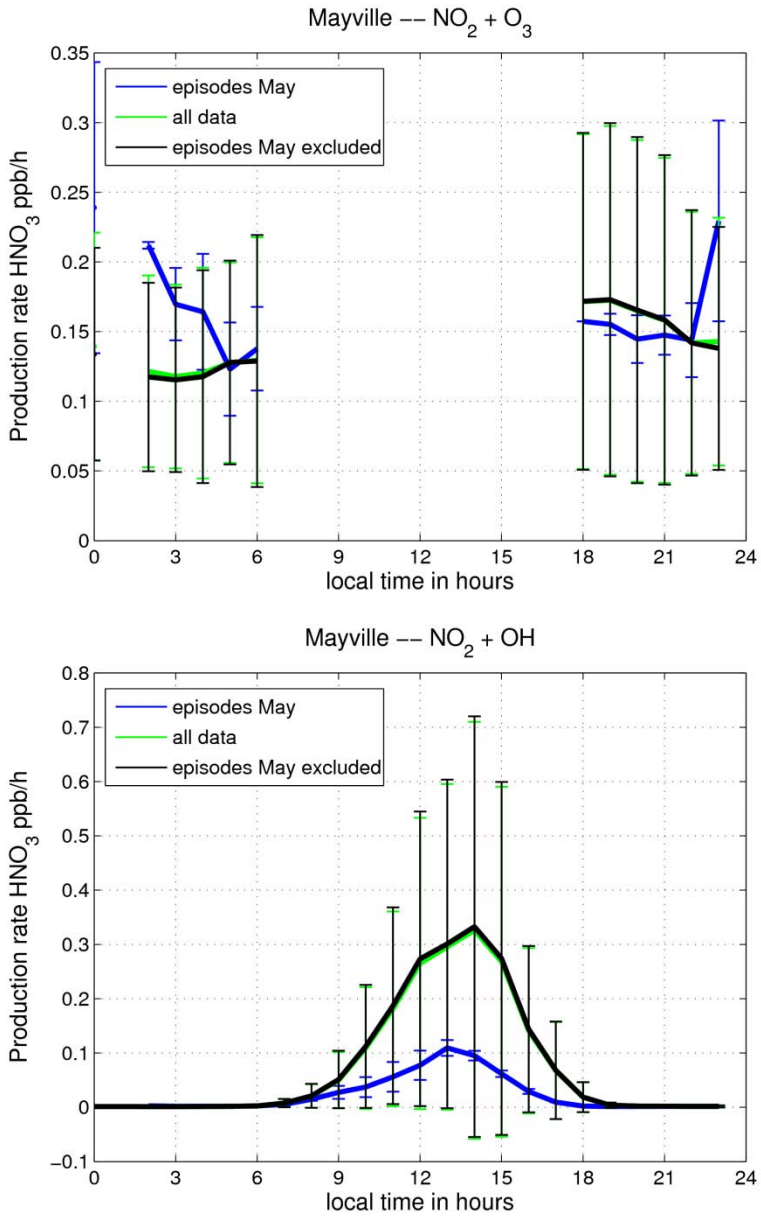

Figure 7-4. As Figure 7-3 but for Mayville.

During episodes the relative importance of daytime and nighttime contributions changed depending on location. In Milwaukee the upper-limit average nighttime production rate was 0.42 ppb/h compared to 0.70 ppb/h for the average daytime production rate.

During episodes in Mayville the upper-limit average nighttime production rate was 0.17 ppb/h compared to only 0.05 ppb/h during daytime. Note that for Mayville the daytime production of

HNO_3 is lower during the episodes (Fig. 7-4, bottom). This reflects the timing of the episodes -- earlier in the year for Mayville, later in the year for Milwaukee -- and the OH concentrations that go along with this; OH in January is about a factor 7 lower than in March. This in turn means that the relative importance of the nighttime pathway is higher in Mayville compared to Milwaukee.

In summary, this estimate shows that the nighttime pathway could contribute up to 50% of the nitrate production in both locations, especially during the earlier (Jan / Feb) episodes.

7.3 Diurnal profiles on weekends versus week days

An interesting question is if day-of-week differences are important for nitrate production in the Wisconsin data set. On weekends anthropogenic activities are different to week day activities, which typically results in lower emissions of NO_x (e.g. Qin et al., 2004). Figure 7-5 shows the diurnal patterns of NO_2, separated into weekend and weekday data. There were 13 weekends during the 3-month measurement period. In Milwaukee, the average concentration reaches about 23 ppb during morning rush hour on week days, while during weekends this value decreases to 14 ppb. In Mayville the NO_2 concentrations are also somewhat lower during weekends than during week days. This is associated with a higher ozone concentration at both stations, most notably in Milwaukee during the morning hours (23 ppb ozone at 6AM on weekends versus 14 ppb on weekdays, see Appendix 3 for Figures). However, the NH_3 concentrations do not show a consistent difference comparing weekends versus weekdays (see Appendix 3). It appears that ammonium nitrate is not very sensitive to changes in NO_x while NH_3 remains essentially unchanged. This results in an absence of a weekend effect regarding total nitrate, total ammonium, particle phase nitrate and ammonium, and $PM_{2.5}$. The diurnal patters for TNO_3 are shown in Figure 7-6, while the complete list of Figures is included in Appendix 3.

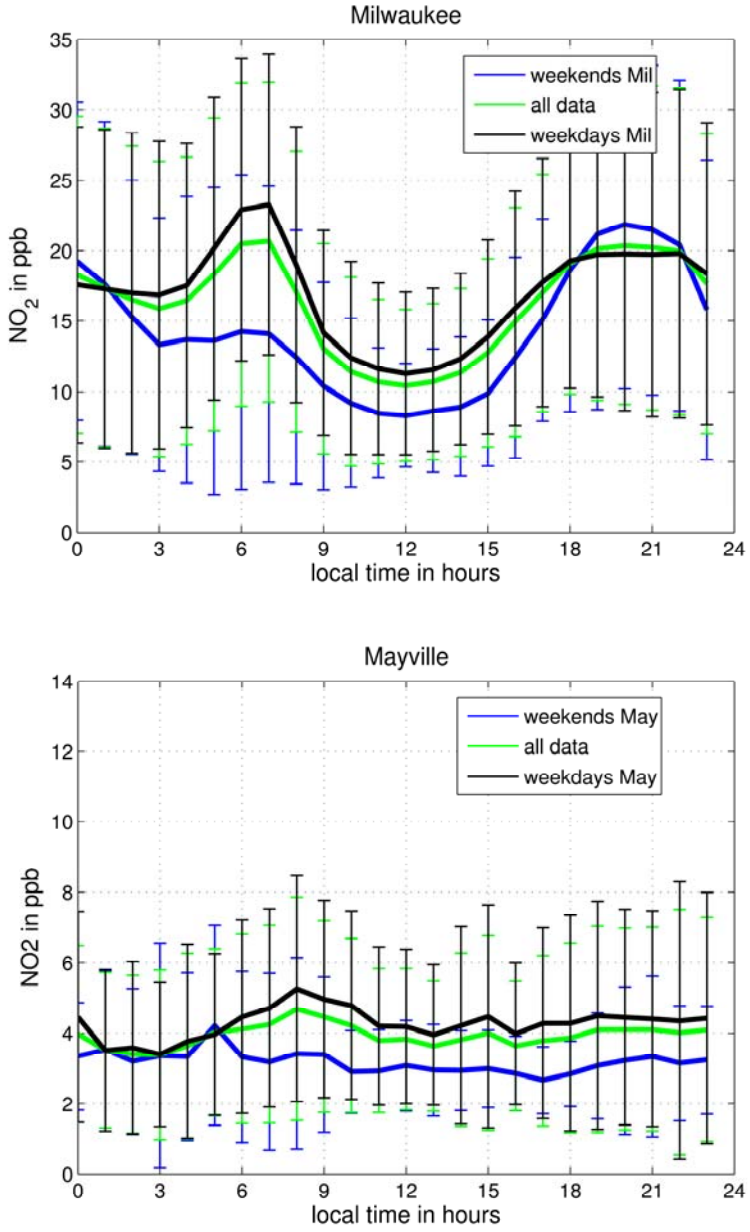

Figure 7-5. Averaged diurnal cycle for NO_2 for the Wisconsin sites. Top: Milwaukee; Bottom Mayville; Three different data collectives are shown: The green line represents the average including all data during the measurement period; The blue line is the average based on data that only includes the weekend hours at the respective site; The black line is the average based on data that includes only the weekday hours at the respective site. Also shown are the corresponding standard deviations.

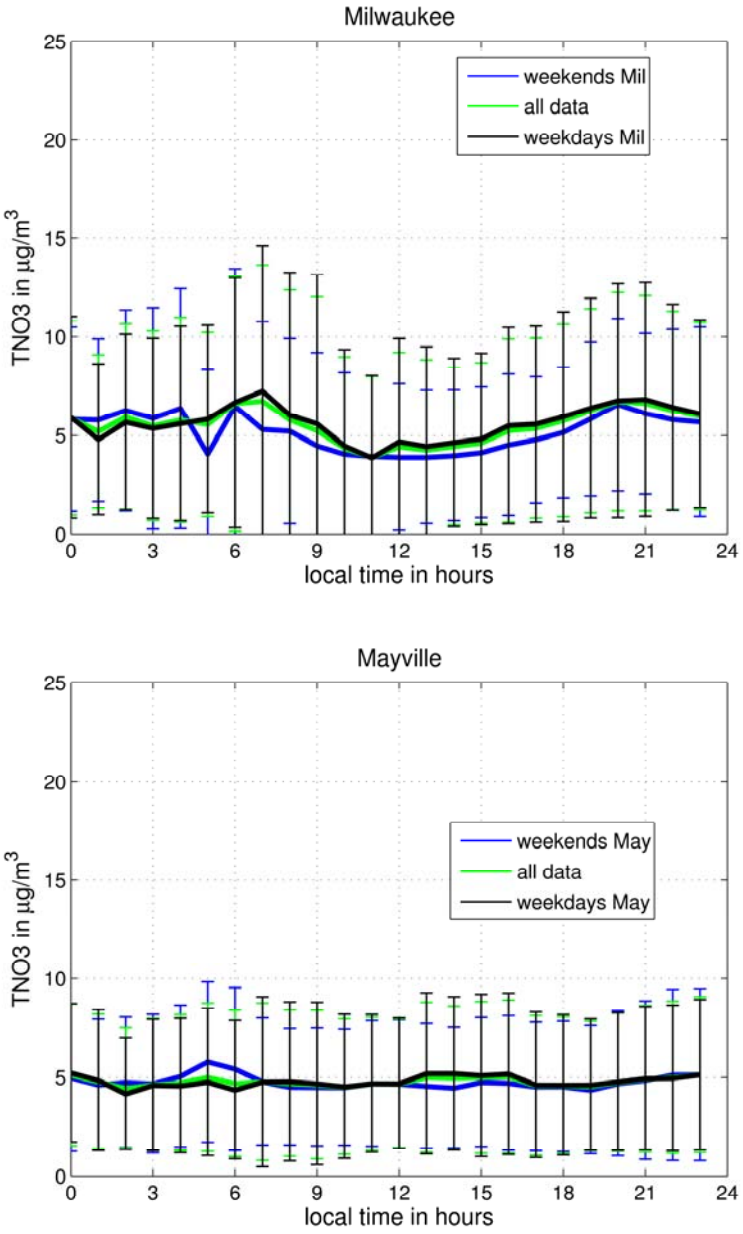

Figure 7-6. As Figure 7-5, but for total nitrate (TNO_3).

7.4 Summary of nitrate/N_2O_5 literature review

The full literature review of nitrate/N_2O_5 related literature is provided in Appendix A13. This Section summarizes the most important points.

- **Key point #1. Aerosols are a mixture of different chemical compounds, coming from a variety of locations** ranging from very local sources, nearby but "fresh" emissions, and regionally transported pollutants that can come from 100s of miles away (e.g. Makar et al., 2009).

- **Key point #2.** During wintertime regional episodes, ammonium nitrate aerosol is the most prevalent aerosol species (e.g. Katzman et al., 2010; Blanchard et al., 2007). The precursors of ammonium nitrate are gas phase nitric acid and ammonia. Nitric acid is formed from atmospheric chemical reactions of NO_x, which is emitted during combustion processes. Ammonia is directly emitted into the atmosphere, with agriculture representing the largest source of ammonia emissions.

- **Key point #3. Ammonium nitrate is (a) semivolatile and (b) requires a specific balance of ammonia and nitric acid.** When there is too little ammonia, ammonium nitrate formation will stop when all the ammonia is gone, leaving nitric acid gas, and creating what is termed an ammonia limited scenario. Conversely, when there is too little nitric acid, ammonium nitrate formation will stop when all the nitric acid is gone, leaving ammonia gas, and creating what is termed a nitric acid limited scenario. Finally, ammonium nitrate is sensitive to temperature and relative humidity. Numerous studies investigate how to assess which regime applies for a given region at a given time in order to infer which control strategies will be most effective (e.g. Makar et al., 2009; Pinder et al., 2007; Ghosh et al., 2010). In addition, the metrics used in Section 6 provide information on the regimes associated with ammonia-limited and nitric acid-limited conditions.

- **Key point #4. There are distinct daytime and nighttime pathways of nitrate formation.** During the daytime the reaction of OH and NO_2 forms HNO_3, which then can partition between gas phase and nitrate in the aerosol phase. In the absence of sunlight, the reaction $NO_2+O_3 \rightarrow NO_3 + O_2$ is followed by the conversion of NO_3 to N_2O_5, which in turn can form HNO_3 via hydrolysis on aqueous aerosols (e.g. Chang et al., 2010). For effective air quality

management, it is important to know the relative importance of each production (and loss) pathway at different times and locations, and to represent them adequately in air quality models. If this is not then case, then we cannot expect to adequately capture the sensitivity of model results towards control strategies.

- **Key point #5. Modeling studies show that the nighttime pathway of nitrate formation can potentially have a large impact, especially in colder climates or during wintertime (e.g. Alexander et al., 2009).** However, regional studies for winter-time conditions or foggy conditions are still lacking. The parameterization of the efficiency of the nighttime pathway is a difficult problem and introduces uncertainty in model simulations (e.g. Riemer et al., 2003, 2009; Evans and Jacob, 2005; Mathur et al., 2008)
- **Key point #6. Gas phase nitric acid may adsorb to mineral dust and form nitrate.** Since dust is predominantly found in the supermicron mode, nitrate is largely found in supermicron mode as well when dust is present, hence the presence of dust can influence the partitioning of nitrate between fine and coarse mode (Song and Carmichael, 1999). The uptake coefficients that characterize these processes are a large source of uncertainties (Bauer et al., 2004). The mineralogy of dust appears to play a role (Krueger et al., 2004). A study by Lee et al. (2008) suggests that these processes may be less important in the Midwest during wintertime compared to other locations and seasons in the U.S.
- **Key point #7. Modeling nitrate is inherently difficult.** Because of the complex interactions of transport and chemistry, state-of-the-art models have difficulties with predicting nitrate (e.g. Tesche et al., 2007; Appel et al., 2008). Mathur et al. (2008) describe that systematic errors in model predictions of nitrate (and $PM_{2.5}$) during the winter period stem from a combination of uncertainties in the magnitude and spatial and temporal allocation of primary $PM_{2.5}$ emissions, current uncertainties in the estimation of chemical production pathways for nitrate, and the representation of boundary layer mixing especially during nighttime conditions. As a consequence, it is even more difficult to develop and evaluate reliable control strategies.

REFERENCES

Appel, K. W., P. V. Bhave, et al. (2008). "Evaluation of the community multiscale air quality (CMAQ) model version 4.5: Sensitivities impacting model performance; Part II - particulate matter." Atmospheric Environment **42**(24): 6057-6066.

Bauer, S.E., Y. Balkanski, M. Schulz, D. A. Hauglustaine, F. Dentener (2004). "Global modeling of heterogeneous chemistry on mineral aerosol surfaces: Influence on tropospheric ozone chemistry and comparison to observations." Journal of Geophysical Research, **109**, doi:10.1029/2003JD003868.

Chang, W.L., P. V. Bhave, S. S. Brown, N. Riemer, J. Stutz, and D. Dabdub (2010). Tropospheric N_2O_5: a review of ambient measurements and model calculations, submitted to *Aerosol Science and Technology*.

Evans, M. J., and Jacob, D. J. (2005). "Impact of new laboratory studies of N_2O_5 hydrolysis on global model budgets of tropospheric nitrogen oxides, ozone and OH." Geophysical Research Letters **32**:L09813, doi:10.1029/2005GL022469.

Ghosh, S.K., P.V. Bhave, J.M. Davis, H. Lee (2010). "Spatio-Temporal Analysis of Total Nitrate Concentrations Using Dynamic Statistical Models." Journal of the American Statistical Association **105**(490):538-551.

Katzman, T.L., A. P. Rutter, J. J. Schauer, G. C. Lough, C. J. Kolb, S. Van Klooster (2010). "PM2.5 and PM10–2.5 Compositions during Wintertime Episodes of Elevated PM Concentrations across the Midwestern USA." Aerosol and Air Quality Research **10**: 140–153.

Lee, T., X.-Y. Yua, B. Ayres, S. M. Kreidenweis, W. C. Malm, J. L. Collett Jr. (2008). "Observations of fine and coarse particle nitrate at several rural locations in the United States" Atmospheric Environment **42**: 2720–2732.

Makar, P.A., M. D. Moran, Q. Zheng, S. Cousineau, M. Sassi, A. Duhamel, M. Besner, D. Davignon, L.-P. Crevier, V. S. Bouchet (2009). "Modelling the impacts of ammonia emissions reductions on North American air quality" Atmospheric Chemistry and Physics, **9**, 7183–7212.

Mathur, R., S. Yu, D. Kang, K. L. Schere (2008). "Assessment of the wintertime performance of developmental particulate matter forecasts with the Eta-Community Multiscale Air Quality modeling system." Journal of Geophysical Research **113**: D02303.

Pinder, R. W., P. J. Adams, et al. (2007). "Ammonia emission controls as a cost-effective strategy for reducing atmospheric particulate matter in the eastern United States." Environmental Science & Technology **41**(2): 380-386.

Qin, Y., G. S. Tonnesen and Z. Wang (2004). "Weekend/weekday differences of ozone, NO_x, CO, VOCs, PM_{10} and the light scatter during ozone season in southern California." Atmospheric Environment, **38**, 3069-3087.

Ren X. et al. (2006). "Behavior of OH and HO_2 in the winter atmosphere in New York City."

Atmospheric Environment, **40**, S2: 252-263.

Riemer, N., Vogel, H., Vogel, B., Schell, B., Ackermann, I., Kessler, C., and Hass, H. (2003). "Impact of the heterogeneous hydrolysis of N_2O_5 on chemistry and nitrate aerosol formation in the lower troposphere under photosmog conditions." Journal of Geophysical Research **108**:4144.

Riemer, N., Vogel, H., Vogel, B., Anttila, T., Mentel, T.F., Kiendler-Scharr, A. (2009). "The relative importance of organic coatings for the heterogeneous hydrolysis of N_2O_5." Journal of Geophysical Research, **114**:D17307, doi:10.1029/2008JD011369.

Sander, S.P., R.R. Friedl, A. R. Ravishankara, D. M. Golden, C.E. Kolb, M. J. Kurylo, R.E. Huie, V.L. Orkin, M.J. Molina, G.K. Moortgat, B.J. Finlayson-Pitts, Chemical Kinetics and Photochemical Data for Use in Atmospheric Studies, Report 02-25, Jet Propul. Lab., Pasadena, Calif., 2003.

Song, C.H., G. R. Carmichael (1999). "The aging process of naturally emitted aerosol (sea-salt and mineral aerosol) during long range transport, Atmospheric Environment." **33**, 2203—2218.

Tesche, T. W., R. Morris, G. Tonnesen, D. McNally, J. Boylan, P. Brewer (2006). "CMAQ/CAMx annual 2002 performance evaluation over the eastern US", Atmospheric Environment **40**, 4906-4919.

Vayenas, D. V., S. Takahama, et al. (2005). "Simulation of the thermodynamics and removal processes in the sulfate-ammonia-nitric acid system during winter: Implications for PM2.5 control strategies." Journal of Geophysical Research-Atmospheres **110**(D7): 11.

Wittig, A. E., S. Takahama, et al. (2004). "Semi-continuous PM2.5 inorganic composition measurements during the Pittsburgh air quality study." Atmospheric Environment **38**(20): 3201-3213.

8. CONCLUSIONS

Analysis of air quality and related measurements obtained during the LADCO Winter Nitrate Study was performed in order to better understand wintertime episodes of elevated fine particle ($PM_{2.5}$) concentrations in the Midwest. This Phase I study was conducted by a team of researchers from the University of Iowa and the University of Illinois. The analysis focused on evaluating and comparing the high time resolution surface observations taken during the three-month period (1 January - 31 March, 2009) at an urban Milwaukee site and a rural site in Mayville, Wisconsin. These were also contrasted with simultaneous measurements taken using similar instrumentation in the SEARCH network. The Milwaukee site (DNR-SERHQ monitor, AQS 55-079-0026) is subjected to higher levels of primary pollutants from nearby highways and industry, while the Mayville site (AQS 55-027-0007), located 65 km northwest of Milwaukee, is largely surrounded by agricultural fields, and is more representative of regional background conditions. The measurements analyzed at these sites included unspeciated hourly $PM_{2.5}$ mass (TEOM, hourly), speciated $PM_{2.5}$ FRM mass (SASS, 24 hour average every 3 days), inorganic gas and aerosol species concentrations (ARA, hourly), precursor gas phase concentrations (denuder, 24 hour average), and various surface meteorological parameters. All data used in the analysis went through QA checks, and the iCAMS continuous monitor concentrations were evaluated and in some cases adjusted for consistency with co-located denuder and filter measurements.

Observations during episode periods were contrasted with those during non-episode periods. Wintertime $PM_{2.5}$ episodes were defined as periods where the seven-hour running average concentrations exceeded 27 $\mu g\ m^{-3}$ for at least four consecutive hours. Thirteen episodes were identified at the Milwaukee site, and seven were identified at Mayville. There were no rural-only episodes, as all episodes at Mayville were concurrent with Milwaukee episodes. The Milwaukee-only (local) episodes occurred in late February and March. Analysis of the species mass concentrations and their diurnal variations revealed the following:

- The diurnal patterns for $PM_{2.5}$ at both sites were very flat during episodes and non-episodes, with a slight (a few microgram per m^3) increase at Milwaukee during episodes at 8 AM. This suggests that large variations in $PM_{2.5}$ in Wisconsin are caused by synoptic disturbance rather than cyclical diurnal changes in boundary layer height and wind speed.
- Episodes (except Milwaukee-only episodes) were characterized by strong enhancements in total nitrate; however, ordering of enhancements differed by site. Episodes had lower ozone concentrations throughout the day.

- During episodes, total nitrate concentrations were about doubled over average concentrations at Milwaukee and tripled at Mayville. About 80% of total nitrate existed in the aerosol phase at these sites, but the partitioning of total nitrate towards the aerosol phase was even stronger (about 90%) during episodes.
- Total ammonia also increased during episodes by a factor of 1.5-2.2. This increase can be attributed almost entirely to an increase in ammonium in the aerosol phase, while gas phase ammonia stayed about at the same level during episodes (Milwaukee) or even decreased (Mayville).
- Gas ratios, an indicator of ammonia availability, decreased slightly as $PM_{2.5}$ increased at these sites (although within the margin of error at Milwaukee). The gas ratios in Mayville were slightly higher than in Milwaukee (e.g. 1.7 vs. 1.5 for all study hours) during non-episodes. During episodes, the ordering switched, with the gas ratios at 1.0 (Mayville) and 1.35 (Milwaukee). The observation that total nitrate concentrations increase more rapidly than total ammonia during most episodes is important to the understanding and control of the episodes, and requires further investigation. One hypothesis as to the cause of this is that local sources of ammonia predominate during the episodes due to low wind speeds, and do not deliver ammonia sufficient to keep up with chemical conversion of NOx to nitric acid during episodes. Enhancement ratios of total ammonia during episodes were similar to those of primary pollutants (OC, EC, NOx) and less than the enhancement ratios of total nitrate.
- NO_y values were much higher at the urban site (26 ppb) than at the rural site (6 ppb). The main difference was in NO, due to local point and area NO_x sources in Milwaukee.
- Milwaukee only-episodes were characterized by the strongest enhancements in sulfate, EC, and OC.

To help place the results for the Wisconsin sites in context, the analysis was repeated for an urban-rural pair in Georgia. The SEARCH network urban site in Atlanta (Jefferson Street) and the rural site in Yorkville, were selected to provide data in a winter environment that had warmer temperatures and less nitrate pollution. There were fewer $PM_{2.5}$ episodes in the period studied at the urban site in Atlanta, Georgia (6) than in Milwaukee. The mean and episode conditions at the Georgia sites displayed a slightly more distinctive diurnal pattern than that at the Wisconsin sites, with a peak at 09:00 and a minimum at 13:00. Despite comparable O_3 levels (22 ppb mean in Milwaukee, 20 ppb mean in Atlanta) and comparable NO_2 levels (16 ppb in Milwaukee, 17 ppb in Atlanta), the total nitrate levels in Milwaukee were on average 2.5 times higher than in Atlanta. These results indicate that nitrate is not much involved in Georgia wintertime episodes. This is due primarily to higher temperatures in Georgia, along with less

favorable nighttime conversion from NO_2 to nitrate, and compounded by the lower lifetime of aerosol nitrate relative to nitric acid gas (on average 62% aerosol fraction for nitrate in Atlanta, versus 91% aerosol fraction in Milwaukee). The total ammonia level in Atlanta was 2.1μg m^{-3}, with 61% in the aerosol phase. For Milwaukee, the total ammonia level was 3.3 μg m^{-3} with 64% in the aerosol phase.

The meteorological conditions for the Midwest winter $PM_{2.5}$ episodes were also analyzed. The number of episodes of $PM_{2.5}$ particle pollution during the 2009 study period was above recent (2002-2008) average levels at both monitoring sites, but was close to average at the regional level. The 2009 winter period was one that featured considerable departures from 1971-2000 climatology, with a colder, drier January and a warm February and March with unusually high precipitation. All fine particle episodes in the 2009 period studied began under similar synoptic conditions, characterized by an approaching high level ridge/surface low pressure system moving into the region. Milwaukee-only episodes were defined throughout primarily by high relative humidity; low pressure; lower visibility; and lighter, more southerly winds at both sites. Mayville experienced the same local meteorological changes as Milwaukee during the Milwaukee-only episodes, even when local fine particle concentrations were not high enough to qualify as an episode. Fog and snow cover were both correlated with episode intensity. Fog was typically due to melting and sublimation of snow cover. Fog accompanied events at Mayville more often than at Milwaukee. Regional snow cover was present over southeastern Wisconsin and northern Illinois at the onset of late winter episodes and usually melted by the end of the episode, contributing moisture to the shallow boundary layer. To better quantify the physical conditions during PM events in future studies, co-located photometer and ceilometer observations may be useful.

Back trajectory analysis showed that in most episodes the air-masses had recently passed over Illinois and Indiana. Trajectory analysis further showed that air pollution transport from Milwaukee to Mayville during episodes was rare, although this conclusion is uncertain due to coarse resolution in the meteorological fields. Directional source analysis based on pollution roses, bivariate polar plots (concentration, wind speed, wind direction), and conditional probability function plots found strong directionality for NO_x at Milwaukee, with high concentrations measured when winds blew from SW – S at wind speeds less than 2 ms^{-1}. This site is located at 700 meter east of interstate 43 and 2.8 km north of interstate 794. NH_3 gas showed SW-WSW directionality at both sites, suggesting that this may not be indicative of local sources. $PM_{2.5}$ showed no directional dependence at either site. At Mayville, NH_3 and NO_y were elevated during periods of southwesterly winds and southeasterly winds, respectively. Bivariate polar plots of $PM_{2.5}$ during episodes showed that the most frequent wind direction was SE, and in this direction higher wind speeds showed higher PM concentrations, possibly indicating some urban-

to-rural transport from Milwaukee to Mayville. Conditional probability functions for NOy and SO_2 at Mayville also showed peak levels under SE winds. Strong directionality was found at Jefferson St. for NO_x indicating local contributions from nearby sources (i.e., there are railroad yards located within 2 km radius). SO_2 at this site showed high directionality with NW winds, where the large Atlanta Railroad station is located. Yorkville, located in a rural area without large anthropogenic combustion sources, showed a weak SE directionality (toward Atlanta) for NO_x and SO2. For NOx, the SE directionality was strongest for higher windspeeds, suggesting urban to rural transport.

Analysis of extensive OC/EC ratios for the Milwaukee and Mayville sites for the period Jan 2001 to Oct 2009 was done to look for patterns as a function of season, ozone levels, RH, temperature, and $PM_{2.5}$ concentration. The analysis confirmed the current conceptual model of OC contributions at these sites, with secondary organic carbon (and the associated increase in OC/EC ratios) only appearing during summer. OC/EC ratios decreased as $PM_{2.5}$ increased in winter

The sensitivity of the inorganic aerosol mass to changes in total ammonia, total nitrate, and total sulfate was evaluated using the ISOROPIA and GFEMN thermodynamic models. These models were validated against previous simulations and experimental data, and against one another. The observed values at Milwaukee and Mayville were used as inputs to the models for the base calculations. The models were run for every hour of the three-month study period for 400 different cases with varying changes in total ammonia (10), total sulfate (4), and total nitrate (10). Changes in the predicted aerosol mass from these simulations were analyzed for all study hours, all episode hours and all non-episode hours. To evaluate the results of these simulations, two new metrics were proposed: relative sensitivity (fractional) and relative sensitivity (mass). Relative sensitivity (mass), defined as ($\Delta PM_{\text{nitrate reduction}}$ / ΔTNO3) / ($\Delta PM_{\text{ammonia reduction}}$ / ΔTNH3) was used as the main quantitative metric for gauging relative sensitivity to changes in ammonia and nitrate. This metric was found to be 1.0 in Mayville during non-episode conditions, and 0.35 during episodes in Mayville. A value of 1.0 indicates that a 1.0 μg m^{-3} reduction in nitrate will have the same effect on $PM_{2.5}$ concentrations as a 1.0 μg m^{-3} reduction in ammonia. A value of 0.35 indicates that a 1.0 μg m^{-3} reduction in nitrate will be only 35% of the effect on $PM_{2.5}$ concentrations as a 1.0 μg m^{-3} reduction in ammonia. In Milwaukee, this metric was 0.63 during non-episodes, decreasing to 0.54 during episodes. Total mass concentrations of nitrate were typically higher than those of ammonia, so equal mass reductions are usually larger percentage reductions in ammonia. The thermodynamic sensitivity is shown graphically in Figure 8-1.

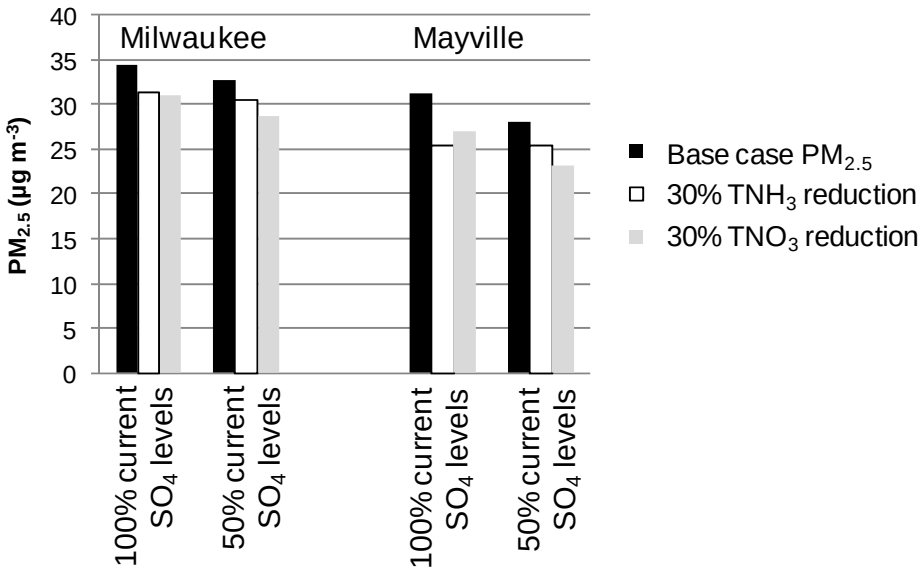

Figure 8-1 (identical to figure 6-8). Summary of thermodynamic modeling results for all episode hours.

Analysis using fractional sensitivity showed that an episode indicator metric defined as the sum of $PM_{2.5}$ minus 35 µg m^{-3} (only for hours with $PM_{2.5}$ above 35 µg m^{-3}) could be cut in half through a reduction in hourly total nitrate levels by ~40%, or by reduction in hourly total ammonia concentrations by ~40%, OR by reduction in both species by ~26%. The Mayville episodes as measured by the same episode indicator metric during the same period (though already cumulatively less than ½ as severe as those in Milwaukee) could be cut in half through a reduction in hourly total nitrate by ~28%, by reduction in hourly total ammonia levels by ~18%, or by reduction in both ammonia and nitrate by ~15%. Control of other species should also be considered in episode control scenarios.

Both fractional sensitivity and relative sensitivity (mass) are needed to forward development of effective control strategies. RS_f has the advantages of comparability to previous work and direct appearance on isopleth diagrams with fractional TNO_3 and TNH_3 as the x and y axes. The disadvantage of fractional sensitivity is that it can remain constant while the actual mass or mole-based sensitivity of the inorganic aerosol system changes, which is precisely what happens during episodes in the Upper Midwest, due to the greater enhancement of total nitrate relative to total ammonia.

Relative sensitivity (mass) was also estimated from the previous Midwest Ammonia Study (Blanchard 2008) and was 2.2 for winter months in Mayville (compared to 1.0 from this study). At the four Midwest

Ammonia Study sites closest to Mayville, the relative sensitivity (mass) ranged from 0.33 to 3.8 during winter months (DJF). At all 4 sites, the relative sensitivity during an air quality episode (only a single episode was analyzed) decreased substantially to values less than 0.5, possibly corroborating the observed drop in the nitrate sensitivity observed in this study.

The findings from this study indicate that a key to understanding winter $PM_{2.5}$ in the Midwest is a better understanding of what controls total nitrate levels. A literature review was conducted to summarize the state of scientific understanding on daytime nitric acid production and nighttime heterogeneous nitrogen chemistry. In the absence of sunlight, gaseous nitrogen dioxide (NO_2) reacts with ozone to produce the nitrate radical (NO_3). This reaction is followed by the conversion of NO_3 to dinitrogen pentoxide (N_2O_5) and eventually to HNO_3. The last step involves the heterogeneous hydrolysis of N_2O_5 on or in aqueous aerosol particles. Since NO_3 is rapidly photolyzed, the dominant pathway for HNO_3 production during daytime is via reaction of NO_2 with the hydroxyl radical (OH), which produces gaseous nitric acid. The daytime and nighttime production rates at Milwaukee and Mayville during the winter study period were estimated assuming that all NO_3 radicals produced yield HNO_3, and using the observed NO_2 and O_3 measurements and recommended reaction rate constants with model estimates of OH. When using all data, the production rates during night were of comparable magnitude to the rates during day for both Milwaukee and Mayville. However, the rates were generally higher in Milwaukee, approximately 0.4 ppb/h compared to 0.15 ppb/h at Mayville, due to the higher NO_2 concentrations in the urban environment. During episodes the relative importance of daytime and nighttime contributions changed depending on location. In Milwaukee the upper-limit average nighttime production rate was 0.42 ppb/h compared to 0.70 ppb/h for the average daytime production rate. During episodes in Mayville the upper-limit average nighttime production rate was 0.17 ppb/h compared to only 0.05 ppb/h during daytime, reflecting differences in the timing of the episodes—earlier in the year for Mayville, later in the year for Milwaukee—and the strong differences in OH concentrations with time of year (OH in January is about a factor of 7 lower than in March). These estimates, while uncertain, show that the nighttime pathway could contribute up to 50% of the nitrate production in both locations, especially during the earlier (Jan/Feb) episodes. More detailed analysis of the impact of nighttime chemistry on nitric acid and particle nitrate using more comprehensive models are needed to refine these estimates.

Phase II of this study will focus on extending this analysis of the measurements obtained during the LADCO Winter Nitrate Study to include three dimensional regional $PM_{2.5}$ modeling using CMAQ and PMCAMx models. Emphasis will be on better understanding the chemical, atmospheric transport, and thermodynamic processes impacting $PM_{2.5}$ levels and their rural-urban gradients in the winter in the

Midwest, evaluation of nitric acid production and its sensitivity to treatments of nighttime chemistry, evaluation of ammonia predictions including spatial patterns, and the sensitivity of modeled PM concentrations and spatial distributions to changes in precursor emissions.